

Supporting information

Photoredox Catalysis via Consecutive ²LMCT and ³MLCT Excitation of an Fe(III/II)-NHC-Complex

Aleksandra Ilic[†], Jesper Schwarz[†], Catherine Johnson[†], Lisa H.M. de Groot, Simon Kaufhold, Reiner Lomoth*, Kenneth Wärnmark*

^aCentre for Analysis and Synthesis (CAS), Department of Chemistry, Lund University, SE-22100 Lund, Sweden;

^bDepartment of Chemistry–Ångström Laboratory, Uppsala University, SE-75120 Uppsala, Sweden.

[†]These authors contributed equally.

*Corresponding Author

E-mail: reiner.lomoth@kemi.uu.se

E-mail: kenneth.warnmark@chem.lu.se

Table of Contents

GENERAL INFORMATION.....	5
Materials and Instruments.....	5
SUBSTRATE SYNTHESIS.....	7
Dimethyl 2-bromo-2-(2-(cyclopent-2-en-1-yl)ethyl)malonate (14a)	7
VISIBLE LIGHT-MEDIATED ATRA REACTION OF C ₈ F ₁₇ I TO 5-HEXEN-1-OL VIA REDUCTIVE QUENCHING OF [Fe(BTZ) ₃](PF ₆) ₃ (1)	8
Optimisations of the visible light-mediated ATRA reaction of C ₈ F ₁₇ I to 5-hexen-1-ol <i>via</i> reductive quenching of [Fe(bt _z) ₃](PF ₆) ₃ using the General Procedure	8
Control Experiments for the visible light-mediated ATRA reaction of perfluorooctyl iodide to 5-hexen-1-ol in presence of TEA using different Fe-catalysts	10
Screening of different alkyl halides for the visible light-mediated ATRA reaction to 5-hexen-1-ol <i>via</i> reductive quenching of [Fe(bt _z) ₃](PF ₆) ₃ using the General Procedure	12
Scope limitations of the visible light-mediated ATRA reaction <i>via</i> reductive quenching of [Fe(bt _z) ₃](PF ₆) ₃ using the General Procedure	12
Synthesis and Isolation of the addition of alkyl halides to alkenes and alkynes using Procedure A	13
5-Iodo-6-perfluorooctylhexanol (3b)	13
5-Iodo-6-perfluorohexylhexanol (3c)	14
5-bromo-7,7,7-trichloroheptan-1-ol (3d)	14
1-bromo-5-iodo-6-perfluorooctylhexane (4b)	15
5-iodo-6-perfluorooctylhexanenitrile (5b)	15
4-(2-iodo-3-perfluorooctyl-propyl)-anisole (6b)	16
1-perfluorooctyl-2-iodo-cyclohexane (7b, 7c)	16
2-iodo-3-perfluorooctylnorbornane (8b)	17
3-iodo-4-perfluorooctyl-but-3-en-1-ol (9b, 9c)	18
5-Iodo-6-perfluorooctylpentanol (10b)	19
5-iodo-6-perfluorooctylpentenoic acid (11b) and 5-(2,2,3,3,4,4,5,5,6,6,7,7,8,8,9,9,9- heptadecafluorononyl)dihydro-2(3H)-Furanone (11c)	19
5-Iodo-6-perfluorooctylhexane-2-one (12b)	20
4-(2-perfluorooctyl-1-iodoethyl)cyclohex-1-en (13b)	21

Intramolecular ATRA reaction of (14a) <i>via</i> reductive quenching of [Fe(bt_z)₃](PF₆)₃ (1)	21
VISIBLE LIGHT-MEDIATED ATRA REACTION OF C₈F₁₇I TO 5-HEXEN-1-OL VIA OXIDATIVE QUENCHING OF [Fe(BTZ)₃](PF₆)₃ (1)	23
Optimisation of the reaction conditions of the oxidative ATRA using the General Procedure	23
Control Experiments for the visible light-mediated ATRA reaction of perfluorooctyl iodide to 5-hexen-1-ol.24	
Scope limitations of the visible light-mediated ATRA reaction <i>via</i> oxidative quenching of [Fe(bt_z)₃](PF₆)₃ using the General Procedure.....	25
Synthesis and Isolation of the addition of alkyl halides to alkenes and alkynes using Procedure B	26
5-Iodo-6-perfluorooctylhexanol (3b)	26
5-Iodo-6-perfluorohexylhexanol (3c).....	26
5-bromo-7,7,7-trichloroheptan-1-ol (3d)	27
1-bromo-5-iodo-6-perfluorooctylhexane (4b).....	27
5-Iodo-6-perfluorooctylhexanenitrile (5b)	28
4-(2-iodo-3-perfluorooctyl-propyl)-anisole (6b).....	28
1-iodo-2-perfluorooctylcyclohexane (7b, 7c)	29
2-iodo-3-(perfluorooctyl)bicyclo[2.2.1]heptane (8b)	30
3-iodo-4-perfluorooctyl-but-3-en-1-ol (9b, 9c).....	30
5-Iodo-6-perfluorooctylpentanol (10b)	31
5-Iodo-6-perfluorooctylpentenoic acid (11b)	32
5-Iodo-6-perfluorooctylhexane-2-one (12b)	32
Intramolecular ATRA reaction of (14a) <i>via</i> oxidative quenching of [Fe(bt_z)₃](PF₆)₃ (1).....	33
MECHANISTIC INVESTIGATIONS	34
The effect of radical scavengers on the visible light-mediated ATRA reaction <i>via</i> reductive quenching of [Fe(bt_z)₃](PF₆)₃ using the General Procedure	34
The effect of different additives on the visible light-mediated ATRA reaction <i>via</i> oxidative quenching of [Fe(bt_z)₃](PF₆)₃ using the General Procedure	34
Investigation of the chemoselectivity of the visible light-mediated ATRA reaction of alkyl halides to alkenes & alkynes <i>via</i> reductive quenching of [Fe(bt_z)₃](PF₆)₃	34

Investigation of the chemoselectivity of the visible light-mediated ATRA reaction of alkyl halides to alkenes & alkynes <i>via</i> oxidative quenching of [Fe(bt_z)₃](PF₆)₃	36
Investigation of the Radical Nature of the visible light-mediated ATRA reaction of alkyl halides to alkenes & alkynes <i>via</i> oxidative quenching of [Fe(bt_z)₃](PF₆)₃.....	37
(±)-diethyl 3-(perfluorooctyl)-methyl-4-(iodomethyl)cyclopentane-1,1-dicarboxylate (16)	37
(<i>E</i>)-5-perfluorooctyl-2-(iodomethyl)pent-3-en-1-ol (17a) and (<i>E</i>)-6-perfluorooctyl-2-iodohex-4-en-1-ol (17b)	37
Investigation of the Radical Nature of the visible light-mediated ATRA reaction of alkyl halides to alkenes & alkynes <i>via</i> reductive quenching of [Fe(bt_z)₃](PF₆)₃	38
(±)-diethyl 3-(perfluorooctyl)-methyl-4-(iodomethyl)cyclopentane-1,1-dicarboxylate (16)	38
(<i>E</i>)-5-perfluorooctyl-2-(iodomethyl)pent-3-en-1-ol (17a) and (<i>E</i>)-6-perfluorooctyl-2-iodohex-4-en-1-ol (17b)	39
Tracing of the visible light-mediated ATRA of perfluorooctyl iodide to 5-hexen-1-ol <i>via</i> reductive & oxidative quenching of [Fe(bt_z)₃](PF₆)₃ using UV-vis absorption spectroscopy	40
Wavelength switching experiment – Fe(III)/[*]Fe(III)/Fe(II)/[*]Fe(II)	41
Quantum Yield Measurements for the ATRA reaction in the reductive and oxidate quenching route	42
Investigation of the longevity of the photoredox catalysts	45
Absorption spectra of [Fe(III)(bt_z)₃]³⁺ and [Fe(II)(bt_z)₃]²⁺	46
Excited State Lifetimes of [Fe(III)(bt_z)₃]³⁺ and [Fe(II)(bt_z)₃]²⁺	47
Excited state reactivity of [Fe(III)(bt_z)₃]³⁺ and [Fe(II)(bt_z)₃]²⁺	48
Cage Escape Yields	51
NMR SPECTRA	53
REFERENCES	92

General Information

Materials and Instruments

Materials. All solvents used in work-up procedures, for silica gel column chromatography, and/or for purification were obtained from commercial suppliers and used without further purification. Reagents *i.e.*, commercially available alkenes, alkyl halides, sacrificial reductants and additives as well as deuterated solvents for NMR-spectroscopy were purchased from Sigma-Aldrich and Acros Organics and used without further purification. $[\text{Fe}(\text{btz})_3](\text{PF}_6)_3$, $[\text{Fe}(\text{btz})_3](\text{PF}_6)_2$ and $[\text{Fe}(\text{bpy})_3](\text{PF}_6)_2$ were prepared according to literature protocol.^[1]

Photoreactions. Generally, photoreactions were performed in a TAK120 AC photoreactor purchased from HK Testsysteme GmbH. The irradiation was performed using the green LED array ($\lambda=530$ nm, 3.03 W/vial) in 6 mL clear glass crimp top vials with septum. The temperature during reaction was maintained at 27–30 °C using air cooling.

For wavelength-switching experiments LED bars were used to irradiate 4 mL vials at 525 nm (Nichia NSPG500DS) or 700 nm (Roithner ELD-700-524). Samples for tracing *via* UV-vis spectroscopy were irradiated in a Photoredox box (EvoluChem LED Spotlight (18 W, 525–530 nm)) purchased from HepatoChem Inc. using a 10 × 10 mm fluorescence quartz cuvette with a screw cap and PTFE septum.

Chromatography. Precoated Merck silica gel 60 F254 plates were used for thin-layer-chromatography (TLC) analysis and products were visualised using UV light or ethanolic KMnO_4 solution and heat as the developing agent. Flash silica gel chromatography was performed using Merck silica gel (pore size 60 Å, 230–400 mesh particle size, particle size 0.043-0.063 mm).

Characterisation. NMR spectra were recorded at ambient temperature on a BrukerAvance II 400 MHz NMR spectrometer (400/101/376 MHz $^1\text{H}/^{13}\text{C}/^{19}\text{F}$). Chemical shifts (δ) for ^1H and ^{13}C NMR spectra were reported in parts per million (ppm), relative to the residual solvent peak of the respective NMR solvent (CDCl_3 ($\delta_{\text{H}} = 7.26$ and $\delta_{\text{C}} = 77.16$ ppm) or CD_3OD ($\delta_{\text{H}} = 3.31$ and $\delta_{\text{C}} = 49.00$ ppm)). Coupling constants (J) are given in Hertz (Hz), with the multiplicities being denoted as follows: singlet (s), doublet (d), triplet (t), quartet (q), quintet (qi), multiplet (m), broad (br). NMR spectra for ^{13}C and ^{19}F we recorded with decoupling from ^1H . Electrospray ionization–high resolution mass spectrometry (ESI–HRMS) and atmospheric pressure chemical ionization (APCI) for mass spectrometry were recorded on a Waters Micromass Q-Tof micro mass spectrometer.

Elemental analyses were performed by Mikroanalytisches Laboratorium KOLBE (Mülheim an der Ruhr, Germany). Melting points were corrected against benzophenone (melting point 48.0 °C^[2]).

UV-vis spectroscopy. UV-vis absorption measurements were performed on a Probe Drum Lab-in-a-box spectrometer. Samples were contained in a 10 × 10 mm fluorescence quartz cuvette with a screw cap and PTFE septum or a 10 mm absorption quartz cuvette. Furthermore, Varian Cary 50 or Cary 5000 spectrophotometers were used to obtain absorption spectra.

Emission Measurements. Steady-state emission measurements were performed on a Fluorolog-3 (Horiba) fluorimeter with slit widths set to 5 nm spectral resolution.

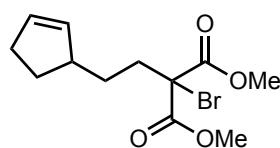
Nanosecond transient absorption measurements. Nanosecond transient absorption measurements were obtained with a LP920-S laser flash photolysis spectrometer (Edinburgh Instruments) equipped with an iStar CCD camera (Andor Technology) for transient spectra and a LP920-K PMT detector connected to a TDS 3052 500 MHz 5 GS/s oscilloscope (Tektronix) for single wavelength kinetics. Probe light was provided by a pulsed XBO 450 W Xenon Arc Lamp (Osram) and samples were excited at 650 nm (for Fe(II)) and 490 nm for Fe(III)) with 8 ns pulses (11.0 ± 0.2 mJ/pulse and 21.6 ± 0.2 mJ/pulse, respectively) provided by a frequency tripled Q-switched Nd:YAG laser (EKSPLA NT342B) combined with an optical parametric oscillator (OPO). Additional nanosecond transient absorption kinetics were obtained with a LKS.60 flash photolysis spectrometer (Applied Photophysics) using a frequency-tripled Nd:YAG laser (Quantel, BrilliantB) with 10 ns pulses at 465 nm (for Fe(II)) or 490 nm (for Fe(III)) at 18.4 ± 0.5 mJ/pulse and 18.2 ± 0.6 mJ/pulse, respectively. Probe light was provided by an unpulsed 150 W Xenon lamp. All measurements were performed at right angle in a 10 × 10 mm quartz cuvette with samples deaerated by purging with Ar (g) and an absorption of around 0.5 at the excitation wavelength.

Femtosecond transient absorption measurements. Fs-TAS was performed probing in the UV-Vis region using a Newport TAS. A Coherent Libra Ti:sapphire amplifier (1.5 mJ, 3kHz, 800 nm, fwhm 40 fs) was used and split into pump and probe beams. Excitation wavelengths of 550 nm (for Fe(III)) and 450 nm (for Fe(II)) were generated by directing the pump beam into the optical parametric amplifiers (TOPAS-Prime and NIRUVVIS, Light Conversion) and then focused and centered on the 1 mm cuvette with a pump power adjusted to 3.05 ± 0.01 mW and 3.10 ± 0.10 mW, respectively. The 800 nm fundamental of the amplifier was focused on a CaF₂ crystal (Crystran), generating the white light supercontinuum probe. A silicon diode array (Newport custom made) was used to record the probe spectrum. A mechanical chopper blocked every other pump pulse, and the transient absorption at each time point was calculated for an

average of 1000 ms chopped/un-chopped pulse pairs. To record the transient absorption spectra at different time points, an optical delay line was used to scan the delay of the probe beam relative to the pump beam from -10.5 ps to 8 ns. A total of ten scans were collected and averaged for each sample. Prior to analysis, the data was corrected for the spectral chirp using Surface Xplorer v4, where single wavelength fits were also performed.

Substrate Synthesis

Dimethyl 2-bromo-2-(2-(cyclopent-2-en-1-yl)ethyl)malonate (**14a**)



(**14a**)

NaH (195 mg, 60 % dispersion in mineral oil, 4.86 mmol, 1.1 equiv.) was washed with dry *n*-hexane (2 × 4 mL) and suspended in dry THF (45 mL) at 0 °C under N₂ (g). To the suspension was added dimethyl 2-(2-(cyclopent-2-en-1-yl)ethyl)malonate^[3] (0.995 g, 4.40 mmol, 1 equiv.) upon which gas evolution occurred. After 10 seconds *N*-bromosuccinimide (955 mg, 5.36 mmol, 1.2 equiv.) was added in one portion. Within 4 min the reaction turned into a light-yellow suspension. After another 10 min, it turned back into a white suspension and was allowed to warm to room temperature. After 2 h the reaction was quenched by addition of water (20 mL) and acidified to pH 2 with hydrochloric acid (aq., 4 %), which caused gas evolution and a transient yellow colour to appear. The mixture was extracted with diethyl ether (3 × 30 mL), washed with brine, dried over MgSO₄ and concentrated *in vacuo*. Silica gel column chromatography (∅ = 5 cm, h = 16 cm, *n*-heptane:EtOAc 10:1) gave the product as a white crystalline solid (718 mg, 54 %).

*R*_f = 0.28 (*n*-heptane:EtOAc, 10:1, visualised with KMnO₄, UV-active). m.p. = 37.7 – 39.2 °C (corrected vs benzophenone) ¹H NMR (400 MHz, CDCl₃) δ (ppm) = 5.75 (dq, *J* = 5.8, 2.3 Hz, 1H, H_{C=C}), 5.64 (dq, *J* = 5.8, 2.1 Hz, 1H, H_{C=C}), 3.82 (s, 6H, H_{MeO}), 2.68 (ddtd, *J* = 10.6, 8.4, 6.2, 2.2 Hz, 1H, H_{CH}), 2.48 – 2.19 (m, 4H, H_{CH₂}), 2.06 (dtd, *J* = 13.2, 8.5, 4.8 Hz, 1H, H_{CH₂}), 1.58 – 1.31 (m, 3H, H_{CH₂}). ¹³C NMR (101 MHz, CDCl₃) δ (ppm) = 167.6 (C_{C=O}), 134.2 (C_{C=C}), 131.3 (C_{C=C}), 63.0 (C_{C-Br}), 54.0 (C_{MeO}), 45.1 (C_{CH}), 36.7 (C_{CH₂}), 32.1 (C_{CH₂}), 31.5 (C_{CH₂}), 29.6 (C_{CH₂}). HRMS (ESI-TOF) calc'd for [C₁₂H₁₇BrO₄+H]⁺ 305.0388; found 305.0380. Elemental analysis (% calc'd, % found for C₁₂H₁₇BrO₄): C (47.23, 47.21), H (5.62, 5.63).

Visible light-mediated ATRA reaction of C₈F₁₇I to 5-hexen-1-ol *via* reductive quenching of [Fe(bt_z)₃](PF₆)₃ (**1**)

Optimisations of the visible light-mediated ATRA reaction of C₈F₁₇I to 5-hexen-1-ol *via* reductive quenching of [Fe(bt_z)₃](PF₆)₃ using the General Procedure

All optimisation reactions were conducted following the General Procedure described in the Experimental section, using 5-hexen-1-ol and perfluorooctyl iodide as starting materials as well as the indicated sacrificial reductants. All equivalent amounts and catalyst loadings were given in relation to the alkene (0.25 mmol) and the reactions were performed in CD₃CN:CD₃OD (4:3) unless otherwise stated.

Table S1: Optimisation of the catalyst loading and control experiments using the General Procedure. 1 equivalent of TEA was used in all reactions. (^atriplicate measurement, ^bduplicate measurement, ^creaction in the dark, heating to 30 °C to simulate generation of heat by light source, ^dnr = no reaction, ^ereaction time given in hours (h), ^fλ = 455 nm, 6.18 W, ^g0.34 equivalents TEA).

Entry	PC	[PC] (mol %)	Sacrificial Reductant	t (min)	NMR yield (%)
1^a	[Fe(bt _z) ₃](PF ₆) ₃	1	TEA	8	>99
2^a	[Fe(bt _z) ₃](PF ₆) ₃	0.75	TEA	10	>99
3^b	[Fe(bt _z) ₃](PF ₆) ₃	0.5	TEA	10	>99
4^b	[Fe(bt _z) ₃](PF ₆) ₃	0.1	TEA	15	90
5^{d,e}	-	-	TEA	65 h ^e	nr ^d
6^f	-	-	Na-(<i>L</i>)-ascorbate	30	>99
7^{c,e}	[Fe(bt _z) ₃](PF ₆) ₃	1	TEA	60 h ^e	nr
8^c	FeBr ₂	1	TEA	24 h ^e	nr
9^g	[Ru(bpy) ₃]Cl ₂ ·6 H ₂ O	0.5	TEA ^f	4	>99

Table S2: Variation of the quenching reagent using the General Procedure (^atriplicate measurement, ^b4-methoxy-*N,N*-diphenylaniline exhibited bad solubility in the solvent mixture.).

Entry	PC	[PC] (mol %)	Sacrificial Reductant	Sacrificial Reductant (equiv.)	t (min)	NMR yield (%)
1^a	[Fe(bt _z) ₃](PF ₆) ₃	0.5	TEA	1	10	>99
2^a	[Fe(bt _z) ₃](PF ₆) ₃	0.5	TEA	0.34	10	>99
3	[Fe(bt _z) ₃](PF ₆) ₃	1	Na-(<i>L</i>)-ascorbate	1	30	82
4^b	[Fe(bt _z) ₃](PF ₆) ₃	0.5	4-methoxy- <i>N,N</i> -diphenylaniline	1 ^b	15	nr
5^b	[Fe(bt _z) ₃](PF ₆) ₃	0.5	4-methoxy- <i>N,N</i> -diphenylaniline	0.34 ^b	15	nr

Sodium-(*L*)-ascorbate was explored as a quenching reagent, but only 82 % conversion was achieved within 0.5 h. An amine donor with suitable solubility properties that does not harbour any α -hydrogens could have aided in eliminating any possible side reactions caused by amine radical cation decomposition via abstraction of a proton and resulting iminium ion formation^[4]. However, use of the electron-rich triarylamine 4-methoxy-*N,N*-diphenylaniline led to no conversion even after 2 h. This is likely due to the charge separation being outpaced by geminate recombination. In contrast, sacrificial electron donors with α -hydrogens such as TEA undergo decomposition processes following the quenching event counteracting charge recombination. (**Table S2**)

Table S3: Optimisation of the amount of TEA using the General Procedure and a catalyst loading of 0.5 mol% (^aduplicate measurement, ^btriplicate measurement, ^cProlongation of the reaction time to 55 min afforded an NMR yield of 55 %).

Entry	PC	[PC] (mol%)	Sacrificial Reductant	TEA (equiv.)	t (min)	NMR yield (%)
1 ^a	[Fe(bt _z) ₃](PF ₆) ₃	0.5	TEA	1	10	>99
2 ^b	[Fe(bt _z) ₃](PF ₆) ₃	0.5	TEA	0.75	10	>99
3 ^b	[Fe(bt _z) ₃](PF ₆) ₃	0.5	TEA	0.5	10	>99
4 ^a	[Fe(bt _z) ₃](PF ₆) ₃	0.5	TEA	0.34	10	>99
5 ^c	[Fe(bt _z) ₃](PF ₆) ₃	0.5	TEA	0.1	10	50 ^c

Table S4: Optimisation of the amount of C₈F₁₇I using the General Procedure and a catalyst loading of 0.5 mol% (^a0.34 equiv. of TEA, ^bProlongation of the reaction time to 25 min did not increase the NMR yield).

Entry	PC	[PC] (mol%)	Sacrificial Reductant ^a	C ₈ F ₁₇ I (equiv.)	t (min)	NMR yield (%)
1	[Fe(bt _z) ₃](PF ₆) ₃	0.5	TEA	1.33	10	>99
2	[Fe(bt _z) ₃](PF ₆) ₃	0.5	TEA	1.0	10	85 ^b

Control Experiments for the visible light-mediated ATRA reaction of perfluorooctyl iodide to 5-hexen-1-ol in presence of TEA using different Fe-catalysts

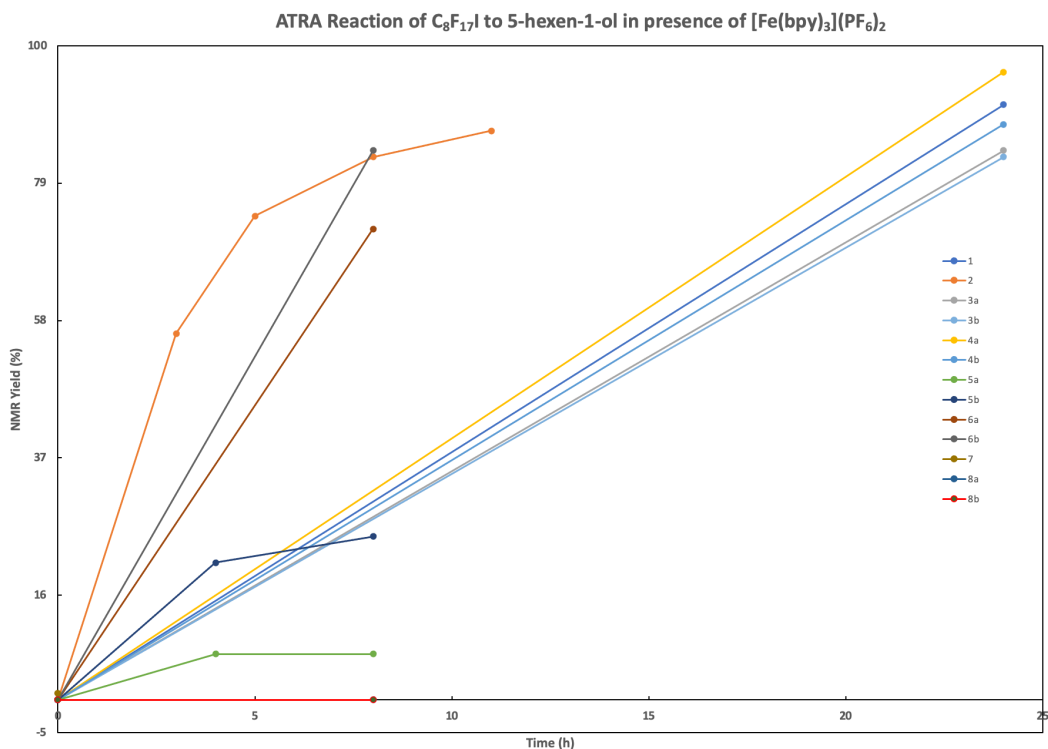


Figure S1: ATRA reaction of perfluorooctyl iodide to 5-hexen-1-ol in the presence of TEA and $[Fe(bpy)_3](PF_6)_2$ (a and b denote duplicate reactions run in parallel); Reaction conditions: 5-hexen-1-ol (0.25 mmol), $C_8F_{17}I$ (0.33 mmol), TEA (0.085 mmol), $[Fe(bpy)_3](PF_6)_2$ (1 mol%) in $CD_3CN:CD_3OD$ (4:3, 3.5 mL), mesitylene (30 μ L, internal standard), $\lambda = 530$ nm.

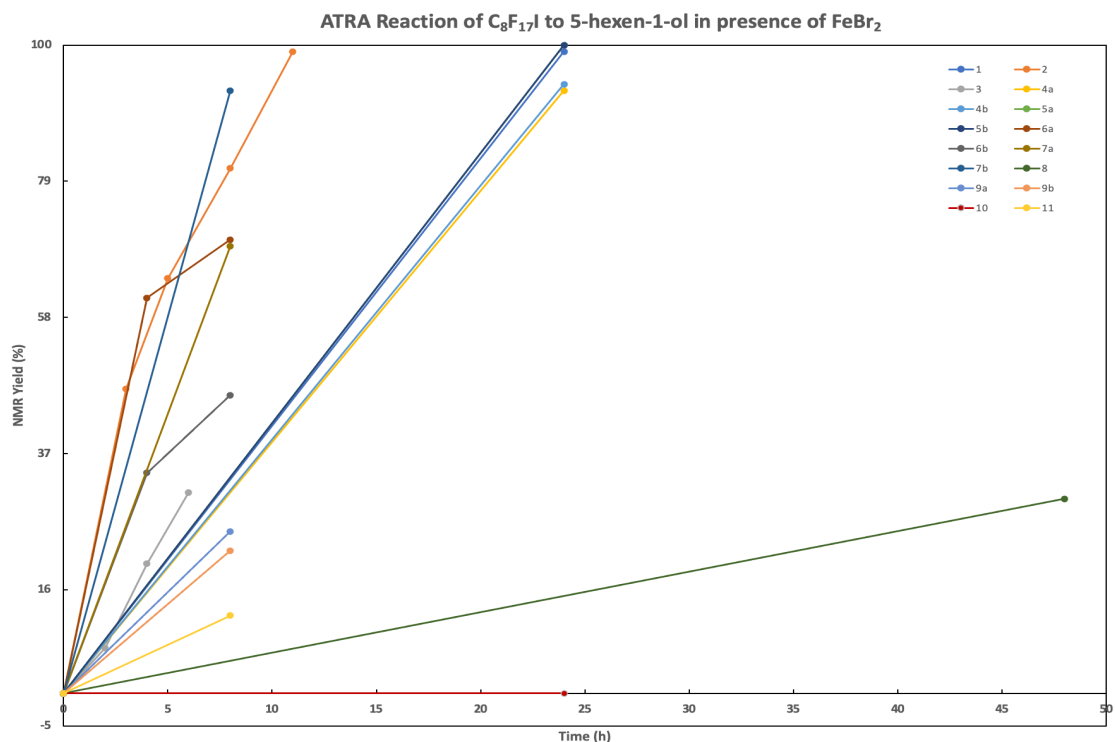


Figure S2: ATRA reaction of perfluorooctyl iodide to 5-hexen-1-ol in the presence of TEA and $FeBr_2$ (a and b denote duplicate reactions run in parallel); Reaction conditions: 5-hexen-1-ol (0.25 mmol), $C_8F_{17}I$ (0.33 mmol), TEA (0.085 mmol), $FeBr_2$ (1 mol%) in $CD_3CN:CD_3OD$ (4:3, 3.5 mL), mesitylene (30 μ L, internal standard), $\lambda = 530$ nm

An array of control reactions was conducted employing different iron compounds such as FeBr₂, FeBr₃ and [Fe(bpy)₃](PF₆)₂ as well as reactions using no catalyst and without irradiation (**Table S1, Entries 6 & 7**). The absence of either catalyst or irradiation both resulted in a lack of conversion of the starting material, even upon prolonging the reaction time to 65 and 60 h respectively. When investigating the efficiency of different iron-based catalysts in the reaction system, particularly in case of FeBr₂ and [Fe(bpy)₃](PF₆)₂, a large variety of differing results was obtained (**Figure S1 & S2**). The reaction times varied from 8–48 h, vastly exceeding the timescale of 10 min for the model reaction using **1** as the photocatalyst, and highly inconsistent yields were afforded, ranging from no conversion to full conversion. Furthermore, it was observed that in some instances the reactions would fail to reach full conversion even upon extended irradiation. The reasons for these inconsistencies could be manifold, ranging from solubility issues to a general lack of robustness of the reaction system. When using FeBr₃ as a catalyst, no conversion occurred even after 48 h of irradiation.

Screening of different alkyl halides for the visible light-mediated ATRA reaction to 5-hexen-1-ol *via* reductive quenching of $[\text{Fe}(\text{btz})_3](\text{PF}_6)_3$ using the General Procedure

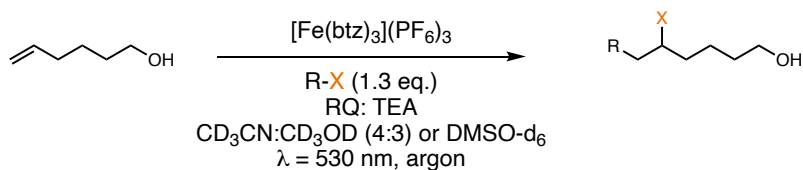


Figure S3: ATRA reaction to 5-hexen-1-ol – Screening of different alkyl halides.

Table S5: Screening of different alkyl halides using the General Procedure (^areaction time in hours (h)).

Entry	R-X	[PC] (mol%)	RQ	t (min)	NMR yield (%)	Additives/Solvents
1 ^a		1	Na-(L)-ascorbate (0.34 eq.)	14 h ^a	nr	$\text{CD}_3\text{CN}:\text{CD}_3\text{OD}$
2		0.5	TEA (0.34 eq.)	45	nr	$\text{CD}_3\text{CN}:\text{CD}_3\text{OD}$
3		0.5	TEA (0.34 eq.)	30	nr	DMSO-d_6
4		0.5	TEA (0.34 eq.)	30	nr	2 equiv. LiBr/ DMSO-d_6
5		0.5	TEA (0.34 eq.)	45	nr	$\text{CD}_3\text{CN}:\text{CD}_3\text{OD}$
6		0.5	TEA (0.34 eq.)	30	nr	DMSO-d_6
7	$\text{C}_8\text{F}_{17}\text{I}$	0.5	TEA (0.34 equiv.)	15	>99	$\text{CD}_3\text{CN}:\text{CD}_3\text{OD}$
8		0.5	TEA (0.34 equiv.)	15	nr	$\text{CD}_3\text{CN}:\text{CD}_3\text{OD}$
9 ^a	$\text{C}_8\text{F}_{17}\text{Br}$	1	TEA (1 equiv.)	24 h ^a	nr	$\text{CD}_3\text{CN}:\text{CD}_3\text{OD}$
10	CBrCl_3	0.5	TEA (0.34 equiv.)	30	48	$\text{CD}_3\text{CN}:\text{CD}_3\text{OD}$

Scope limitations of the visible light-mediated ATRA reaction *via* reductive quenching of $[\text{Fe}(\text{btz})_3](\text{PF}_6)_3$ using the General Procedure

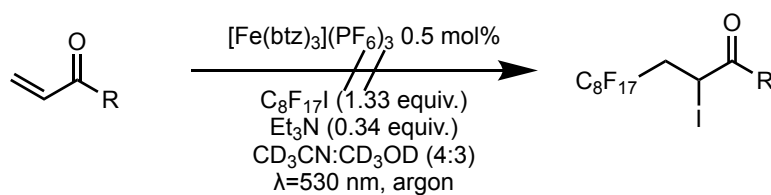


Table S6: ATRA reaction (RQ) using Michael Acceptors as substrates.

Entry	Alkene	NMR yield (%)
1		<5
2		<5

Synthesis and Isolation of the addition of alkyl halides to alkenes and alkynes using Procedure A

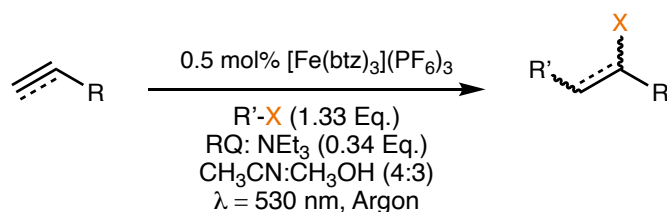
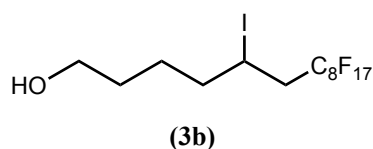


Figure S4: General reaction scheme for the reductively quenched ATRA catalyzed by [Fe(btz)₃](PF₆)₃ (**1**) using Procedure A (see Experimental Section).

The following reactions were performed following Procedure A (see Experimental Section) unless otherwise stated.

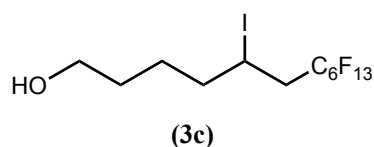
5-Iodo-6-perfluorooctylhexanol (**3b**)



The reaction mixture was prepared according to Procedure A using 5-hexen-1-ol (30.0 μL, 0.25 mmol, 1 equiv.) and perfluorooctyl iodide (88 μL, 0.33 mmol, 1.33 equiv.) and illuminated for 10 min at 530 nm. Purification by silica gel column chromatography (16.5 × 3.5 cm, PE:EtOAc 5:1) afforded the product as a colourless oil, which solidified upon standing to give a white wax-like solid (**3b**) (587 mg, 91 %, over 4 batches). NMR-spectroscopic data was in accordance with literature.^[5]

$R_f = 0.29$ (EtOAc:PE, 1:4 v/v, visualised with KMnO₄, UV-active). ¹H NMR (400 MHz, CDCl₃) δ (ppm) = 4.32 (tt, $J = 8.7, 4.8$ Hz, 1H), 3.65 (t, $J = 5.9$ Hz, 2H), 2.84 (dddd, $J = 57.9, 27.6, 15.8, 7.0$ Hz, 2H), 1.81 (pd, $J = 9.7, 4.4$ Hz, 2H), 1.70 – 1.57 (m, 3H), 1.55 – 1.42 (m, 1H). ¹³C NMR (101 MHz, CDCl₃): δ (ppm) = 121.9 – 104.8 (m), 62.31, 41.65 (t, $J = 20.8$ Hz), 40.0, 31.5, 26.0, 20.4. ¹⁹F NMR (376 MHz, CDCl₃): δ (ppm) = -80.3 (t, $J = 10.1$ Hz), -109.9 – -112.1 (m), -113.0 – -115.0 (m), -120.5 – -121.0 (m), -121.2 (m), -121.7 – -122.4 (m), -122.6 – -123.0 (m), -124.8 – -126.7 (m). ESI-HRMS calculated $m/z = 680.9350$, found $m/z = 680.9366$ for [C₁₄H₁₂F₁₇IO + Cl]⁻. Elemental analysis for C₁₄H₁₂F₁₇IO (% calc'd, % found): C (26.02, 25.73), H (1.87, 2.01).

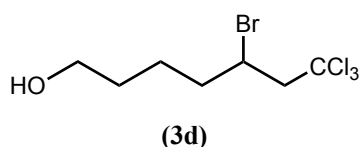
5-Iodo-6-perfluorohexylhexanol (**3c**)



The reaction mixture was prepared according to Procedure A using 5-hexen-1-ol (30.0 μ L, 0.25 mmol, 1 equiv.) and perfluorohexyl iodide (111 μ L, 0.33 mmol, 1.33 equiv.) and illuminated for 10 min at 530 nm. Purification by silica gel column chromatography (16 \times 2.5 cm, *n*-heptane:EtOAc, 4:1) afforded the product as a colourless oil (**3c**) (127 mg, 93 %). NMR-spectroscopic data was in accordance with literature.^[5]

$R_f = 0.3$ (*n*-heptane:EtOAc, 3:1 v/v, visualised with UV). ^1H NMR (400 MHz, CDCl_3): δ (ppm) = 4.34 (tdd, $J = 8.4, 5.5, 4.4$ Hz, 1H), 3.73 – 3.62 (m, 2H), 3.02 – 2.83 (m, 1H), 2.86 – 2.68 (m, 1H), 1.94 – 1.73 (m, 2H), 1.74 – 1.50 (m, 4H). ^{13}C NMR (101 MHz, CDCl_3): δ (ppm) = 122.9 – 105.7 (m), 62.6, 41.80 (t, $J = 20.9$ Hz), 40.2, 31.7, 26.2, 20.6. ^{19}F NMR (376 MHz, CDCl_3): δ (ppm) = -80.9 (tt, $J = 10.1, 2.6$ Hz), -109.9 – -112.7 (m), -113.4 – -116.1 (m), -121.2 – -122.3 (m), -122.4 – -123.4 (m), -123.5 – -123.7 (m), -125.6 – -126.6 (m). ESI-HRMS calculated $m/z = 580.9414$, found $m/z = 580.9413$ for $[\text{C}_{12}\text{H}_{12}\text{F}_{13}\text{IO} + \text{Cl}]^-$. Elemental analysis for $\text{C}_{12}\text{H}_{12}\text{F}_{13}\text{IO}$ (% calc'd, % found): C (26.39, 26.23), H (2.21, 2.28).

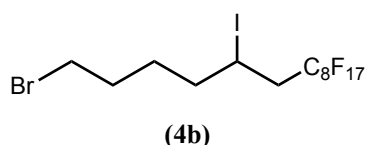
5-bromo-7,7,7-trichloroheptan-1-ol (**3d**)



The reaction mixture was prepared according to Procedure A using 5-hexen-1-ol (30.0 μ L, 0.25 mmol, 1 equiv.) and CBrCl_3 (32.5 μ L, 0.33 mmol, 1.33 equiv.) and illuminated for 60 min at 530 nm. Purification by silica gel column chromatography (24 \times 2.5 cm, DCM:EtOAc, 24:1) afforded the product as a colourless oil (**3d**) (162 mg, 43 %, over 5 batches).

$R_f = 0.46$ (DCM:EtOAc, 24:1 v/v, visualised with KMnO_4). ^1H NMR (400 MHz, CDCl_3): δ (ppm) = 4.31 (dtd, $J = 9.4, 5.2, 4.3$ Hz, 1H), 3.68 – 3.61 (m, 2H), 3.44 (dd, $J = 15.8, 5.0$ Hz, 1H), 3.21 (dd, $J = 15.8, 5.3$ Hz, 1H), 2.12 – 1.88 (m, 2H), 1.77 – 1.47 (m, 4H). ^{13}C NMR (101 MHz, CDCl_3): δ (ppm) = 97.2, 62.7 (d, $J = 7.6$ Hz), 49.0, 39.3, 31.8, 23.8. ESI-HRMS calculated $m/z = 330.8826$, found $m/z = 330.8825$ for $[\text{C}_7\text{H}_{12}\text{BrCl}_3\text{O} + \text{Cl}]^-$. Elemental analysis for $\text{C}_7\text{H}_{12}\text{BrCl}_3\text{O}$ (% calc'd, % found): C (28.17, 28.06), H (4.05, 4.09).

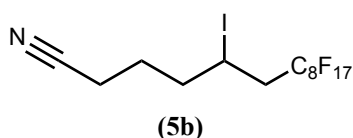
1-bromo-5-iodo-6-perfluorooctylhexane (**4b**)



The reaction mixture was prepared according to Procedure A using 6-bromo-1-hexene (33.4 μL , 0.25 mmol, 1 equiv.) and perfluorooctyl iodide (88 μL , 0.33 mmol, 1.33 equiv.) and illuminated for 10 min at 530 nm. Purification by silica gel column chromatography (25 \times 3.5 cm, PE) afforded the product (**4b**) as a colourless oil, which solidified upon standing to give a wax-like solid (478 mg, 90 %, over 3 batches). NMR-spectroscopic data was in accordance with literature.^[5]

R_f = 0.42 (PE, visualised with KMnO_4). ^1H NMR (400 MHz, CDCl_3): δ (ppm) = 4.33 (tdd, J = 8.4, 5.4, 4.2 Hz, 1H), 3.43 (t, J = 6.8 Hz, 2H), 3.04 – 2.85 (m, 1H), 2.85 – 2.68 (m, 1H), 2.02 – 1.66 (m, 5H), 1.66 – 1.51 (m, 1H). ^{13}C NMR (101 MHz, CDCl_3): δ (ppm) = 125.3 – 104.0 (m), 41.9 (t, J = 20.9 Hz), 39.5, 33.1, 31.7, 28.5, 20.0. ^{19}F NMR (376 MHz, CDCl_3): δ (ppm) = -81.0 (t, J = 10.0 Hz), -109.7 – -112.7 (m), -114.2 – -115.3 (m), -121.5 – -122.3 (m), -122.6 – -123.2 (m), -123.3 – -124.0 (m), -126.2 – -126.4 (m). ESI-HRMS calculated m/z = 742.8506, found m/z = 742.8505 for $[\text{C}_{14}\text{H}_{11}\text{BrF}_{17}\text{I} + \text{Cl}]^-$. Elemental analysis for $\text{C}_{14}\text{H}_{11}\text{BrF}_{17}\text{I}$ (% calc'd, % found): C (23.72, 23.79), H (1.56, 1.55).

5-iodo-6-perfluorooctylhexanenitrile (**5b**)

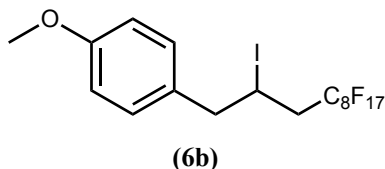


The reaction mixture was prepared according to Procedure A using 5-hexanenitrile (28.4 μL , 0.25 mmol, 1 equiv.) and perfluorooctyl iodide (88 μL , 0.33 mmol, 1.33 equiv.) and illuminated for 40 min at 530 nm. Purification by silica gel column chromatography (20 \times 3.5 cm, PE:Et₂O 9:1) afforded the product (**5b**) as a colourless to slightly red oil, which solidified upon standing (478 mg, 76 %, over 4 batches). NMR-spectroscopic data was in accordance with literature.^[5]

R_f = 0.22 (PE:Et₂O, 9:1 v/v, visualised with UV/ KMnO_4). ^1H NMR (400 MHz, CDCl_3): δ (ppm) = 4.36 – 4.25 (m, 1H), 3.05 – 2.68 (m, 2H), 2.51 – 2.34 (m, 2H), 2.06 – 1.89 (m, 3H), 1.90 – 1.74 (m, 1H). ^{13}C NMR (101 MHz, CDCl_3): δ (ppm) = 123.5 – 104.6 (m), 118.9, 41.8 (t, J = 21.0 Hz), 38.9, 26.0, 18.1, 16.5. ^{19}F NMR (376 MHz, CDCl_3): δ (ppm) = -81.0, -111.1 – -112.1 (m), -113.8 – -115.7 (m), -121.3 – -122.4 (m), -121.75 – -122.06 (m), -122.53 – -

122.88 (m), -123.5 – -123.7 (m), -126.1 – -126.4 (m). ESI-HRMS calculated $m/z = 675.9197$, found $m/z = 675.9190$ for $[C_{14}H_9F_{17}IN + Cl]^-$. Elemental analysis for $C_{14}H_9F_{17}IN$ (% calc'd, % found): C (26.23, 26.28), H (1.42, 1.41), N(2.18, 2.16).

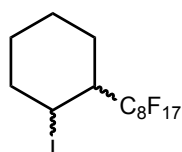
4-(2-iodo-3-perfluorooctyl-propyl)-anisole (**6b**)



The reaction mixture was prepared according to Procedure A using 4-allyl-anisole (38.4 μ L, 0.25 mmol, 1 equiv.) and perfluorooctyl iodide (88 μ L, 0.33 mmol, 1.33 equiv.) and illuminated for 40 min at 530 nm. Purification by silica gel column chromatography (20 \times 3.5 cm, PE) afforded the product (**6b**) as a white solid (478 mg, 76 %, over 4 batches).

$R_f = 0.55$ (PE, visualised with UV/ $KMnO_4$). 1H NMR (400 MHz, $CDCl_3$): δ (ppm) = 7.16 – 7.08 (m, 2H), 6.92 – 6.84 (m, 2H), 4.42 (dq, $J = 8.5, 6.4$ Hz, 1H), 3.81 (s, 3H), 3.19 (qd, $J = 14.7, 7.2$ Hz, 2H), 2.97 – 2.74 (m, 2H). ^{13}C NMR (101 MHz, $CDCl_3$): δ (ppm) = 159.0, 130.8, 130.2, 119.6 – 108.0 (m), 114.1, 55.4, 46.4, 40.8 (t, $J = 20.9$ Hz), 20.4. ^{19}F NMR (376 MHz, $CDCl_3$): δ (ppm) = -80.8 (t, $J = 10.1$ Hz), -111.1 – -112.7 (m), -113.4 (t, $J = 14.3$ Hz), -114.1 (t, $J = 14.1$ Hz), -121.4 – -122.1 (m), -122.6 – -122.9 (m), -123.5 – -123.7 (m), -126.2 (dpd, $J = 14.0, 6.8, 3.0$ Hz). ESI-HRMS calculated $m/z = 728.9350$, found $m/z = 728.9368$ for $[C_{18}H_{12}F_{17}IO + Cl]^-$. Elemental analysis for $C_{18}H_{12}F_{17}IO$ (% calc'd, % found): C(31.14, 31.09), H(1.74, 1.68)

1-perfluorooctyl-2-iodo-cyclohexane (**7b**, **7c**)



cis (**7b**), *trans* (**7c**)

The reaction mixture was prepared according to Procedure A using cyclohexene¹ (25.3 μ L, 0.25 mmol, 1 equiv.) and perfluorooctyl iodide (88 μ L, 0.33 mmol, 1.33 equiv.) and illuminated for 15 min at 530 nm. Purification by silica gel column chromatography (20 \times 2.5 cm, *n*-heptane) afforded diastereomer (**7b**) as a colourless, slightly waxy solid (78 mg, 17 %, over 3 batches) and diastereomer (**7c**) as a colourless oil (25 mg, 5 %, over 3 batches). NMR-spectroscopic data was in accordance with literature.^[6]

¹ The starting material was added after degassing of the reaction solution with Argon due to its high volatility.

cis-Isomer (**7b**):

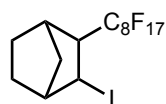
$R_f = 0.49$ (*n*-heptane, visualised with KMnO_4). ^1H NMR (400 MHz, CDCl_3): δ (ppm) = 4.75 – 4.69 (m, 1H), 2.22 (ddt, $J = 14.3, 5.9, 3.1$ Hz, 1H), 2.01 – 1.75 (m, 5H), 1.78 – 1.60 (m, 2H), 1.40 (tt, $J = 14.0, 9.9, 8.6, 3.6$ Hz, 1H). ^{13}C NMR (101 MHz, CDCl_3): δ (ppm) = 119.7 – 107.2 (m), 44.6 (t, $J = 20.8$ Hz), 37.5, 27.6 (t, $J = 4.7$ Hz), 25.3, 22.9 (q, $J = 3.7$ Hz), 22.2.

^{19}F NMR (376 MHz, CDCl_3): δ (ppm) = -80.9 (t, $J = 10.0$ Hz), -117.7 (tdq, $J = 16.5, 11.4, 6.3, 4.8$ Hz), -119.9 – -120.5 (m), -120.9 – -121.3 (m), -121.5 – -122.2 (m), -122.7 – -122.9 (m), -126.1 – -126.4 (m). APCI-HRMS calculated $m/z = 501.0511$, found $m/z = 501.0497$ for $[\text{C}_{14}\text{H}_{10}\text{F}_{17} - \text{I}]^+$. Elemental analysis for $\text{C}_{14}\text{H}_{10}\text{F}_{17}\text{I}$ (% calc'd, % found): C (26.77, 26.79), H (1.60, 1.59).

trans-Isomer (**7c**):

$R_f = 0.69$ (*n*-heptane, visualised with KMnO_4). ^1H NMR (400 MHz, CDCl_3): δ (ppm) = 4.97 (q, $J = 4.0$ Hz, 1H), 2.77 – 2.62 (m, 1H), 2.20 (dq, $J = 14.9, 7.1$ Hz, 1H), 2.01 (dq, $J = 15.3, 4.2$ Hz, 1H), 1.90 (tt, $J = 12.9, 3.2$ Hz, 2H), 1.80 – 1.72 (m, 1H), 1.60 (dq, $J = 14.9, 5.9, 5.0$ Hz, 3H). ^{13}C NMR (101 MHz, CDCl_3): δ (ppm) = 119.7 – 106.6 (m), 45.2 (t, $J = 19.4$ Hz), 34.9, 25.4, 22.8, 22.0, 21.5. ^{19}F NMR (376 MHz, CDCl_3): δ (ppm) = -80.8 (t, $J = 10.0$ Hz), -107.5 – -113.5 (m), -119.8, -120.4 – -120.7 (m), -121.0 (dq, $J = 22.3, 12.1, 9.1$ Hz), -121.3 – -122.1 (m), -122.6 – -122.9 (m), -126.1 (tp, $J = 21.1, 7.7, 6.8$ Hz). APCI-HRMS calculated $m/z = 501.0511$, found $m/z = 501.0511$ for $[\text{C}_{14}\text{H}_{10}\text{F}_{17} - \text{I}]^+$. Elemental analysis for $\text{C}_{14}\text{H}_{10}\text{F}_{17}\text{I}$ (% calc'd, % found): C (26.77, 26.71), H (1.60, 1.57).

2-Iodo-3-perfluorooctylnorbornane (**8b**)



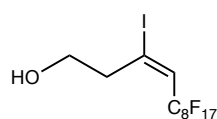
(**8b**)

The reaction mixture was prepared according to Procedure A using norbornene (23.5 μL , 0.25 mmol, 1 equiv.) and perfluorooctyl iodide (88 μL , 0.33 mmol, 1.33 equiv.) and illuminated for 15 min at 530 nm. Purification by silica gel column chromatography (15 \times 2.5 cm, *n*-heptane) afforded the product as a colourless oil, which solidified upon standing to give a colourless wax-like solid (**8b**) (256 mg, 80 %, over 2 batches). NMR-spectroscopic data was in accordance with literature.^[6]

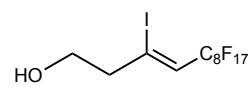
$R_f = 0.60$ (*n*-heptane, visualised with KMnO_4). ^1H NMR (400 MHz, CDCl_3): δ (ppm) = 4.31 (ddd, $J = 6.0, 3.8, 2.1$ Hz, 1H), 2.50 (d, $J = 4.2$ Hz, 1H), 2.46 – 2.30 (m, 2H), 1.96 – 1.84 (m, 1H), 1.76 – 1.55 (m, 3H), 1.38 – 1.20 (m, 2H). ^{13}C NMR (101 MHz, CDCl_3): δ (ppm) = 122.6

- 106.0 (m), 55.8 (dd, $J = 21.7, 19.0$ Hz), 44.7, 38.0, 35.2 (d, $J = 2.2$ Hz), 29.9, 27.6, 26.1 (t, $J = 3.4$ Hz). ^{19}F NMR (376 MHz, CDCl_3): δ (ppm) = -80.9 (tt, $J = 9.9, 2.4$ Hz), -115.2 (ddq, $J = 25.2, 15.2, 4.7$ Hz), -116.0 (tdt, $J = 18.3, 9.1, 4.7$ Hz), -118.6 (dtt, $J = 12.3, 8.1, 4.3$ Hz), -119.3 (qt, $J = 12.3, 4.2$ Hz), -120.7 – -121.0 (m), -121.6 – -122.1 (m), -122.6 – -122.9 (m), -126.2 (ddp, $J = 17.4, 10.8, 3.6$ Hz). APCI-HRMS calculated $m/z = 513.0511$, found $m/z = 513.0507$ for $[\text{C}_{15}\text{H}_{10}\text{F}_{17} - \text{I}]^+$. Elemental analysis for $\text{C}_{15}\text{H}_{10}\text{F}_{17}\text{I}$ (% calc'd, % found): C (28.15, 28.18), H (1.57, 1.55).

3-iodo-4-perfluorooctyl-but-3-en-1-ol (**9b**, **9c**)



(9b)



(9c)

The reaction mixture was prepared according to Procedure A using 3-butyn-1-ol (19.0 μL , 0.25 mmol, 1 equiv.) and perfluorooctyl iodide (88 μL , 0.33 mmol, 1.33 equiv.) and illuminated for 20 min at 530 nm. Purification by silica gel column chromatography (21 \times 3.5 cm, PE:EtOAc, 9:1) afforded the two separate stereoisomers as waxy white solids (over 5 batches: Isomer **9b**: 323 mg, 42 %, Isomer **9c**: 154 mg, 20 %). NMR-spectroscopic data was in accordance with literature.^[5]

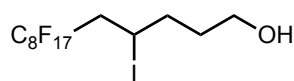
E-Isomer (**9b**):

$R_f = 0.50$ (PE:EtOAc, 9:1 v/v, visualised with KMnO_4). ^1H NMR (400 MHz, CDCl_3): δ (ppm) = 6.49 (t, $J = 14.3$ Hz, 1H), 3.87 (t, $J = 6.3$ Hz, 2H), 2.94 (ddt, $J = 8.0, 6.4, 1.6$ Hz, 2H). ^{13}C NMR (101 MHz, CDCl_3): δ (ppm) = 129.2 (t, $J = 23.8$ Hz), 117.6 – 104.0 (m), 62.0, 43.8. ^{19}F NMR (376 MHz, CDCl_3): δ (ppm) = -80.8 (t, $J = 9.9$ Hz), -105.0 (tt, $J = 12.6, 3.5$ Hz), -121.1 – -122.2 (m), -122.4 – -123.4 (m), -126.0 – -126.3 (m). ESI-HRMS calculated $m/z = 650.8880$, found $m/z = 650.8887$ for $[\text{C}_{12}\text{H}_6\text{F}_{17}\text{IO} + \text{Cl}]^-$. Elemental analysis for $\text{C}_{12}\text{H}_6\text{F}_{17}\text{IO}$ (% calc'd, % found): C (23.40, 23.39), H (0.98, 0.99).

Z-Isomer (**9c**):

$R_f = 0.19$ (PE:EtOAc, 9:1 v/v, visualised with KMnO_4). ^1H NMR (400 MHz, CDCl_3): δ (ppm) = 6.41 (t, $J = 13.0$ Hz, 1H), 3.85 (t, $J = 5.8$ Hz, 2H), 2.92 (tq, $J = 5.8, 1.8$ Hz, 2H). ^{13}C NMR (101 MHz, CDCl_3): δ (ppm) = 124.5 (t, $J = 23.8$ Hz), 121.6 – 105.9 (m), 60.8, 51.1. ^{19}F NMR (376 MHz, CDCl_3): δ (ppm) = -80.8 (t, $J = 9.9$ Hz), -108.8 (td, $J = 15.9, 14.7, 4.0$ Hz), -121.4 – -121.6 (m), -121.69 – -122.1 (m), -122.6 – -123.0 (m), -126.1 – -126.3 (m). ESI-HRMS calculated $m/z = 650.8880$, found $m/z = 650.8896$ for $[\text{C}_{12}\text{H}_6\text{F}_{17}\text{IO} + \text{Cl}]^-$. Elemental analysis for $\text{C}_{12}\text{H}_6\text{F}_{17}\text{IO}$ (% calc'd, % found): C (23.40, 23.52), H (0.98, 1.05).

5-Iodo-6-perfluorooctylpentanol (**10b**)

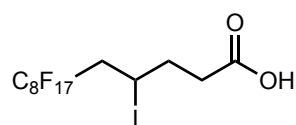


(**10b**)

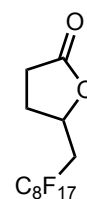
The reaction mixture was prepared according to Procedure A using 4-penten-1-ol (25.8 μ L, 0.25 mmol, 1 equiv.) and perfluorooctyl iodide (88 μ L, 0.33 mmol, 1.33 equiv.) and illuminated for 10 min at 530 nm. Purification by silica gel column chromatography (15 x 2.5 cm, *n*-heptane:EtOAc, 5:1) afforded the product as a colourless oil, which solidified upon standing to give a white wax-like solid (**10b**) (147 mg, 93 %). NMR-spectroscopic data was in accordance with literature.^[5]

$R_f = 0.27$ (*n*-heptane:EtOAc, 5:1 v/v, visualised with UV/KMnO₄). ¹H NMR (400 MHz, CDCl₃): δ (ppm) = 4.37 (tt, $J = 8.1, 5.4$ Hz, 1H), 3.70 (t, $J = 6.2$ Hz, 2H), 3.04 – 2.82 (m, 1H), 2.86 – 2.69 (m, 1H), 2.01 – 1.86 (m, 2H), 1.90 – 1.76 (m, 1H), 1.76 – 1.61 (m, 1H). ¹³C NMR (101 MHz, CDCl₃): δ (ppm) = 120.6 – 108.2 (m), 61.8, 41.8 (t, $J = 20.8$ Hz), 37.0, 32.8, 20.4. ¹⁹F NMR (376 MHz, CDCl₃): δ (ppm) = -80.6 – -81.2 (m), -111.5 (tt, $J = 14.8, 3.6$ Hz), -112.21 (ddt, $J = 18.4, 14.8, 3.7$ Hz), -114.3 (tt, $J = 14.1, 3.2$ Hz), -115.0 (td, $J = 13.5, 6.9$ Hz), -121.4 – -122.2 (m), -122.6 – -123.0 (m), -123.5 – -123.8 (m), -126.1 – -126.4 (m). ESI-HRMS calculated $m/z = 666.9193$, found $m/z = 666.9202$ for [C₁₃H₁₀F₁₇IO + Cl]⁻. Elemental analysis for C₁₃H₁₀F₁₇IO (% calc'd, % found): C (24.70, 24.76), H (1.59, 1.61)

5-iodo-6-perfluorooctylpentenoic acid (**11b**) and 5-(2,2,3,3,4,4,5,5,6,6,7,7,8,8,9,9,9-heptafluorononyl)dihydro-2(3*H*)-Furanone (**11c**)



(**11b**)



(**11c**)

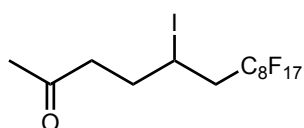
The reaction mixture was prepared according to Procedure A using 4-pentenoic acid (25.5 μ L, 0.25 mmol, 1 equiv.) and perfluorooctyl iodide (88 μ L, 0.33 mmol, 1.33 equiv.) and illuminated for 30 min at 530 nm. Purification by silica gel column chromatography (20 x 2.5 cm, DCM \rightarrow DCM:EtOAc 4:1, 1 % AcOH) afforded two products as white solids ((**11b**): 139 mg, 43 %, (**11c**): 83 mg, 26 %). NMR-spectroscopic data for both products was in accordance with literature.^[7]

(11b):

$R_f = 0.38$ (DCM:EtOAc, 4:1 + 1 % AcOH, v/v, visualised with KMnO_4). $^1\text{H NMR}$ (400 MHz, CDCl_3): δ (ppm) = 4.45 – 4.34 (m, 1H), 3.08 – 2.87 (m, 1H), 2.79 (ddd, $J = 33.5, 15.3, 7.4$ Hz, 1H), 2.72 – 2.60 (m, 1H), 2.60 – 2.52 (m, 1H), 2.26 – 2.13 (m, 1H), 2.13 – 2.00 (m, 1H). $^{13}\text{C NMR}$ (101 MHz, CDCl_3): δ (ppm) = 178.5, 122.3 – 105.7 (m), 41.8 (t, $J = 20.9$ Hz), 34.9, 34.4, 18.7. $^{19}\text{F NMR}$ (376 MHz, CDCl_3): δ (ppm) = -81.0 (t, $J = 10.0$ Hz), -111.2 (tt, $J = 14.8, 3.7$ Hz), -111.7 – -112.0 (m), -114.2 (t, $J = 13.8$ Hz), -114.8 – -115.0 (m), -121.5 – -122.2 (m), -122.8 (ddtt, $J = 22.1, 17.3, 10.9, 6.3$ Hz), -123.5 – -123.8 (m), -126.3 (tq, $J = 11.4, 5.5$ Hz). ESI-HRMS calculated $m/z = 680.8986$, found $m/z = 680.8997$ for $[\text{C}_{13}\text{H}_{18}\text{F}_{13}\text{IO}_2 + \text{Cl}]^-$. Elemental analysis for $\text{C}_{13}\text{H}_8\text{F}_{17}\text{IO}_2$ (% calc'd, % found): C (24.17, 24.17), H (1.25, 1.26).

(11c):

$R_f = 0.30$ (DCM, visualised with UV/ KMnO_4). $^1\text{H NMR}$ (400 MHz, CDCl_3): δ (ppm) = 4.87 (dq, $J = 8.3, 6.1$ Hz, 1H), 2.80 – 2.45 (m, 5H), 2.44 – 2.31 (m, 1H), 2.05 (dq, $J = 12.7, 9.3$ Hz, 1H). $^{13}\text{C NMR}$ (101 MHz, CDCl_3): δ (ppm) = 175.6, 122.4 – 105.5 (m), 74.5 – 71.1 (m), 36.6 (t, $J = 21.2$ Hz), 28.8, 28.2. $^{19}\text{F NMR}$ (376 MHz, CDCl_3): δ (ppm) = -81.0 (t, $J = 10.1$ Hz), -112.8 (tq, $J = 10.8, 3.5$ Hz), -121.4 – -123.1 (m), -123.1 – -123.8 (m), -126.3 (tt, $J = 14.3, 6.9, 2.8$ Hz). ESI-HRMS calculated $m/z = 552.9863$, found $m/z = 552.9861$ for $[\text{C}_{13}\text{H}_7\text{F}_{17}\text{O}_2 + \text{Cl}]^-$. Elemental analysis for $\text{C}_{13}\text{H}_7\text{F}_{17}\text{O}_2$ (% calc'd, % found): C (30.13, 30.08), H (1.36, 1.34).

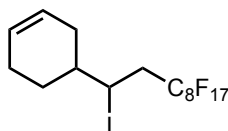
5-Iodo-6-perfluorooctylhexane-2-one (**12b**)**(12b)**

The reaction mixture was prepared according to Procedure A using 5-hexen-2-one (29 μL , 0.25 mmol, 1 equiv.) and perfluorooctyl iodide (88 μL , 0.33 mmol, 1.33 equiv.) and illuminated for 15 min at 530 nm. Purification by silica gel column chromatography (20 \times 2.5 cm, DCM) afforded the product as a colourless oil, which solidified upon standing to give a colourless wax-like solid (**12b**) (159 mg, 98 %).^[8]

$R_f = 0.78$ (DCM, visualised with KMnO_4). $^1\text{H NMR}$ (400 MHz, CDCl_3): δ (ppm) = 4.35 (dddd, $J = 9.3, 7.8, 5.6, 3.5$ Hz, 1H), 3.03 – 2.55 (m, 4H), 2.17 (s, 3H), 2.12 (dddd, $J = 10.1, 8.2, 5.0, 2.7$ Hz, 1H), 2.05 – 1.88 (m, 1H). $^{13}\text{C NMR}$ (101 MHz, CDCl_3): δ (ppm) = 206.5, 123.3 – 105.3 (m), 43.8, 41.8, 34.3, 30.2, 19.9. $^{19}\text{F NMR}$ (376 MHz, CDCl_3): δ (ppm) = -81.0 (t, $J = 10.1$ Hz), -111.5 (tt, $J = 14.7, 3.7$ Hz), -112.2 (ddt, $J = 18.2, 14.7, 3.6$ Hz), -114.1 (tt, $J = 14.0, 3.0$ Hz), -

114.8 (td, $J = 13.5, 7.2$ Hz), -121.5 – -122.2 (m), -122.7 – -123.1 (m), -123.5 – -123.8 (m), -126.3 (dtd, $J = 14.0, 7.0, 3.0$ Hz). ESI-HRMS calculated $m/z = 666.9403$, found $m/z = 666.9407$ for $[C_{14}H_{10}F_{17}IO + Na]^+$. Elemental analysis for $C_{14}H_{10}F_{17}IO$ (% calc'd, % found): C (26.11, 26.32), H (1.56, 1.51).

4-(2-perfluorooctyl-1-iodoethyl)cyclohex-1-en (**13b**)

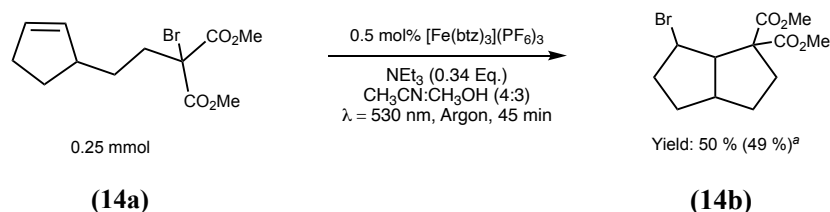


(**13b**)

The reaction mixture was prepared according to Procedure A using 4-vinyl-cyclohex-1-en (32.6 μ L, 0.25 mmol, 1 equiv.) and perfluorooctyl iodide (88 μ L, 0.33 mmol, 1.33 equiv.) and illuminated for 30 min at 530 nm. Purification by silica gel column chromatography (20 \times 2.5 cm, *n*-heptane) afforded the product as a colourless oil, which solidified upon standing to give a white wax-like solid (**13b**) (103 mg, 63 %, mixture of diastereomers).

$R_f = 0.58$ (*n*-heptane, visualised with $KMnO_4$). 1H NMR (400 MHz, $CDCl_3$): δ (ppm) = δ 5.75 – 5.62 (m, 2H), 4.45 (dtd, $J = 27.3, 6.7, 3.2$ Hz, 1H), 3.03 – 2.74 (m, 2H), 2.21 – 1.88 (m, 4H), 1.83 – 1.60 (m, 1H), 1.53 – 1.30 (m, 1H), 1.14 (dtdd, $J = 21.7, 10.9, 5.5, 2.9$ Hz, 1H). ^{13}C NMR (101 MHz, $CDCl_3$): δ (ppm) = 127.1 (d, $J = 19.6$ Hz), 125.2 (d, $J = 32.1$ Hz), 119.4 – 106.6 (m), 40.4, 40.1, 39.3 (t, $J = 20.8$ Hz), 32.2, 30.8, 30.5, 29.1, 28.6, 26.8, 25.2. ^{19}F NMR (376 MHz, $CDCl_3$): δ (ppm) = -80.8 (t, $J = 10.0$ Hz), -112.7 (dtt, $J = 33.0, 14.7, 3.6$ Hz), -114.1 – -114.4 (m), -115.0 (dt, $J = 41.8, 13.8$ Hz), -121.4 – -121.66 (m), -121.8 – -122.0 (m), -122.6 – -122.9 (m), -123.4 – -123.6 (m), -126.1 (tdd, $J = 11.5, 8.2, 4.0$ Hz). APCI-HRMS calculated $m/z = 527.0668$, found $m/z = 527.0663$ for $[C_{16}H_{12}F_{17}I]^+$. Elemental analysis for $C_{16}H_{12}F_{17}I$ (% calc'd, % found): C (29.38, 29.33), H (1.85, 1.83).

Intramolecular ATRA reaction of (**14a**) via reductive quenching of $[Fe(btz)_3](PF_6)_3$ (**1**)



^aYield after purification by silica gel column chromatography.

The reaction mixture was prepared according to Procedure A using (**14a**) (76.29 mg, 0.25 mmol, 1 equiv.) and illuminated for 45 min at 530 nm. Purification by silica gel column

chromatography (20 × 2.5 cm, DCM) afforded the product as a colourless oil, which solidified upon standing to give a colourless wax-like solid (**14b**) (76 mg, 49 %, over 2 batches).

(14b):

R_f = 0.32 (DCM, visualised with UV/KMnO₄). ¹H NMR (400 MHz, CDCl₃): δ (ppm) = 3.85 – 3.65 (m, 7H), 3.43 (ddd, J = 9.4, 7.8, 1.1 Hz, 1H), 2.78 (pd, J = 8.9, 2.1 Hz, 1H), 2.26 – 2.01 (m, 4H), 1.90 (dddd, J = 12.6, 11.5, 9.9, 6.9 Hz, 1H), 1.58 – 1.37 (m, 2H), 1.10 (dddd, J = 12.9, 11.4, 8.3, 6.1 Hz, 1H). ¹³C NMR (101 MHz, CDCl₃): δ (ppm) = 171.9, 170.1, 63.2, 58.3, 52.9, 52.5, 49.6, 42.4, 39.1, 32.4, 32.2, 30.0. ESI-HRMS calculated m/z = 327.0208, found m/z = for 327.0208 [C₁₂H₁₇BrO₄ + Na]⁺. Elemental analysis for C₁₂H₁₇BrO₄ (% calc'd, % found): C (47.23, 47.06), H (5.62, 5.75).

Visible light-mediated ATRA reaction of C₈F₁₇I to 5-hexen-1-ol *via* oxidative quenching of [Fe(bt_z)₃](PF₆)₃ (**1**)

Optimisation of the reaction conditions of the oxidative ATRA using the General Procedure

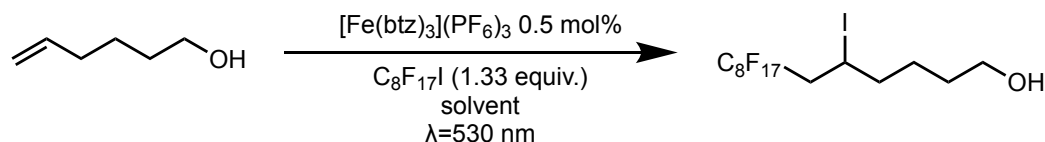


Table S7: Optimisation of the solvent in the oxidative ATRA reaction. (^aDuplicate reactions. ^b[Fe(bt_z)₃](PF₆)₃ poorly soluble in the solvent. All yields were determined by ¹H NMR spectroscopy using mesitylene as internal standard.)

Entry	Solvent	Time (h)	NMR-yield (%)
1	CD ₃ CN:CD ₃ OD (4:3)	2	41
2 ^a	CD ₃ CN	2	66, 73 ^a
3	Acetone-d ₆	2	72
4	DMSO-d ₆	2	67
5 ^b	THF-d ₈	2	<5 ^b
6 ^b	CD ₃ OD	2	17 ^b

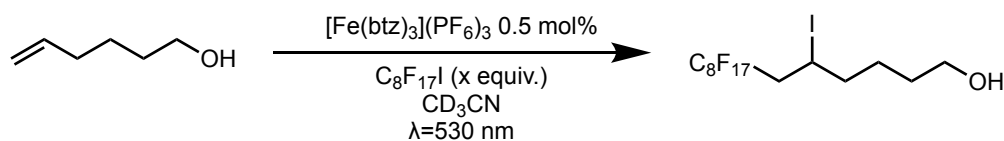


Table S8: Optimisation of equivalents of perfluorooctyl iodide used in the oxidative ATRA-reaction. (^aDuplicate reactions. All yields were determined by ¹H NMR spectroscopy using mesitylene as internal standard. ^bAccurate determination of the NMR yield was not possible at this high concentration of C₈F₁₇I due to the generation of a biphasic system.)

Entry	C ₈ F ₁₇ I (equiv.)	Time (h)	NMR-yield (%)
1 ^a	1.33	2	66, 73
2	2	2	66
3	4	2	57
4	10	2	~70 ^b

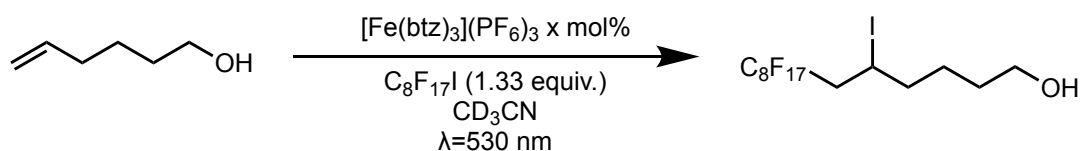


Table S9: Optimisation of PC loading in the oxidative ATRA reaction. (^a Duplicate reactions. All yields were determined by ¹H NMR spectroscopy using mesitylene as internal standard.)

Entry	PS (mol%)	Time	NMR-yield (%)
1	5	2 h	>99
2	2.5	2 h	>99
3	1	1 h	96
4	0.5	2 h	66–73 ^a
5	1.5	40 min	>99 ^a

Control Experiments for the visible light-mediated ATRA reaction of perfluorooctyl iodide to 5-hexen-1-ol

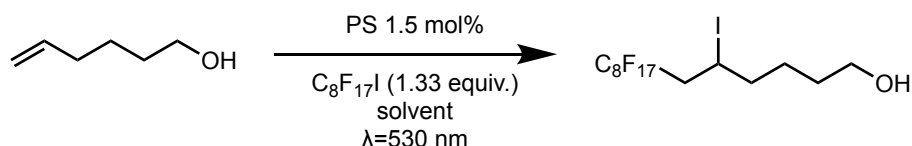


Table S10: Control reactions for the oxidative ATRA (^a1 % PS. ^breaction run in the dark. All yields were determined by ¹H NMR spectroscopy using mesitylene as internal standard.)

Entry	PS	Solvent	Reaction time	NMR-yield (%)
1	FeBr ₂	CD ₃ CN	24 h	<5
2	FeBr ₃	CD ₃ CN	24 h	16
3	[Fe(bpy) ₃](PF ₆) ₂	CD ₃ CN	24 h	<5
4	[Fe(bpy) ₃](PF ₆) ₃	CD ₃ CN	24 h	<5
5	-	CD ₃ CN	24 h	<5
6	[Ru(bpy) ₃]Cl ₂ ·6 H ₂ O	CD ₃ CN	40 min 12 h	34 50
7 ^a	[Ru(bpy) ₃]Cl ₂ ·6 H ₂ O ^a	DMSO-d ₆	40 min 12 h	36 69
8	[Ru(bpy) ₃]Cl ₂ ·6 H ₂ O	DMSO-d ₆	40 min 12 h	42 66
9	-	DMSO-d ₆	12 h	< 5
10 ^b	[Fe(phtmeimb) ₂]PF ₆	CD ₃ CN	24 h	< 5

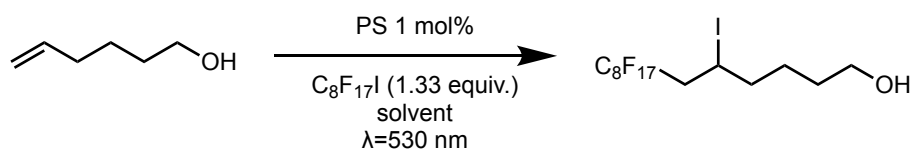


Table S11: Control reactions for the oxidative ATRA using different PSs. (^a1.5 mol% PS. All yields were determined by ¹H NMR spectroscopy using mesitylene as internal standard.)

Entry	PS	Solvent	Reaction time	Atmosphere	NMR-yield (%)
1	[Fe(bpy) ₃](PF ₆) ₂	CD ₃ CN:CD ₃ OD (4:3)	48 h	argon	<5
2	[Fe(bpy) ₃](PF ₆) ₂	CD ₃ CN:CD ₃ OD (4:3)	24 h	air	<5
3	[Fe(bpy) ₃](PF ₆) ₂	DMSO-d ₆	24 h	argon	<5
4	[Fe(bpy) ₃](PF ₆) ₂	DMSO-d ₆	24 h	air	<5
5	[Fe(bpy) ₃](PF ₆) ₃	CD ₃ CN:CD ₃ OD (4:3)	48 h	argon	21
6	FeBr ₃	CD ₃ CN:CD ₃ OD (4:3)	48 h	air	<5
7	FeBr ₃	CD ₃ CN:CD ₃ OD (4:3)	48 h	argon	31
8	FeBr ₂	CD ₃ CN:CD ₃ OD (4:3)	48 h	air	<5
9	[Ru(bpy) ₃]Cl ₂ ·6 H ₂ O	CD ₃ CN:CD ₃ OD (4:3)	24 h	argon	7
10	[Ru(bpy) ₃]Cl ₂ ·6 H ₂ O	DMSO-d ₆	40 min	argon	42 ^a
			12 h		74
11	[Ru(bpy) ₃]Cl ₂ ·6 H ₂ O	CD ₃ CN:CD ₃ OD (4:3)	24 h	air	6
12	[Ru(bpy) ₃]Cl ₂ ·6 H ₂ O	DMSO-d ₆	12 h	air	62
13	-	DMSO-d ₆	12 h	argon	<5
14	-	DMSO-d ₆	12 h	air	<5

Scope limitations of the visible light-mediated ATRA reaction *via* oxidative quenching of [Fe(bt_z)₃](PF₆)₃ using the General Procedure



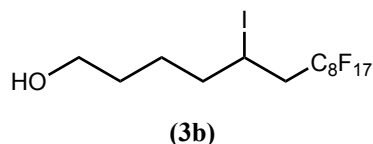
Table S12: ATRA reaction (OQ) using Michael Acceptors as substrates.

Entry	Alkene	NMR yield (%)
1		<5
2		<5

Synthesis and Isolation of the addition of alkyl halides to alkenes and alkynes using Procedure B

The following reactions were performed following Procedure B (see Experimental Section) unless otherwise stated.

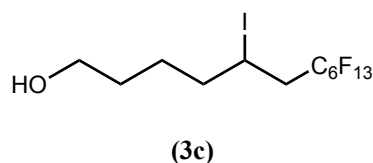
5-Iodo-6-perfluorooctylhexanol (**3b**)



Procedure B was applied using 5-hexenol (30.0 μL , 0.25 mmol, 1 equiv.), perfluorooctyl iodide (87.7 μL , 0.33 mmol, 1.33 equiv.), $[\text{Fe}(\text{btz})_3](\text{PF}_6)_3$ (5.7 mg, 3.8 μmol , 0.015 equiv.) and acetonitrile (3.5 mL). Purification by silica gel chromatography (PE:EtOAc 5:1) gave the product as a colourless oil (148 mg, 92 %). The NMR-data was in accordance with literature data.^[5]

$R_f = 0.13$ (*n*-heptane:EtOAc 5:1, UV-active, visualised with KMnO_4). ^1H NMR (400 MHz, CDCl_3) δ (ppm) = 4.34 (tdd, $J = 8.4, 5.5, 4.3$ Hz, 1H), 3.69 (t, $J = 6.1$ Hz, 2H), 3.03 – 2.69 (m, 2H), 1.95 – 1.76 (m, 2H), 1.73 – 1.44 (m, 4H). ^{13}C NMR (101 MHz, CDCl_3) δ (ppm) = 123.0 – 105.5 (m), 62.7, 41.8 (t, $J = 20.8$ Hz), 40.2, 31.7, 26.2, 20.6. ^{19}F NMR (376 MHz, CDCl_3) δ (ppm) = -80.2 – -81.5 (m), -111.1 – -115.2 (m), -121.2 – -121.7 (m), -121.7 – -122.1 (m), -122.5 – -122.9 (m), -123.4 – -123.8 (m), -125.9 – -126.3 (m). HRMS (ESI-TOP) calc'd for $[\text{C}_{14}\text{H}_{12}\text{F}_{17}\text{IO}+\text{Cl}]^-$ 680.9350; found 680.9359. Elemental analysis (% calc'd, % found for $\text{C}_{14}\text{H}_{12}\text{F}_{17}\text{IO}$): C (26.02, 26.06), H (1.87, 1.85).

5-Iodo-6-perfluorohexylhexanol (**3c**)

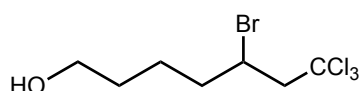


Procedure B was applied using 5-hexenol (30.0 μL , 0.25 mmol, 1 equiv.), perfluorohexyl iodide (71.9 μL , 0.33 mmol, 1.33 equiv.), $[\text{Fe}(\text{btz})_3](\text{PF}_6)_3$ (5.7 mg, 3.8 μmol , 0.015 equiv.) and acetonitrile (3.5 mL). Purification by silica gel chromatography (*n*-heptane:EtOAc 5:1) gave the product as a colourless oil (133 mg, 93 %). The NMR-data was in accordance with literature data.^[5]

$R_f = 0.11$ (*n*-heptane:EtOAc 5:1, UV-active, visualised with KMnO_4). ^1H NMR (400 MHz, CDCl_3) δ (ppm) = 4.34 (tdd, $J = 8.4, 5.5, 4.3$ Hz, 1H), 3.69 (t, $J = 6.1$ Hz, 2H), 3.03 – 2.68 (m, 2H), 1.83 (ddt, $J = 14.5, 9.9, 4.3$ Hz, 2H), 1.71 – 1.46 (m, 4H). ^{13}C NMR (101 MHz, CDCl_3) δ

(ppm) = 122.6 – 104.6 (m), 62.5, 41.80 (t, $J = 20.8$ Hz), 40.2, 31.6, 26.2, 20.6. ^{19}F NMR (376 MHz, CDCl_3) δ (ppm) = -80.76 (tt, $J = 10.0, 2.5$ Hz), -110.88 – -115.46 (m), -121.59 – -121.96 (m), -122.61 – -123.04 (m), -123.39 – -123.75 (m), -125.90 – -126.35 (m). HRMS (ESI-TOF) calc'd for $[\text{C}_{12}\text{H}_{12}\text{F}_{13}\text{IO}+\text{Cl}]^-$ 580.9414; found 580.9428. Elemental analysis (% calc'd, % found for $\text{C}_{12}\text{H}_{12}\text{F}_{13}\text{IO}$): C (26.39, 26.21), H (2.21, 2.27), N (0.00, 0.00)

5-bromo-7,7,7-trichloroheptan-1-ol (**3d**)

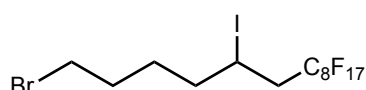


(**3d**)

Procedure B was applied using 5-hexenol (30.0 μL , 0.25 mmol, 1 equiv.), bromotrichloromethane (32.8 μL , 0.33 mmol, 1.33 equiv.), $[\text{Fe}(\text{btz})_3](\text{PF}_6)_3$ (5.7 mg, 3.8 μmol , 0.015 equiv.) and acetonitrile (3.5 mL). Purification by silica gel chromatography (DCM:EtOAc, 20:1) gave the product as a white solid (29 mg, 39 %). NMR-spectroscopic data was in accordance with literature.

$R_f = 0.11$ (*n*-heptane:EtOAc 5:1, UV-active, visualised with KMnO_4). ^1H NMR (400 MHz, CDCl_3) δ (ppm) = 4.33 (dtd, $J = 9.4, 5.2, 4.3$ Hz, 1H), 3.73 – 3.63 (m, 2H), 3.46 (dd, $J = 15.8, 5.0$ Hz, 1H), 3.23 (dd, $J = 15.8, 5.3$ Hz, 1H), 2.14 – 1.89 (m, 2H), 1.78 – 1.51 (m, 4H). ^{13}C NMR (101 MHz, CDCl_3) δ (ppm) = 97.3, 62.7 (d, $J = 7.6$ Hz), 49.0, 39.4, 31.9, 23.8. HRMS (ESI-TOF) calc'd for $[\text{C}_7\text{H}_{12}\text{BrCl}_3\text{O}+\text{Cl}]^-$ 330.8826; found 330.8826. Elemental analysis (% calc'd, % found for $\text{C}_7\text{H}_{12}\text{BrCl}_3\text{O}$): C (28.17, 28.11), H (4.05, 4.03).

1-bromo-5-iodo-6-perfluorooctylhexane (**4b**)



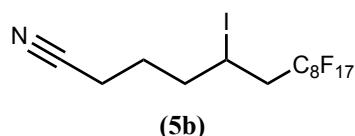
(**4b**)

Procedure B was applied using 6-bromo-1-hexene (33.4 μL , 0.25 mmol, 1 equiv.), perfluorooctyl iodide (87.7 μL , 0.33 mmol, 1.33 equiv.), $[\text{Fe}(\text{btz})_3](\text{PF}_6)_3$ (5.7 mg, 3.8 μmol , 0.015 equiv.) and acetonitrile (3.5 mL). Purification by silica gel chromatography (*n*-heptane) gave the product as a colourless oil (166 mg, 94 %). The NMR-data was in accordance with literature data.^[5]

$R_f = 0.24$ (*n*-heptane, UV-active, visualised with KMnO_4). ^1H NMR (400 MHz, CDCl_3) δ (ppm) = 4.33 (tdd, $J = 8.5, 5.3, 4.2$ Hz, 1H), 3.42 (t, $J = 6.7$ Hz, 2H), 3.03 – 2.66 (m, 2H), 2.02 – 1.66 (m, 5H), 1.66 – 1.51 (m, 1H). ^{13}C NMR (101 MHz, CDCl_3) δ (ppm) = 122.04 – 106.12 (m), 41.9 (t, $J = 20.9$ Hz), 39.5 (d, $J = 2.3$ Hz), 33.1, 31.7, 28.5, 20.0. ^{19}F NMR (376 MHz,

CDCl₃) δ (ppm) = -81.0 (t, J = 10.0 Hz), -111.1 – -115.3 (m), -121.5 – -121.8 (m), -121.8 – -122.3 (m), -122.7 – -123.0 (m), -123.5 – -123.9 (m), -126.2 – -126.4 (m). HRMS (ESI-TOF) calc'd for [C₁₄H₁₂BrF₁₇I+Cl]⁻ 742.8506; found 742.8522. Elemental analysis (% calc'd, % found for C₁₄H₁₂BrF₁₇I): C (23.68, 23.58), H (1.70, 1.41), N (0.00, 0.02).

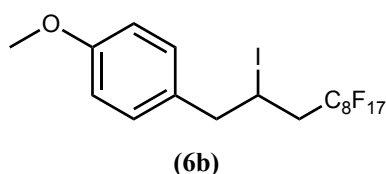
5-Iodo-6-perfluorooctylhexanenitrile (5b)



Procedure B was applied using 5-hexenenitrile (29.9 μ L, 0.25 mmol, 1 equiv.), perfluorooctyl iodide (87.7 μ L, 0.33 mmol, 1.33 equiv.), [Fe(bt_z)₃](PF₆)₃ (5.7 mg, 3.8 μ mol, 0.015 equiv.) and acetonitrile (3.5 mL). Purification by silica gel chromatography (*n*-heptane:Et₂O, 9:1 – 4:1) gave the product as a colourless oil (92 mg, 57 %). The NMR-data was in accordance with literature data.^[5]

R_f = 0.31 (*n*-heptane:EtOAc 5:1, UV-active, visualised with KMnO₄). ¹H NMR (400 MHz, CDCl₃) δ (ppm) = 4.37 – 4.26 (m, 1H), 3.06 – 2.69 (m, 2H), 2.52 – 2.35 (m, 2H), 2.05 – 1.91 (m, 3H), 1.89 – 1.73 (m, 1H). ¹³C NMR (101 MHz, CDCl₃) δ (ppm) = 122.1 – 106.3 (m), 118.9, 41.66 (t, J = 20.9 Hz), 38.9, 26.0, 18.1, 18.1, 16.5. ¹⁹F NMR (376 MHz, CDCl₃) δ (ppm) = -80.65 – -80.90 (m), -110.94 – -115.19 (m), -121.40 – -121.68 (m), -121.75 – -122.06 (m), -122.53 – -122.88 (m), -123.36 – -123.67 (m), -125.93 – -126.31 (m). HRMS (ESI-TOF) calc'd for [C₁₄H₉F₁₇IN+Na]⁺ 663.9406; found 663.9407. Elemental analysis (% calc'd, % found for C₁₄H₉F₁₇IN): C (26.23, 26.27), H (1.42, 1.45), N (2.18, 2.16).

4-(2-iodo-3-perfluorooctyl-propyl)-anisole (6b)

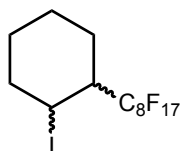


Procedure B (irradiation for 80 min) was applied using 4-allylanisole (38.4 μ L, 0.25 mmol, 1 equiv.), perfluorooctyl iodide (87.7 μ L, 0.33 mmol, 1.33 equiv.), [Fe(bt_z)₃](PF₆)₃ (5.7 mg, 3.8 μ mol, 0.015 equiv.) and acetonitrile (3.5 mL). Purification by silica gel chromatography (EtOAc in *n*-heptane, 1 – 4 %) gave the product as a white solid (129 mg, 74 %).

R_f = 0.22 (2 % EtOAc in *n*-heptane, UV-active, visualised with KMnO₄). ¹H NMR (400 MHz, CDCl₃) δ (ppm) = 7.16 – 7.08 (m, 2H), 6.91 – 6.83 (m, 2H), 4.42 (dq, J = 8.5, 6.4 Hz, 1H), 3.81 (s, 3H), 3.18 (qd, J = 14.7, 7.2 Hz, 2H), 2.97 – 2.78 (m, 2H). ¹³C NMR (101 MHz, CDCl₃) δ (ppm) = 159.0, 130.8, 130.2, 121.3 – 106.5 (m), 114.1, 55.4, 46.4, 40.8 (t, J = 20.8 Hz), 20.3.

^{19}F NMR (376 MHz, CDCl_3) δ (ppm) = -80.75 (t, J = 10.0 Hz), -111.40 – -114.31 (m), -121.5, -121.8, -122.7, -123.6, -126.1. HRMS (ESI-TOF) calc'd for $[\text{C}_{18}\text{H}_{12}\text{F}_{17}\text{IO}+\text{Cl}]^-$ 728.9350; found 728.9366. Elemental analysis (% calc'd, % found for $\text{C}_{18}\text{H}_{12}\text{F}_{17}\text{IO} \cdot 0.05 \text{ C}_7\text{H}_{16}$): C (31.52, 31.63), H (1.85, 1.64).

1-iodo-2-perfluorooctylcyclohexane (**7b**, **7c**)



cis (**7b**), *trans* (**7c**)

Procedure B was applied using cyclohexene (25.3 μL , 0.25 mmol, 1 equiv.), perfluorooctyl iodide (87.7 μL , 0.33 mmol, 1.33 equiv.), $[\text{Fe}(\text{btz})_3](\text{PF}_6)_3$ (5.7 mg, 3.8 μmol , 0.015 equiv.) and acetonitrile (3.5 mL). Purification by silica gel chromatography (*n*-heptane) gave the two diastereomers (*cis*: 39 mg, 25 %, *trans*: 11 mg, 7 %). The NMR-data was in accordance with literature data.^[6]

$R_{f, \text{cis}} = 0.50$, $R_{f, \text{trans}} = 0.72$ (*n*-heptane, UV-active, stain with KMnO_4).

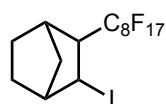
cis-Isomer (**7b**):

^1H NMR (400 MHz, CDCl_3) δ (ppm) = 4.72 (s, 1H), 2.22 (dd, J = 15.1, 3.6 Hz, 1H), 2.01 – 1.60 (m, 7H), 1.47 – 1.32 (m, 1H). ^{13}C NMR (101 MHz, CDCl_3) δ (ppm) = 123.2 – 104.9 (m), 44.6 (t, J = 20.8 Hz), 37.5, 27.6 (t, J = 4.6 Hz), 25.3, 22.9 (q, J = 3.6 Hz), 22.2. ^{19}F NMR (376 MHz, CDCl_3) δ (ppm) = -80.82 (t, J = 10.0 Hz), -117.6, -120.2, -121.0, -121.8, -121.9, -122.7, -126.1. HRMS (APCI-TOF) calc'd for $[\text{C}_{15}\text{H}_{10}\text{F}_{17}\text{I}]^+$ 513.0511; found 513.0502. Elemental analysis (% calc'd, % found for $\text{C}_{14}\text{H}_{10}\text{F}_{17}\text{I}$): C (26.77, 26.72), H (1.60, 1.59).

trans-Isomer (**7c**)

^1H NMR (400 MHz, CDCl_3) δ (ppm) = 4.97 (q, J = 4.0 Hz, 1H), 2.70 (t, J = 18.3 Hz, 1H), 2.27 – 2.15 (m, 1H), 2.06 – 1.84 (m, 3H), 1.77 (s, 1H), 1.65 – 1.55 (m, 3H). ^{13}C NMR (101 MHz, CDCl_3) δ (ppm) = 119.9 – 107.0 (m), 44.6 (t, J = 20.8 Hz), 37.5, 27.6 (t, J = 4.7 Hz), 25.3, 22.9 (q, J = 3.6 Hz), 22.2. ^{19}F NMR (376 MHz, CDCl_3) δ (ppm) = -80.76 (tt, J = 9.9, 2.3 Hz), -106.73 – -111.63 (m), -119.7, -120.5, -121.0, -121.8, -122.7, -126.1.

2-iodo-3-(perfluorooctyl)bicyclo[2.2.1]heptane (**8b**)

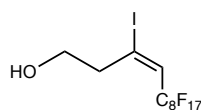


(**8b**)

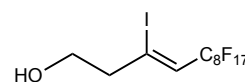
Procedure B was applied using norbornene (23.5 mg, 0.25 mmol, 1 equiv.), perfluorooctyl iodide (87.7 μ L, 0.33 mmol, 1.33 equiv.), [Fe(btz)₃](PF₆)₃ (5.7 mg, 3.8 μ mol, 0.015 equiv.) and acetonitrile (3.5 mL). Purification by silica gel chromatography (*n*-heptane) gave the product as a white solid (151 mg, 94 %). NMR-spectroscopic data was in accordance with literature.^[6]

R_f = 0.58 (*n*-heptane, UV-active, visualised with KMnO₄). ¹H NMR (400 MHz, CDCl₃) δ (ppm) = 4.31 (ddd, J = 6.1, 3.7, 2.1 Hz, 1H), 2.55 – 2.30 (m, 3H), 1.96 – 1.84 (m, 1H), 1.78 – 1.56 (m, 3H), 1.41 – 1.21 (m, 2H). ¹³C NMR (101 MHz, CDCl₃) δ (ppm) = 124.1 – 104.9 (m), 55.9 (dd, J = 21.8, 19.1 Hz), 44.7, 38.0, 35.2 (d, J = 2.3 Hz), 29.9, 27.6, 26.1 (t, J = 3.4 Hz). ¹⁹F NMR (376 MHz, CDCl₃) δ (ppm) = -80.86 (tt, J = 9.9, 2.4 Hz), -115.06 – -119.41 (m), -120.8, -120.9, -121.7, -121.9, -122.7, -126.2. HRMS (APCI-TOF) calc'd for [C₁₅H₁₀F₁₇]⁺ 513.0511; found 513.0502. Elemental analysis (% calc'd, % found for C₁₅H₁₀F₁₇I): C (28.15, 28.06), H (1.57, 1.58).

3-iodo-4-perfluorooctyl-but-3-en-1-ol (**9b**, **9c**)



(**9b**)



(**9c**)

Procedure B was applied using 3-butynol (18.9 μ L, 0.25 mmol, 1 equiv.), perfluorooctyl iodide (87.7 μ L, 0.33 mmol, 1.33 equiv.), [Fe(btz)₃](PF₆)₃ (5.7 mg, 3.8 μ mol, 0.015 equiv.) and acetonitrile (3.5 mL). Purification by silica gel chromatography (*n*-heptane:EtOAc 6:1) gave (*E*)-3-iodo-4-perfluorooctyl-but-3-en-1-ol (**9b**) (100 mg, 65 %) and the (*Z*)-3-iodo-4-perfluorooctyl-but-3-en-1-ol (**9c**) (25 mg, 16 %), both as white solids. NMR-spectroscopic data was in accordance with literature.^[5]

(*E*)-3-iodo-4-perfluorooctyl-but-3-en-1-ol (**9b**)

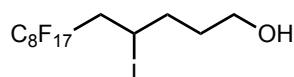
R_f = 0.36 (*n*-heptane:EtOAc, 5:1, UV-active, visualised with KMnO₄). ¹H NMR (400 MHz, CDCl₃) δ (ppm) = 6.49 (t, J = 14.3 Hz, 1H), 3.87 (t, J = 6.3 Hz, 2H), 2.99 – 2.90 (m, 2H). ¹³C NMR (101 MHz, CDCl₃) δ (ppm) = 129.2 (t, J = 23.7 Hz), 120.2 – 105.3 (m), 62.0, 43.8. ¹⁹F NMR (376 MHz, CDCl₃) δ (ppm) = -80.8 (tt, J = 9.8, 2.3 Hz), -105.0 (tt, J = 13.0, 3.2 Hz),

-121.4, -121.8, -122.7, -123.0, -126.1. HRMS (ESI-TOF) calc'd for $[\text{C}_{12}\text{H}_6\text{F}_{17}\text{IO}+\text{Cl}]^+$ 650.8880; found 650.8871. Elemental analysis (% calc'd, % found for $\text{C}_{12}\text{H}_6\text{F}_{17}\text{IO}$): C (23.40, 23.36), H (0.98, 0.97).

(Z)-3-iodo-4-perfluorooctyl-but-3-en-1-ol (**9c**)

$R_f = 0.18$ (*n*-heptane:EtOAc, 5:1, UV-active, visualised with KMnO_4). ^1H NMR (400 MHz, CDCl_3) δ (ppm) = 6.41 (t, $J = 13.0$ Hz, 1H), 3.85 (t, $J = 5.8$ Hz, 2H), 2.97 – 2.88 (m, 2H). ^{13}C NMR (101 MHz, CDCl_3) δ (ppm) = 124.5 (t, $J = 23.8$ Hz), 119.9 – 107.23 (m), 60.8, 51.1. ^{19}F NMR (376 MHz, CDCl_3) δ (ppm) = -80.8 (tt, $J = 9.8, 2.4$ Hz), -108.7 – -108.9 (m), -121.4, -121.9, -122.7, -122.8, -126.1. HRMS (ESI-TOF) calc'd for $[\text{C}_{12}\text{H}_6\text{F}_{17}\text{IO}+\text{Cl}]^-$ 650.8880; found 650.8870. Elemental analysis (% calc'd, % found for $\text{C}_{12}\text{H}_6\text{F}_{17}\text{IO}$): C (23.40, 23.74), H (0.98, 1.11).

5-iodo-6-perfluorooctylpentanol (**10b**)

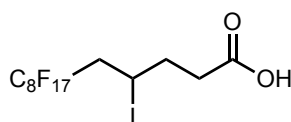


(**10b**)

Procedure B was applied using 4-pentenol (25.8 μL , 0.25 mmol, 1 equiv.), perfluorooctyl iodide (87.7 μL , 0.33 mmol, 1.33 equiv.), $[\text{Fe}(\text{btz})_3](\text{PF}_6)_3$ (5.7 mg, 3.8 μmol , 0.015 equiv.) and acetonitrile (3.5 mL). Purification by silica gel chromatography (*n*-heptane:EtOAc 4:1) gave the product as a white solid (141 mg, 89 %). NMR-spectroscopic data was in accordance with literature.^[5]

$R_f = 0.17$ (*n*-heptane:EtOAc 4:1, UV-active, visualised with KMnO_4). ^1H NMR (400 MHz, CDCl_3) δ (ppm) = 4.38 (tt, $J = 8.1, 5.4$ Hz, 1H), 3.71 (t, $J = 6.1$ Hz, 2H), 3.04 – 2.69 (m, 3H), 2.06 – 1.62 (m, 3H). ^{13}C NMR (101 MHz, CDCl_3) δ (ppm) = 120.6 – 108.2 (m), 61.8, 42.1 (t, $J = 20.9$ Hz), 37.0, 32.8, 20.4. ^{19}F NMR (376 MHz, CDCl_3) δ (ppm) = -80.9 (t, $J = 10.0$ Hz), -110.7 – -115.5 (m), -121.6, -122.0, -122.8, -123.7, -126.2. HRMS (ESI-TOF) calc'd for $[\text{C}_{13}\text{H}_{10}\text{F}_{17}\text{IO}+\text{Cl}]^-$ 666.9193; found 666.9182. Elemental analysis (% calc'd, % found for $\text{C}_{13}\text{H}_{10}\text{F}_{17}\text{IO}$): C (24.70, 24.72), H (1.59, 1.57).

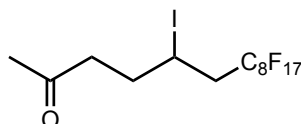
5-Iodo-6-perfluorooctylpentenoic acid (**11b**)



(**11b**)

Procedure B was applied using 5-pentenoic acid (25.5 μ L, 0.25 mmol, 1 equiv.), perfluorooctyl iodide (87.7 μ L, 0.33 mmol, 1.33 equiv.), [Fe(bt_z)₃](PF₆)₃ (5.7 mg, 3.8 μ mol, 0.015 equiv.) and acetonitrile (3.5 mL). Purification by silica gel chromatography (DCM) gave the product as a white solid (140 mg, 87 %). NMR-spectroscopic data was in accordance with literature.^[7a] R_f = 0.46 (DCM:EtOAc 4:1 + 1 % AcOH, UV-active, visualised with KMnO₄). ¹H NMR (400 MHz, CDCl₃) δ (ppm) = 4.40 (dddd, J = 9.9, 8.6, 5.3, 3.5 Hz, 1H), 3.08 – 2.51 (m, 4H), 2.20 (dddd, J = 15.3, 8.4, 6.9, 3.5 Hz, 1H), 2.07 (dddd, J = 15.2, 9.9, 8.4, 5.4 Hz, 1H). ¹³C NMR (101 MHz, CDCl₃) δ (ppm) = 178.4, 123.0 – 105.7 (m), 42.0 (t, J = 20.9 Hz), 35.1, 34.5, 18.9. ¹⁹F NMR (376 MHz, CDCl₃) δ (ppm) = -80.87 (t, J = 9.9 Hz), -110.61 – -115.41 (m), -121.6, -121.9, -122.8, -123.6, -126.2. HRMS (ESI-TOF) calc'd for [C₁₃H₈F₁₇IO₂+Cl]⁻ 680.8986; found 680.8995. Elemental analysis (% calc'd, % found for C₁₃H₈F₁₇IO₂): C (24.17, 24.15), H (1.25, 1.24).

5-Iodo-6-perfluorooctylhexane-2-one (**12b**)

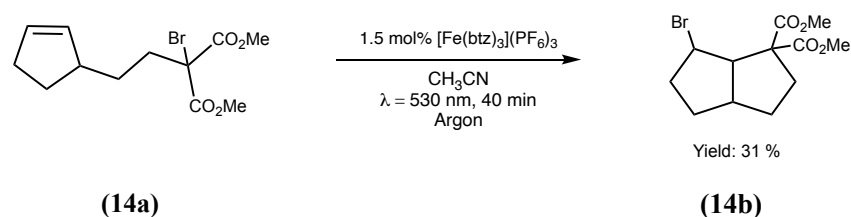


(**12b**)

Procedure B was applied using 5-hexene-2-one (29.0 μ L, 0.25 mmol, 1 equiv.), perfluorooctyl iodide (87.7 μ L, 0.33 mmol, 1.33 equiv.), [Fe(bt_z)₃](PF₆)₃ (5.7 mg, 3.8 μ mol, 0.015 equiv.) and acetonitrile (3.5 mL). Purification by silica gel chromatography (DCM) gave the product as a white solid (157 mg, 97 %).^[8]

R_f = 0.82 (DCM, visualised with KMnO₄). ¹H NMR (400 MHz, CDCl₃) δ (ppm) = 4.36 (dddd, J = 10.0, 7.9, 5.6, 3.5 Hz, 1H), 3.04 – 2.57 (m, 4H), 2.19 (s, 3H), 2.19 – 2.08 (m, 1H), 1.99 (dddd, J = 15.3, 10.0, 8.2, 5.4 Hz, 1H). ¹³C NMR (101 MHz, CDCl₃) δ (ppm) = 206.6, 122.1 – 106.0 (m), 43.8, 42.1 (t, J = 21.0 Hz), 34.2, 30.2, 19.9. ¹⁹F NMR (376 MHz, CDCl₃) δ (ppm) = -80.7 – -80.9 (m), -110.7 – -115.5 (m), -121.5, -121.9, -122.7, -123.6, -126.1. HRMS (ESI-TOF) calc'd for [C₁₄H₁₀F₁₇IO+Cl]⁻ 678.9193; found 678.9204. Elemental analysis (% calc'd, % found for C₁₄H₁₀F₁₇IO): C (26.11, 26.21), H (1.56, 1.55).

Intramolecular ATRA reaction of **(14a)** *via* oxidative quenching of $[\text{Fe}(\text{btz})_3](\text{PF}_6)_3$ (**1**)



General procedure B was applied using dimethyl 2-bromo-2-(2-(cyclopent-2-en-1-yl)ethyl)malonate (154.8 mg, 0.50 mmol, 1 equiv), $[\text{Fe}(\text{btz})_3](\text{PF}_6)_3$ (11.4 mg, 7.6 mmol, 0.03 equiv.) and acetonitrile (7 mL) divided into two vials. Purification by silica gel chromatography (DCM) gave product **(14b)** as a white solid (48 mg, 31%).

$R_f = 0.31$ (DCM, visualised with UV/ KMnO_4). $^1\text{H NMR}$ (400 MHz, CDCl_3) δ (ppm) = 3.85 – 3.65 (m, 7H), 3.43 (ddd, $J = 9.4, 7.8, 1.1$ Hz, 1H), 2.78 (pd, $J = 8.9, 2.1$ Hz, 1H), 2.26 – 2.01 (m, 4H), 1.90 (dddd, $J = 12.6, 11.5, 9.9, 6.9$ Hz, 1H), 1.58 – 1.37 (m, 2H), 1.10 (dddd, $J = 12.9, 11.4, 8.3, 6.1$ Hz, 1H). $^{13}\text{C NMR}$ (101 MHz, CDCl_3) δ (ppm) = 172.0, 170.2, 63.3, 58.4, 53.0, 52.6, 49.7, 42.6, 39.2, 32.5, 32.3, 30.1. HRMS (ESI-TOF) calc'd for $[\text{C}_{12}\text{H}_{17}\text{BrO}_4 + \text{Na}]^+$ 327.0208; found 327.0204. Elemental analysis (% calc'd, % found for $\text{C}_{12}\text{H}_{17}\text{BrO}_4$): C (47.23, 47.40), H (5.62, 5.51).

Mechanistic Investigations

The effect of radical scavengers on the visible light-mediated ATRA reaction via reductive and oxidative quenching of $[\text{Fe}(\text{btz})_3](\text{PF}_6)_3$ using the General Procedure

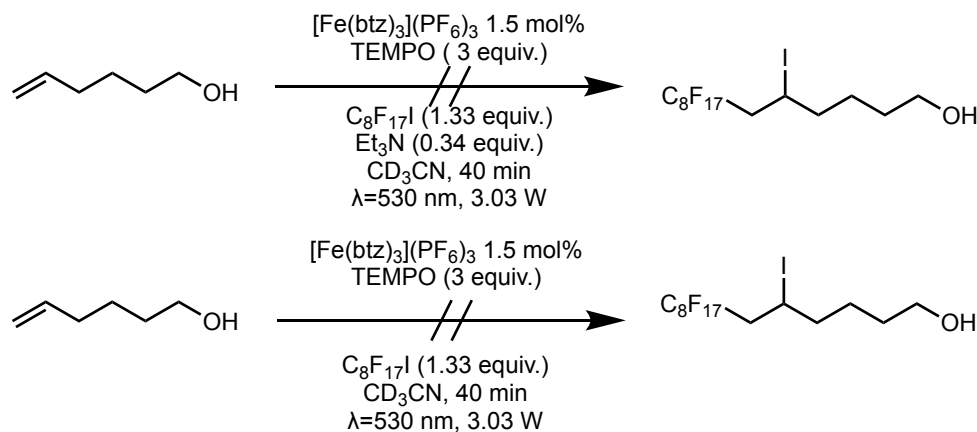
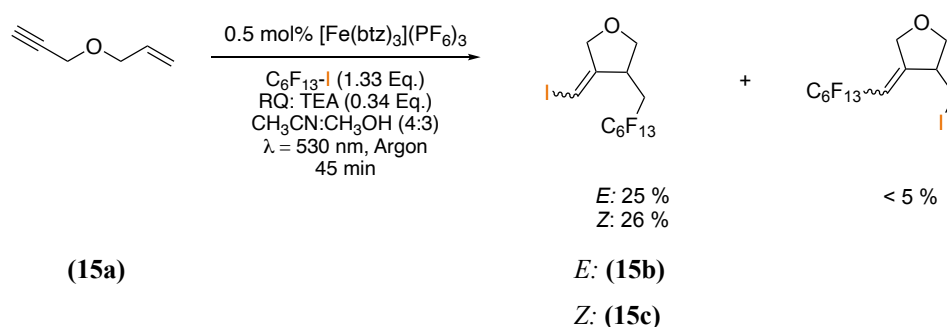


Figure S5: Addition of TEMPO (2,2,6,6-tetramethylpiperidine-1-oxyl) to the ATRA reaction (RQ above, OQ below) resulting in complete inhibition of the reaction.

Table S13: Addition of TEMPO (2,2,6,6-tetramethylpiperidine-1-oxyl) to the ATRA reaction (OQ) resulting in complete inhibition of the reaction. (^a RQ, ^b OQ)

Entry	Additive	Equiv.	NMR yield (%)
1 ^a	TEMPO	3	<5
2 ^b	TEMPO	3	<5

Investigation of the chemoselectivity of the visible light-mediated ATRA reaction of alkyl halides to alkenes & alkynes *via* reductive quenching of $[\text{Fe}(\text{btz})_3](\text{PF}_6)_3$



Following the reaction conditions described in Procedure A 3-(allyloxy)-1-propyne (27.9 μL , 0.25 mmol, 1 equiv.) and perfluorohexyl iodide (111 μL , 0.33 mmol, 1.33 equiv.) were used and the reaction mixture was illuminated for 2 h at 530 nm. Filtration over silica gel (2.5 x 10 cm, *n*-heptane:EtOAc 5:1) afforded a mixture of two stereoisomers (**x**) as an off-white slightly waxy solid (160 mg, over 2 batches).

The stereoisomers were separated and purified by additional silica gel column chromatography (2.5 x 23 cm, *n*-heptane:EtOAc 49:1) affording (**15b**) (81 mg, 25 %) and (**15c**) (86 mg, 26 %) as white solids. NMR-spectroscopic data was in accordance with literature^[9].

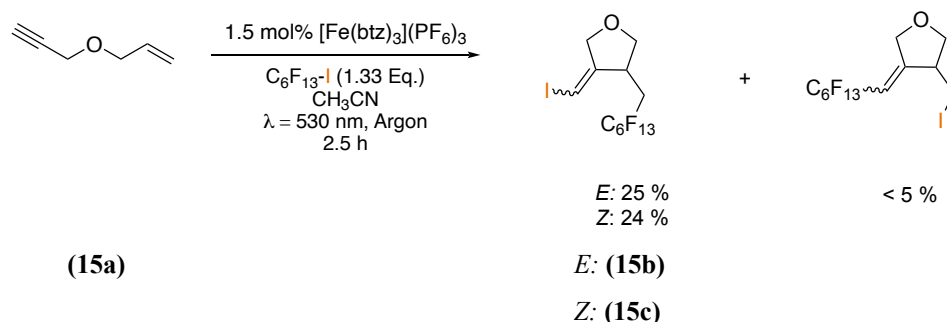
E-Isomer (**15b**):

$R_f = 0.43$ (*n*-heptane:EtOAc 5:1, visualised with UV/KMnO₄). ¹H NMR (400 MHz, CDCl₃): δ (ppm) = 6.19 (q, $J = 1.9$ Hz, 1H), 4.36 (dt, $J = 13.3, 1.8$ Hz, 1H), 4.23 (dd, $J = 13.3, 1.9$ Hz, 1H), 4.06 (dd, $J = 9.6, 2.5$ Hz, 1H), 3.96 (dd, $J = 9.5, 5.5$ Hz, 1H), 3.23 – 3.13 (m, 1H), 2.68 – 2.48 (m, 1H), 2.35 – 2.14 (m, 1H). ¹³C NMR (101 MHz, CDCl₃): δ (ppm) = 153.0, 121.0 – 102.3 (m), 72.9, 71.6, 69.9, 41.3, 31.9 (t, $J = 20.9$ Hz). ¹⁹F NMR (376 MHz, CDCl₃): δ (ppm) = δ -80.8 (tt, $J = 10.0, 2.6$ Hz), -112.3 – -112.5 (m), -113.1 (tt, $J = 14.3, 4.3$ Hz), -113.7 (tq, $J = 13.3, 4.3$ Hz), -114.3 – -114.5 (m), -121.7 (dp, $J = 24.4, 9.3, 6.5$ Hz), -122.8 (tdd, $J = 22.9, 10.3, 6.0$ Hz), -123.6 (dddq, $J = 20.6, 12.7, 9.0, 5.0, 4.4$ Hz), -126.0 – -126.2 (m). APCI-HRMS calculated $m/z = 542.9490$, found $m/z = 542.9486$ for [C₁₂H₈F₁₃IO + H]⁺. Elemental analysis for C₁₂H₈F₁₃IO (% calc'd, % found): C (26.59, 26.36), H (1.49, 1.46).

Z-Isomer (**15c**):

$R_f = 0.65$ (*n*-heptane:EtOAc, 5:1 v/v, visualised with UV/KMnO₄). ¹H NMR (400 MHz, CDCl₃): δ (ppm) = 6.13 (td, $J = 2.7, 2.0$ Hz, 1H), 4.36 – 4.19 (m, 3H), 3.75 (dd, $J = 9.1, 7.0$ Hz, 1H), 3.11 (dtt, $J = 8.6, 3.4, 1.8$ Hz, 1H), 2.52 – 2.32 (m, 1H), 2.31 – 2.11 (m, 1H). ¹³C NMR (101 MHz, CDCl₃): δ (ppm) = 153.1, 120.1 – 100.2 (m), 75.8, 75.0, 68.9, 39.6, 33.2 (t, $J = 21.5$ Hz). ¹⁹F NMR (376 MHz, CDCl₃): δ (ppm) = -80.8 (tt, $J = 9.9, 2.6$ Hz), -111.8 (tt, $J = 14.3, 3.7$ Hz), -112.5 (tp, $J = 14.7, 3.7$ Hz), -113.5 (tq, $J = 13.8, 3.7$ Hz), -114.2 (tt, $J = 12.8, 3.0$ Hz), -121.6 – -121.9 (m), -122.7 – -123.0 (m), -123.4 (dpt, $J = 20.1, 8.3, 3.2$ Hz), -126.1 (ddq, $J = 18.4, 10.9, 3.5$ Hz). APCI-HRMS calculated $m/z = 542.9490$, found $m/z = 542.9486$ for [C₁₂H₈F₁₃IO + H]⁺. Elemental analysis for C₁₂H₈F₁₃IO (% calc'd, % found): C (26.59, 26.39), H (1.49, 1.47).

Investigation of the chemoselectivity of the visible light-mediated ATRA reaction of alkyl halides to alkenes & alkynes *via* oxidative quenching of [Fe(btz)₃](PF₆)₃



Following the reaction conditions described in Procedure B 3-(allyloxy)-1-propyne (27.9 μL , 0.25 mmol, 1 equiv.) and perfluorohexyl iodide (111 μL , 0.33 mmol, 1.33 equiv.) were used and the reaction mixture was illuminated for 2 h at 530 nm. Filtration over silica gel (2.5 x 10 cm, *n*-heptane:EtOAc 5:1) afforded a mixture of two stereoisomers (**y**) as a off-white slightly waxy solid (235 mg, over 2 batches).

The stereoisomers were separated and purified by additional silica gel column chromatography (2.5 x 23 cm, *n*-heptane:EtOAc 49:1) affording **15b** (82 mg, 25 %) and **15c** (78 mg, 24 %) as white solids. NMR-spectroscopic data was in accordance with literature^[9].

E-Isomer (**15b**):

$R_f = 0.43$ (*n*-heptane:EtOAc 5:1, visualised with UV/KMnO₄). ¹H NMR (400 MHz, CDCl₃): δ (ppm) = 6.19 (q, $J = 1.9$ Hz, 1H), 4.36 (dt, $J = 13.3, 1.8$ Hz, 1H), 4.23 (dd, $J = 13.3, 1.9$ Hz, 1H), 4.06 (dd, $J = 9.6, 2.5$ Hz, 1H), 3.96 (dd, $J = 9.5, 5.5$ Hz, 1H), 3.23 – 3.13 (m, 1H), 2.68 – 2.48 (m, 1H), 2.35 – 2.14 (m, 1H). ¹³C NMR (101 MHz, CDCl₃): δ (ppm) = 153.0, 121.0 – 102.3 (m), 72.9, 71.6, 69.9, 41.3, 31.9 (t, $J = 20.9$ Hz). ¹⁹F NMR (376 MHz, CDCl₃): δ (ppm) = δ -80.8 (tt, $J = 10.0, 2.6$ Hz), -112.3 – -112.5 (m), -113.1 (tt, $J = 14.3, 4.3$ Hz), -113.7 (tq, $J = 13.3, 4.3$ Hz), -114.3 – -114.5 (m), -121.7 (dp, $J = 24.4, 9.3, 6.5$ Hz), -122.8 (tdd, $J = 22.9, 10.3, 6.0$ Hz), -123.6 (dddq, $J = 20.6, 12.7, 9.0, 5.0, 4.4$ Hz), -126.0 – -126.2 (m). APCI-HRMS calculated $m/z = 542.9490$, found $m/z = 542.9486$ for [C₁₂H₈F₁₃IO + H]⁺. Elemental analysis for C₁₂H₈F₁₃IO (% calc'd, % found): C (26.59, 26.36), H (1.49, 1.46).

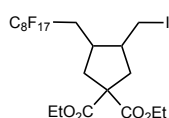
Z-Isomer (**15c**):

$R_f = 0.65$ (*n*-heptane:EtOAc, 5:1 v/v, visualised with UV/KMnO₄). ¹H NMR (400 MHz, CDCl₃): δ (ppm) = 6.13 (td, $J = 2.7, 2.0$ Hz, 1H), 4.36 – 4.19 (m, 3H), 3.75 (dd, $J = 9.1, 7.0$ Hz, 1H), 3.11 (dtt, $J = 8.6, 3.4, 1.8$ Hz, 1H), 2.52 – 2.32 (m, 1H), 2.31 – 2.11 (m, 1H). ¹³C NMR (101 MHz, CDCl₃): δ (ppm) = 153.1, 120.1 – 100.2 (m), 75.8, 75.0, 68.9, 39.6, 33.2 (t, $J = 21.5$

Hz). ^{19}F NMR (376 MHz, CDCl_3): δ (ppm) = -80.8 (tt, J = 9.9, 2.6 Hz), -111.8 (tt, J = 14.3, 3.7 Hz), -112.5 (tp, J = 14.7, 3.7 Hz), -113.5 (tq, J = 13.8, 3.7 Hz), -114.2 (tt, J = 12.8, 3.0 Hz), -121.6 – -121.9 (m), -122.7 – -123.0 (m), -123.4 (dpt, J = 20.1, 8.3, 3.2 Hz), -126.1 (ddq, J = 18.4, 10.9, 3.5 Hz). APCI-HRMS calculated m/z = 542.9490, found m/z = 542.9486 for $[\text{C}_{12}\text{H}_8\text{F}_{13}\text{IO} + \text{H}]^+$. Elemental analysis for $\text{C}_{12}\text{H}_8\text{F}_{13}\text{IO}$ (% calc'd, % found): C (26.59, 26.39), H (1.49, 1.47).

Investigation of the Radical Nature of the visible light-mediated ATRA reaction of alkyl halides to alkenes & alkynes *via* oxidative quenching of $[\text{Fe}(\text{btz})_3](\text{PF}_6)_3$

(±)-diethyl 3-(perfluorooctyl)-methyl-4-(iodomethyl)cyclopentane-1,1-dicarboxylate (**16**)

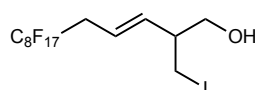


(**16**)

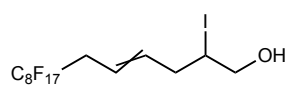
Procedure B was applied using diethyl 2,2-diallylmalonate (60.4 μL , 0.25 mmol, 1 equiv.), perfluorooctyl iodide (87.7 μL , 0.33 mmol, 1.33 equiv.), $[\text{Fe}(\text{btz})_3](\text{PF}_6)_3$ (5.7 mg, 3.8 μmol , 0.015 equiv.) and acetonitrile (3.5 mL). Purification by silica gel chromatography (*n*-heptane:EtOAc 50:1 – 20:1) gave the product (**16**) (189 mg, 96 %) as a colourless oil. The NMR-data was in accordance with literature data.^[7a]

R_f = 0.35 (*n*-heptane:EtOAc 10:1, UV-active, visualised with KMnO_4). ^1H NMR (400 MHz, CDCl_3) δ (ppm) = 4.29 – 4.13 (m, 4H), 3.16 (dd, J = 10.0, 5.5 Hz, 1H), 3.04 (t, J = 9.7 Hz, 1H), 2.67 – 2.46 (m, 4H), 2.37 – 1.94 (m, 4H), 1.25 (td, J = 7.1, 4.6 Hz, 6H). ^{13}C NMR (101 MHz, CDCl_3) δ (ppm) = 172.4, 172.1, 123.0 – 104.1 (m), 62.0, 61.9, 58.4, 45.6, 39.9, (d, J = 2.5 Hz), 35.5, 29.84 (t, J = 21.6 Hz), 14.1, 14.0, 5.6. ^{19}F NMR (376 MHz, CDCl_3) δ (ppm) = -80.7 (t, J = 9.9 Hz), -111.5 – -115.0 (m), -121.6, -121.9, -122.7, -123.4, -126.1. HRMS (ESI-TOF) calc'd for $[\text{C}_{21}\text{H}_{20}\text{F}_{17}\text{IO}_4 + \text{Na}]^+$ 808.0033; found 808.0018.

(*E*)-5-perfluorooctyl-2-(iodomethyl)pent-3-en-1-ol (**17a**) and (*E*)-6-perfluorooctyl-2-iodohex-4-en-1-ol (**17b**)



(**17a**)



(**17b**)

Procedure B was applied using *trans*-(2-vinylcyclopropyl)methanol **17** (25.7 mg, 0.25 mmol, 1 equiv.), perfluorooctyl iodide (87.7 μL , 0.33 mmol, 1.33 equiv.), $[\text{Fe}(\text{btz})_3](\text{PF}_6)_3$ (5.7 mg, 3.8 μmol , 0.015 equiv.) and acetonitrile (3.5 mL). Purification by silica gel chromatography

(*n*-heptane:EtOAc 5:1) gave (*E*)-6-perfluorooctyl-2-iodohex-4-en-1-ol (**17a**) (58 mg, 36 %) and 5-perfluorooctyl-2-(iodomethyl)pent-3-en-1-ol (**17b**) (61 mg, 38 %), both as sticky white solids.

(*E*)-6-perfluorooctyl-2-iodohex-4-en-1-ol (**17a**):

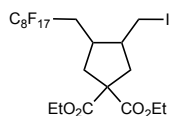
$R_f = 0.15$ (*n*-heptane:EtOAc 5:1, UV-active, Visualised with KMnO_4). $^1\text{H NMR}$ (400 MHz, CDCl_3) δ (ppm) = 5.62 (q, $J = 2.8$ Hz, 2H), 3.68 (dd, $J = 6.0, 1.3$ Hz, 2H), 3.39 – 3.21 (m, 2H), 2.98 – 2.78 (m, 2H), 2.52 – 2.39 (m, 1H). $^{13}\text{C NMR}$ (101 MHz, CDCl_3) δ (ppm) = 137.5, 120.7 (t, $J = 4.4$ Hz), 120.3 – 106.6 (m), 65.3, 46.3, 35.0 (t, $J = 22.6$ Hz), 7.9. $^{19}\text{F NMR}$ (376 MHz, CDCl_3) δ (ppm) = -80.72 (t, $J = 9.9$ Hz), -113.1, -121.7, -121.9, -122.7, -122.9, -126.1. HRMS (ESI-TOF) calc'd for $[\text{C}_{14}\text{H}_{10}\text{F}_{17}\text{IO} + \text{Cl}]^-$ 678.9193; found 678.9207. Elemental analysis (% calc'd, % found for $\text{C}_{14}\text{H}_{10}\text{F}_{17}\text{IO}$): C (26.11, 26.22), H (1.56, 1.67).

5-perfluorooctyl-2-(iodomethyl)pent-3-en-1-ol (**17b**):

$R_f = 0.18$ (*n*-heptane:EtOAc 5:1, UV-active, Visualised with KMnO_4). $^1\text{H NMR}$ (400 MHz, CDCl_3) δ (ppm) = 5.86 – 5.56 (m, 2H), 4.20 (dq, $J = 7.8, 5.6$ Hz, 1H), 3.75 (dd, $J = 5.5, 1.6$ Hz, 2H), 2.91 (td, $J = 18.3, 7.3$ Hz, 2H), 2.82 – 2.61 (m, 2H). $^{13}\text{C NMR}$ (101 MHz, CDCl_3) δ (ppm) (mixture of isomers) = 135.8, 135.8, 120.5, 120.0, 119.6-107.5 (m) 67.9, 65.5, 41.8, 39.3, 37.6, 34.9, 30.3, 7.4. $^{19}\text{F NMR}$ (376 MHz, CDCl_3) δ (ppm) = -80.72 (t), -112.56 – -113.23 (m), -121.49 – -122.01 (m), -122.57 – -122.80 (m), -122.85 – -123.30 (m), -125.84 – -126.30 (m). HRMS (ESI-TOF) calc'd for $[\text{C}_{14}\text{H}_{10}\text{F}_{17}\text{IO} + \text{Cl}]^-$ 678.9193; found 678.9210. Elemental analysis (% calc'd, % found for $\text{C}_{14}\text{H}_{10}\text{F}_{17}\text{IO}$): C (26.11, 26.18), H (1.56, 1.55), N (0.00, 0.00).

Investigation of the Radical Nature of the visible light-mediated ATRA reaction of alkyl halides to alkenes & alkynes *via* reductive quenching of $[\text{Fe}(\text{btz})_3](\text{PF}_6)_3$

(±)-diethyl 3-(perfluorooctyl)-methyl-4-(iodomethyl)cyclopentane-1,1-dicarboxylate (**16**)

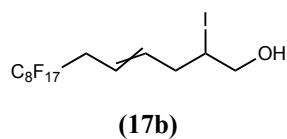
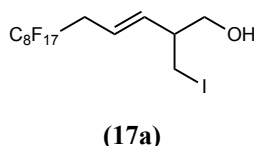


(**16**)

Procedure A was applied using diethyl 2,2-diallylmalonate (60.4 μL , 0.25 mmol, 1 equiv.), perfluorooctyl iodide (87.7 μL , 0.33 mmol, 1.33 equiv.), $[\text{Fe}(\text{btz})_3](\text{PF}_6)_3$ (1.92 mg, 1.3 μmol , 0.005 equiv.) and acetonitrile:methanol (4:3, 3.5 mL) and irradiation for 20 min. Purification by silica gel chromatography (*n*-heptane:EtOAc 40:1 – 20:1) gave the product (**16**) (153 mg, 78 %) as a colourless oil. The NMR-data was in accordance with literature data.^[7a]

$R_f = 0.35$ (*n*-heptane:EtOAc 10:1, UV-active, visualised with KMnO_4). ^1H NMR (400 MHz, CDCl_3) δ (ppm) = 4.29 – 4.13 (m, 4H), 3.16 (dd, $J = 10.0, 5.5$ Hz, 1H), 3.04 (t, $J = 9.7$ Hz, 1H), 2.67 – 2.46 (m, 4H), 2.37 – 1.94 (m, 4H), 1.25 (td, $J = 7.1, 4.6$ Hz, 6H). ^{13}C NMR (101 MHz, CDCl_3) δ (ppm) = 172.4, 172.1, 123.0 – 104.1 (m), 62.0, 61.9, 58.4, 45.6, 39.9, 38.5 (d, $J = 2.5$ Hz), 35.5, 29.84 (t, $J = 21.6$ Hz), 14.1, 14.0, 5.6. ^{19}F NMR (376 MHz, CDCl_3) δ (ppm) = -80.7 (t, $J = 9.9$ Hz), -111.5 – -115.0 (m), -121.6, -121.9, -122.7, -123.4, -126.1. HRMS (ESI-TOF) calc'd for $[\text{C}_{21}\text{H}_{20}\text{F}_{17}\text{IO}_4 + \text{Na}]^+$ 808.0033; found 808.0022.

(*E*)-5-perfluorooctyl-2-(iodomethyl)pent-3-en-1-ol (**17a**) and (*E*)-6-perfluorooctyl-2-iodohex-4-en-1-ol (**17b**)



Procedure A was applied using *trans*-(2-vinylcyclopropyl)methanol **17** (25.7 mg, 0.25 mmol, 1 equiv.), perfluorooctyl iodide (87.7 μL , 0.33 mmol, 1.33 equiv.), $[\text{Fe}(\text{btz})_3](\text{PF}_6)_3$ (1.91 mg, 1.3 μmol , 0.005 equiv.) and acetonitrile:methanol (4:3, 3.5 mL) and irradiation for 20 min. Purification by silica gel chromatography (*n*-heptane:EtOAc 5:1) gave (*E*)-6-perfluorooctyl-2-iodohex-4-en-1-ol (**17b**) (50 mg, 31 %) and 5-perfluorooctyl-2-(iodomethyl)pent-3-en-1-ol (**17a**) (63 mg, 39 %), both as sticky white solids.

(*E*)-6-perfluorooctyl-2-iodohex-4-en-1-ol (**17a**):

$R_f = 0.15$ (*n*-heptane:EtOAc 5:1, UV-active, visualised with KMnO_4). ^1H NMR (400 MHz, CDCl_3) δ (ppm) = 5.62 (q, $J = 2.8$ Hz, 2H), 3.68 (dd, $J = 6.0, 1.3$ Hz, 2H), 3.39 – 3.21 (m, 2H), 2.98 – 2.78 (m, 2H), 2.52 – 2.39 (m, 1H). ^{13}C NMR (101 MHz, CDCl_3) δ (ppm) = 137.5, 120.7 (t, $J = 4.4$ Hz), 120.3 – 106.6 (m), 65.3, 46.3, 35.0 (t, $J = 22.6$ Hz), 7.9. ^{19}F NMR (376 MHz, CDCl_3) δ (ppm) = -80.72 (t, $J = 9.9$ Hz), -113.1, -121.7, -121.9, -122.7, -122.9, -126.1.

5-perfluorooctyl-2-(iodomethyl)pent-3-en-1-ol (**17b**):

$R_f = 0.18$ (*n*-heptane:EtOAc 5:1, UV-active, visualised with KMnO_4). ^1H NMR (400 MHz, CDCl_3) δ (ppm) = 5.86 – 5.56 (m, 2H), 4.20 (dq, $J = 7.8, 5.6$ Hz, 1H), 3.75 (dd, $J = 5.5, 1.6$ Hz, 2H), 2.91 (td, $J = 18.3, 7.3$ Hz, 2H), 2.82 – 2.61 (m, 2H). ^{13}C NMR (101 MHz, CDCl_3) δ (ppm) (mixture of isomers) = 135.8, 135.8, 120.5, 120.0, 119.6-107.5 (m) 67.9, 65.5, 41.8, 39.3, 37.6, 34.9, 30.3, 7.4. ^{19}F NMR (376 MHz, CDCl_3) δ (ppm) = -80.72 (t), -112.56 – -113.23 (m), -121.49 – -122.01 (m), -122.57 – -122.80 (m), -122.85 – -123.30 (m), -125.84 – -126.30 (m).

Tracing of the visible light-mediated ATRA of perfluorooctyl iodide to 5-hexen-1-ol *via* reductive & oxidative quenching of $[\text{Fe}(\text{btz})_3](\text{PF}_6)_3$ using UV-vis absorption spectroscopy

Samples were contained in a 10×10 mm fluorescence quartz cuvette with a screw cap and PTFE septum and deaerated by flushing with Ar (g) for 10 min. The reaction mixtures were prepared according to Procedure A & Procedure B respectively, maintaining the same concentrations. All samples, where specifically stated, where illuminated in the cuvette as a reaction vessel using an EvoluChem LED Spotlight (18 W, 525–530 nm) purchased from HepatoChem Inc.

UV-vis absorption spectra were recorded with a Probe Drum Lab-in-a-box spectrometer.

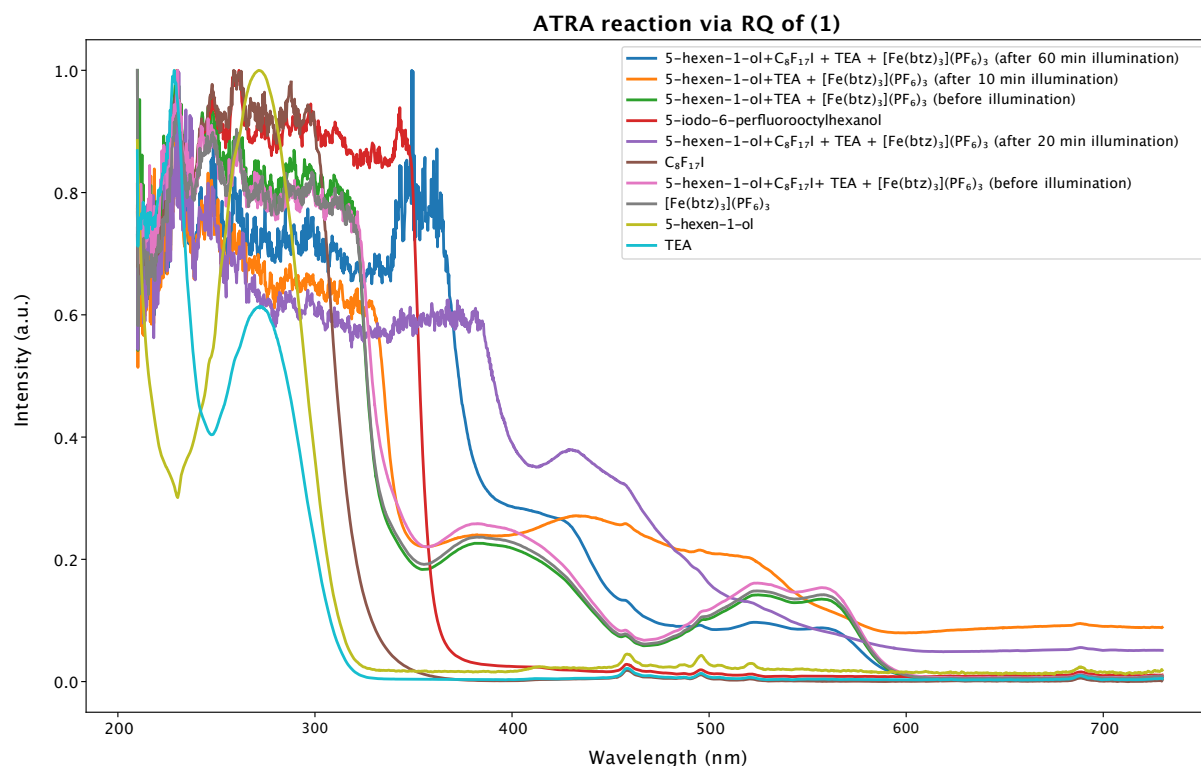


Figure S6: Tracking of the visible light-mediated ATRA of perfluorooctyl iodide to 5-hexen-1-ol *via* reductive quenching (RQ) of $[\text{Fe}(\text{btz})_3](\text{PF}_6)_3$ using UV-vis absorption spectroscopy under the reaction conditions described in Procedure A.

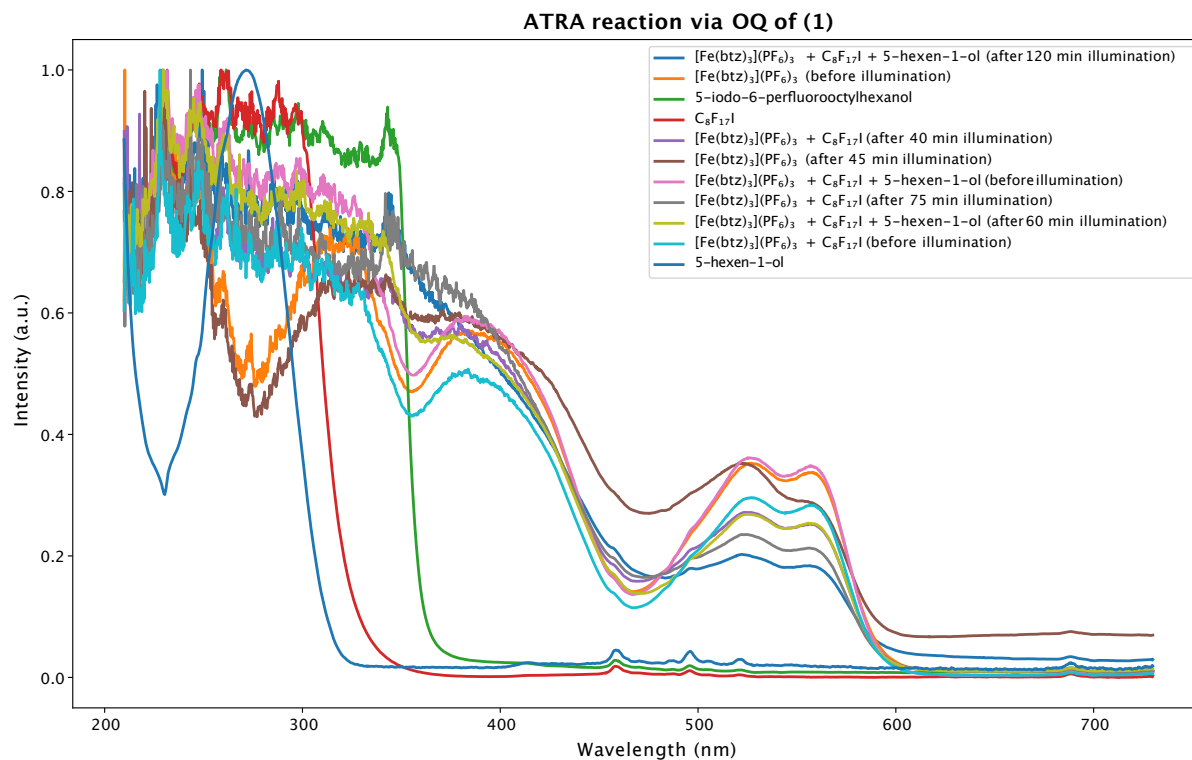


Figure S7: Tracking of the visible light-mediated ATRA of perfluorooctyl iodide to 5-hexen-1-ol *via* oxidative quenching (OQ) of [Fe(btz)₃](PF₆)₃ using UV-vis absorption spectroscopy under the reaction conditions described in Procedure B.

Wavelength switching experiment – Fe(III)/*Fe(III)/Fe(II)/*Fe(II)

Two samples (1.75 mL each) were prepared following Procedure A using 5-hexen-1-ol – initially without addition of the halide reagent C₈F₁₇I – and charged to two 4 mL-glass vials topped with a PTFE septum screw cap. The reaction solutions were then deaerated by flushing with Ar (g) for 10 min. Both vials were then illuminated at 525 nm for 25 min using an LED bar (Nichia NSPG500DS). After a colour change from red to brown, indicative of the formation of [Fe(btz)₃]²⁺ (shown by UV vis absorption (**Figure 2**, brown)), C₈F₁₇I was added to both vials under argon. While one of the vials was thereafter stored in the dark (**H**), the other (**G**) was then illuminated at 700 nm (LED bar, Roithner ELD-700-524) for 60 min. Within 5 min the illuminated sample had regained the initial red colouring (**Figure 2**, red), which was maintained throughout further illumination, whereas the dark sample exhibited no visible colour or spectral change. The conversion of starting material was quantified *via* ¹H NMR spectroscopy, which showed that in the dark sample (**H**) none of the starting material was converted (**Figure S93–Figure S95**), whereas in sample (**G**) 5 % NMR yield were noted (**Figure S90–Figure S92**).

Quantum Yield Measurements for the ATRA reaction in the reductive and oxidate quenching route

The quantum yields of the reductive and oxidative ATRA reaction were determined using a method developed by Pitre *et al.*^[10], wherein the oxidation of 9,10-diphenylanthracene (DPA) catalysed by $[\text{Ru}(\text{bpy})_3]\text{Cl}_2$ in acetonitrile was used to quantify the number of moles of photons absorbed by the sample. All samples were irradiated for 5 min in the same slot at 530 nm (3.02W/slot) in a TAK120 AC photoreactor purchased from HK Testsysteme GmbH. UV-vis absorption measurements were performed on a Probe Drum Lab-in-a-box spectrometer and samples were contained in a 10 mm quartz cuvette.

The concentrations of $[\text{Ru}(\text{bpy})_3]\text{Cl}_2 \cdot 6 \text{H}_2\text{O}$ were chosen as to match the absorbance of $[\text{Fe}(\text{btz})_3](\text{PF}_6)_3$ (**1**), when using the respective concentrations employed in the RQ (0.36 mM (**1**)) and OQ (1.07 mM (**1**)) ATRA reaction. All reactions were performed in duplicates and absorption spectra of solutions of $[\text{Ru}(\text{bpy})_3]\text{Cl}_2 \cdot 6 \text{H}_2\text{O}$ in MeCN in the same concentrations as used for the actinometry were recorded as to ensure that the absorbance at 372 nm – the wavelength of interest for quantifying the consumption of DPA – was lower than in the reaction solution after the reaction time of 5 min. This was done to ensure that the consumption of the starting material was being determined accurately.

The reaction solutions were prepared under exclusion of light and stored in amber glass vials before transferring to the reaction vessel and the cuvette for UV-vis spectroscopy.

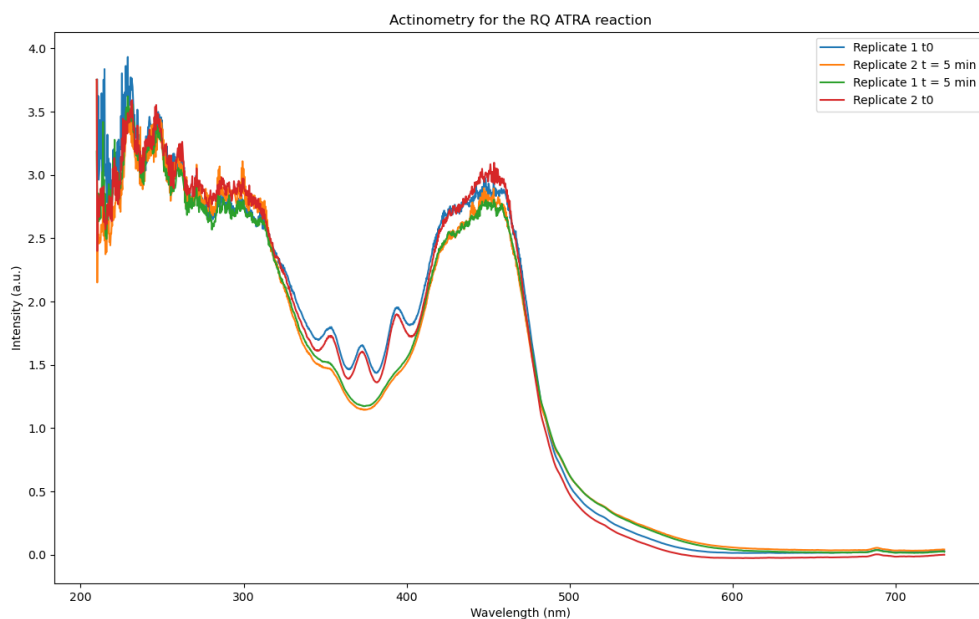


Figure S8: Absorption spectra for the oxidation of DPA using $[\text{Ru}(\text{bpy})_3]\text{Cl}_2 \cdot 6 \text{H}_2\text{O}$; The concentration of Ru-PC was chosen as to match the absorption of $[\text{Fe}(\text{III})(\text{btz})_3](\text{PF}_6)_3$ in the concentration used in Procedure A (RQ).

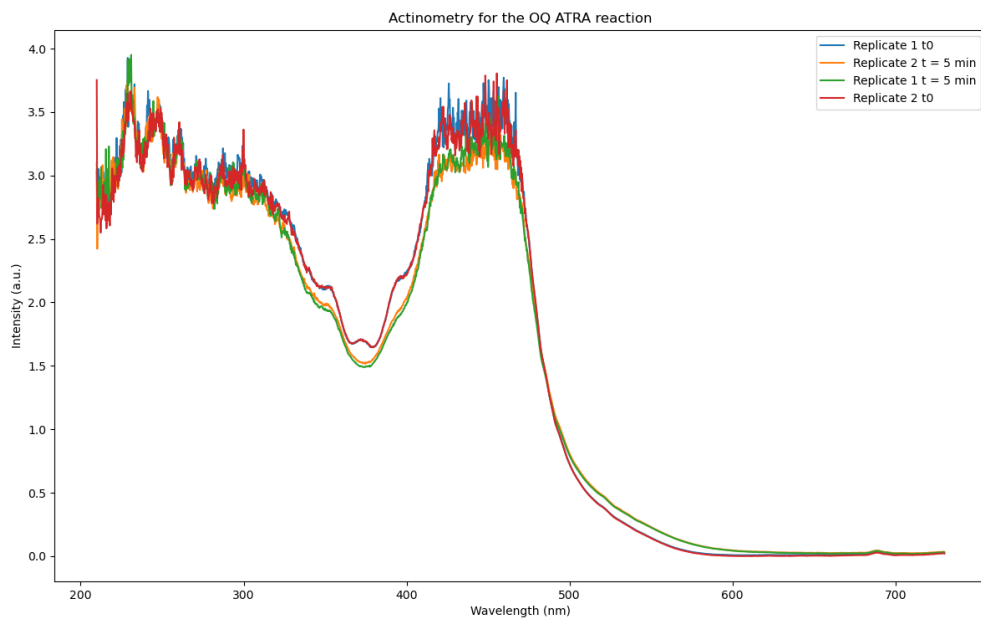


Figure S9: Absorption spectra for the oxidation of DPA using $[\text{Ru}(\text{bpy})_3]\text{Cl}_2 \cdot 6 \text{H}_2\text{O}$; The concentration of Ru-PC was chosen as to match the absorption of $[\text{Fe}(\text{III})(\text{btz})_3](\text{PF}_6)_3$ in the concentration used in Procedure B (OQ).

The calculations were done following the procedure described in the reference manual^[10] and gave the results afforded in **Table S15**.

$$n \text{ (mol of DPA consumed)} = \left(\frac{A_{\text{initial}} - A_{\text{final}}}{\epsilon_{372 \text{ nm}} l} \right) \cdot V \quad (\text{Eq. 1})$$

$$\frac{N_{\text{hv}}}{t} = \frac{n \text{ (moles of DPA consumed)}}{\Phi_{\text{actinometer}} t} \quad (\text{Eq. 2})$$

$$\Phi_{\text{ATRA}} = \frac{n \text{ (moles of ATRA product formed)}}{t} \cdot \left(\frac{N_{\text{hv}}}{t} \right)^{-1} \quad (\text{Eq. 3})$$

- A_{initial} ...absorbance of the solution at 372 nm before irradiation
- A_{final} ...absorbance of the solution at 372 nm after 5 min of irradiation
- $\epsilon_{372 \text{ nm}}$...molar extinction coefficient of DPA at 372 nm in acetonitrile ($11100 \text{ M}^{-1}\text{cm}^{-1}$)
- l ...path length of the cuvette (cm)
- V ...Volume (L)
- $\frac{N_{\text{hv}}}{t}$...moles of absorbed photons by sample per time unit
- $\Phi_{\text{actinometer}}$...quantum yield of the actinometer (0.019)
- Φ_{ATRA} ...quantum yield of the ATRA reaction

Table S14: Data for the determination of the Quantum Yield for the reductively (RQ) and oxidatively quenched (OQ) ATRA reaction of 5-hexen-1-ol with $\text{C}_8\text{F}_{17}\text{I}$ using Procedure A and B respectively (^aThe amount of ATRA product formed was determined *via* ^1H NMR spectroscopy using mesitylene as internal standard and corrected by a factor of 0.21 to account for the differences in sample volume compared to the actinometer reaction.).

RQ			
	$A_{\text{initial}}(372 \text{ nm})$	$A_{\text{final}}(372 \text{ nm})$	$n \text{ (moles of ATRA product produced in 5 min)}^{\text{a}}$
Replicate 1	1.6518	1.18	0.0378E-3
Replicate 2	1.5989	1.149	
OQ			
	$A_{\text{initial}}(372 \text{ nm})$	$A_{\text{final}}(372 \text{ nm})$	$n \text{ (moles of ATRA product produced in 10 min)}^{\text{a}}$
Replicate 1	1.7072	1.4946	0.0315E-3
Replicate 2	1.7037	1.5275	

Table S15: Results of the Quantum Yield Measurements for the reductively (RQ) and oxidatively quenched (OQ) ATRA reaction of 5-hexen-1-ol with $\text{C}_8\text{F}_{17}\text{I}$ using Procedure A and B respectively. (^aThe amount of DPA consumed was determined using Eq. 1. Aliquots of 750 μL of the reaction solutions were diluted for UV/vis absorption spectroscopy with a dilution factor of 2 for the RQ and 4.67 for the OQ cycle. ^bThe initially obtained quantum yield was divided by 2 to account for the two photons involved in the product formation in the RQ route and the corresponding result is given here under Φ).

	$n(\text{DPA consumed}) \text{ (mol)}^{\text{a}}$	$(N_{\text{hv}})/t$	Φ^{b}
RQ	6,38E-08	1,12E-08	6
	6,08E-08	1,07E-08	6
OQ	$n(\text{DPA consumed}) \text{ (mol)}^{\text{a}}$	$(N_{\text{hv}})/t$	Φ
	6,70E-08	1,18E-08	4
	5,56E-08	9,75E-09	5

The obtained quantum yields provide strong evidence for a chain propagation mechanism^[11] being operative in both the reductive ($\phi = 6$ (RQ)) as well as the oxidative ($\phi = 4.5$ (OQ)) ATRA reaction, as $\Phi \gg 1$.

Investigation of the longevity of the photoredox catalysts

In order to test the longevity of **(1)** in both the reductive and the oxidative cycle the model reaction (alkene: 5-hexen-1-ol, R-X: C₈F₁₇I) was conducted using the conditions described in Procedure A and B respectively. Reaction times were chosen according to the optimisation experiments (RQ: **Table S1-Table S4**, OQ: **Table S9**).

After the initial reaction, the conversion of starting material was determined *via* ¹H NMR-spectroscopy using mesitylene as an internal standard. Thereafter, the required amounts of alkene, R-X and – where applicable – TEA were added and a new sample for NMR analysis was taken as a reference point before irradiating again.

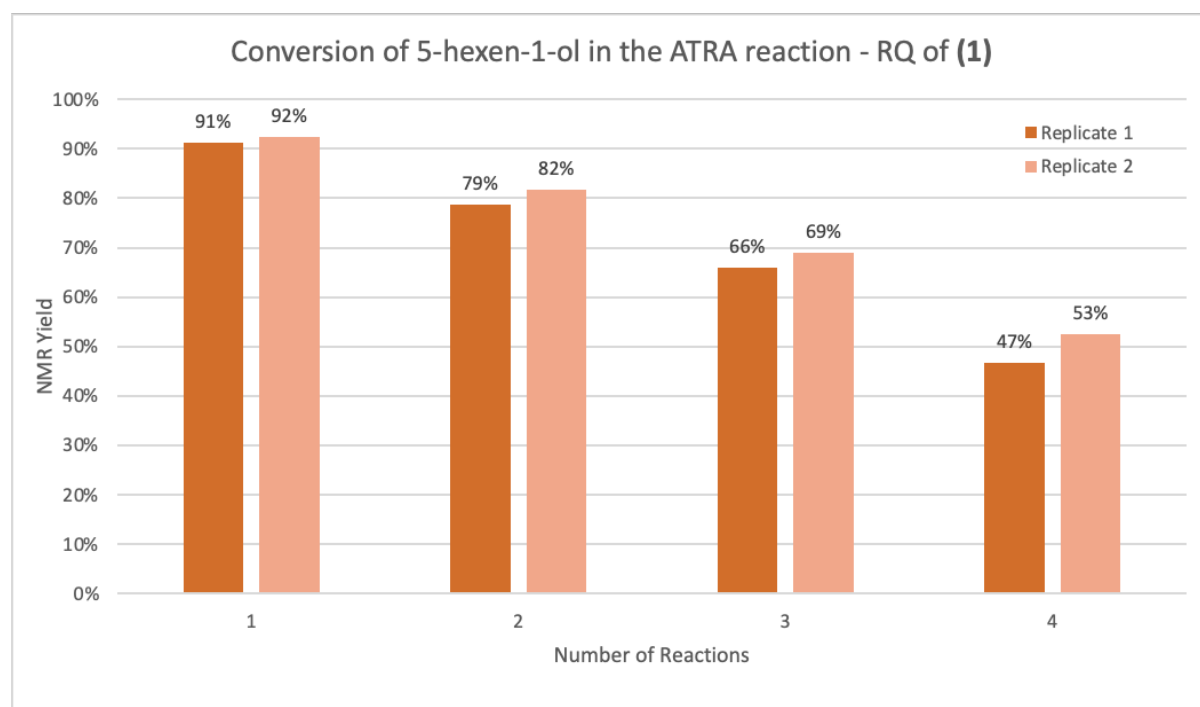


Figure S10: Investigation of the longevity of **(1)** in the reductive quenching cycle by repeated addition of the starting materials to the reaction mixture in intervals of 10 min.

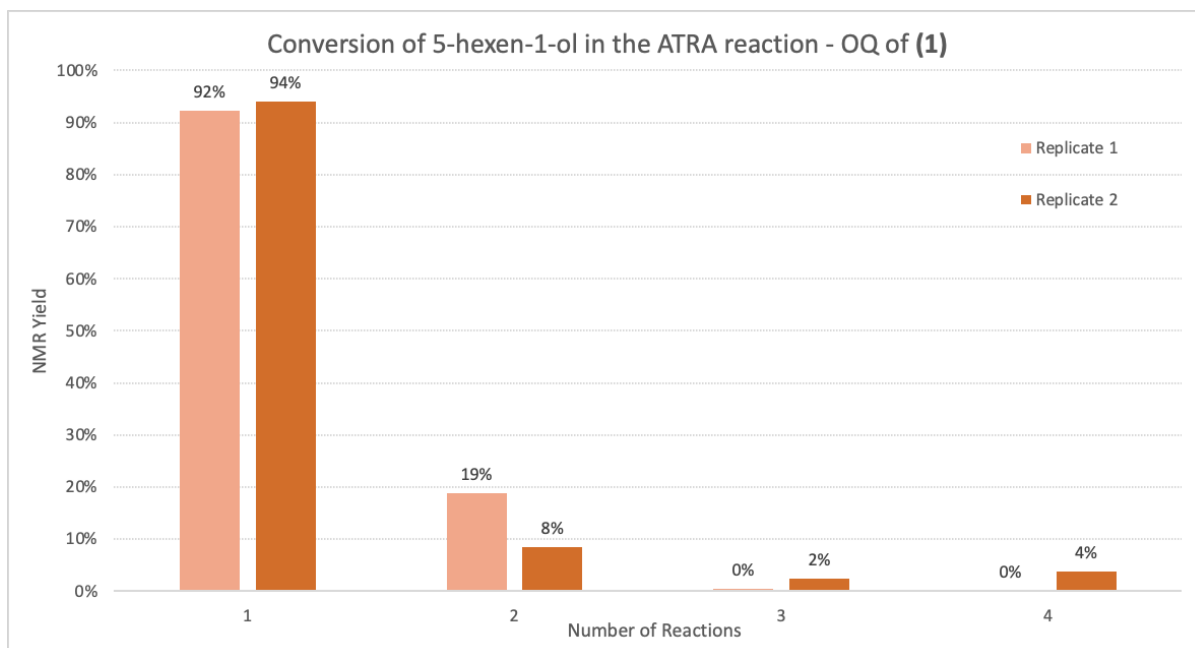


Figure S11: Investigation of the longevity of (1) in the oxidative quenching cycle by repeated addition of the starting materials to the reaction mixture in intervals of 40 min.

Absorption spectra of $[\text{Fe(III)}(\text{btz})_3]^{3+}$ and $[\text{Fe(II)}(\text{btz})_3]^{2+}$

The absorption spectra of $[\text{Fe(III)}(\text{btz})_3]^{3+}$ and $[\text{Fe(II)}(\text{btz})_3]^{2+}$ in MeCN:MeOH (4:3) are shown in **Figure S12**. The spectra are similar to spectra in acetonitrile that have been previously reported^[1b] and were used to calculate the difference spectra superimposed on the transient absorption spectra (**Figure 3** and **Figure 4**).

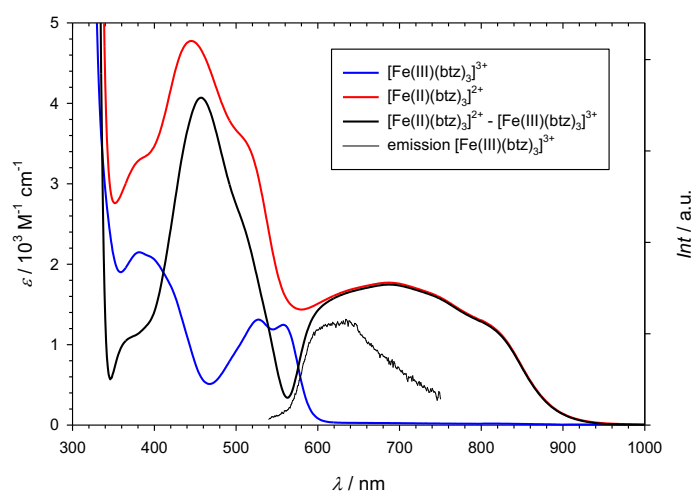


Figure S12: Absorption and emission spectra of $[\text{Fe(III)}(\text{btz})_3](\text{PF}_6)_3$ **1** and absorption spectrum of $[\text{Fe(II)}(\text{btz})_3](\text{PF}_6)_2$ **2** in MeCN:MeOH (4:3).

Excited State Lifetimes of $[\text{Fe(III)(btz)}_3]^{3+}$ and $[\text{Fe(II)(btz)}_3]^{2+}$

Excited state lifetimes of the iron complexes in MeCN:MeOH (4:3) were determined through femtosecond transient absorption spectroscopy. The transient spectra of $[\text{Fe(III)(btz)}_3]^{3+}$ (**Figure S13**) show a excited state absorption band peaking at about 470 nm next to the ground state bleach around 550 nm and additional broad transient absorption at wavelengths >570 nm. The transient spectra are very similar to the previously reported spectra in MeCN^[1a] and in good correspondence to the LMCT character of the excited state considering the difference between Fe(III) and Fe(II) ground state spectra and attributing the intense transient absorption below 400 nm to the ligand radical cation. A fit of the 465 nm kinetics returned a lifetime of 94 ps, which is within error margins essentially identical to what was observed by transient absorption in MeCN (101 ± 7 ps).^[1a]

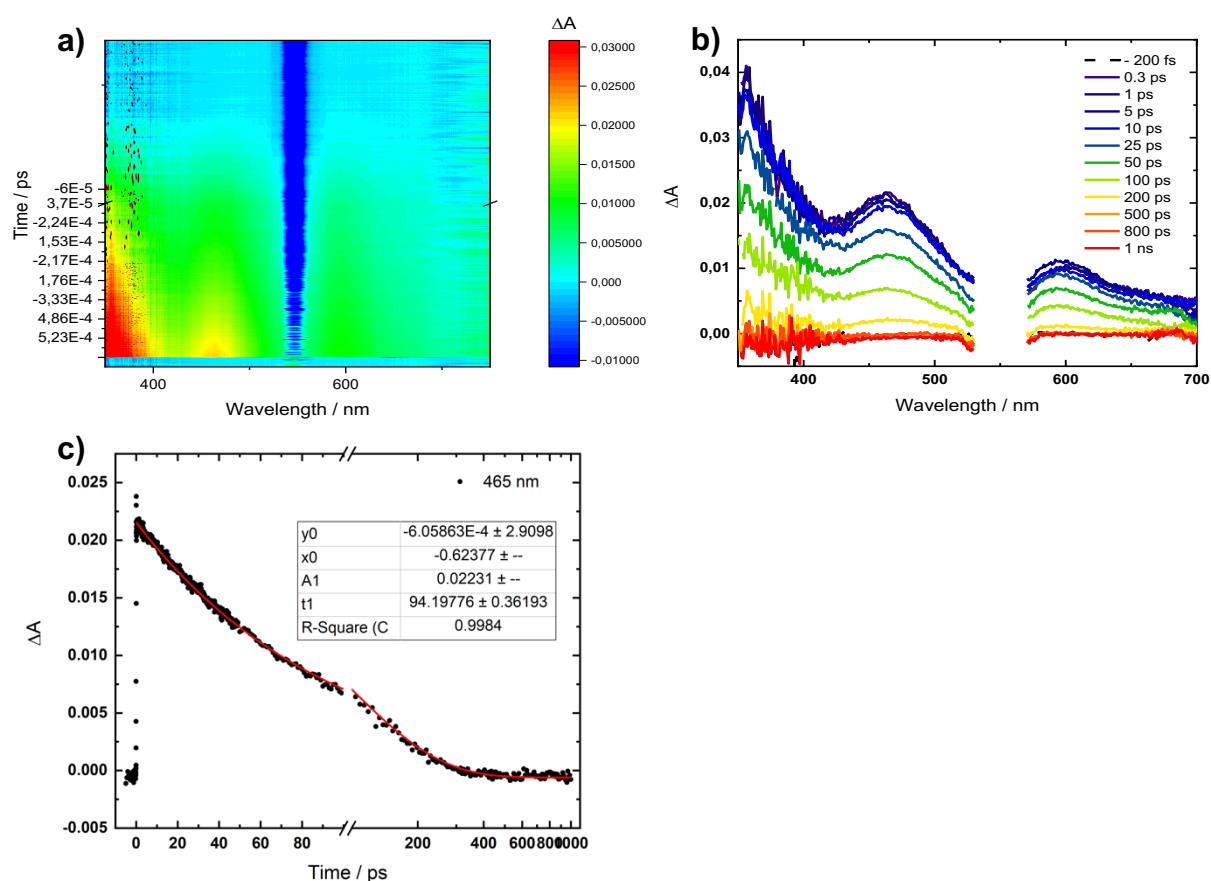


Figure S13: a) Contour graph and b) transient absorption spectra ($\lambda_{\text{ex}} = 550$ nm, 3.05 ± 0.01 mW, 10 scans averaged) of $[\text{Fe(III)(btz)}_3](\text{PF}_6)_3$ **1** in MeCN:MeOH (4:3); c) kinetics selected at 465 nm (black dots) and corresponding fit (red line).

The fs-TAS spectra of $[\text{Fe(II)(btz)}_3]^{2+}$ show a broad ground state bleach (430 – 650 nm) that is superimposed on a pronounced excited state absorption below 430 nm (with a peak at 370 nm)

and a minor excited state absorption between 550 and 600 nm. Also for the Fe(II) complex the spectrum of the excited state is very similar to the reported spectrum in neat MeCN^[1b] and in good agreement with its MLCT character based on the differences between Fe(III) and Fe(II) ground state spectra and attributing the intense transient absorption at 370 nm to the ligand radical anion. Fits of the excited state decay (360 nm) and ground state recovery (640 nm) return a lifetime of around 340 ps, which is significantly shorter than the previously reported value observed in neat acetonitrile (528 ps).^[1b]

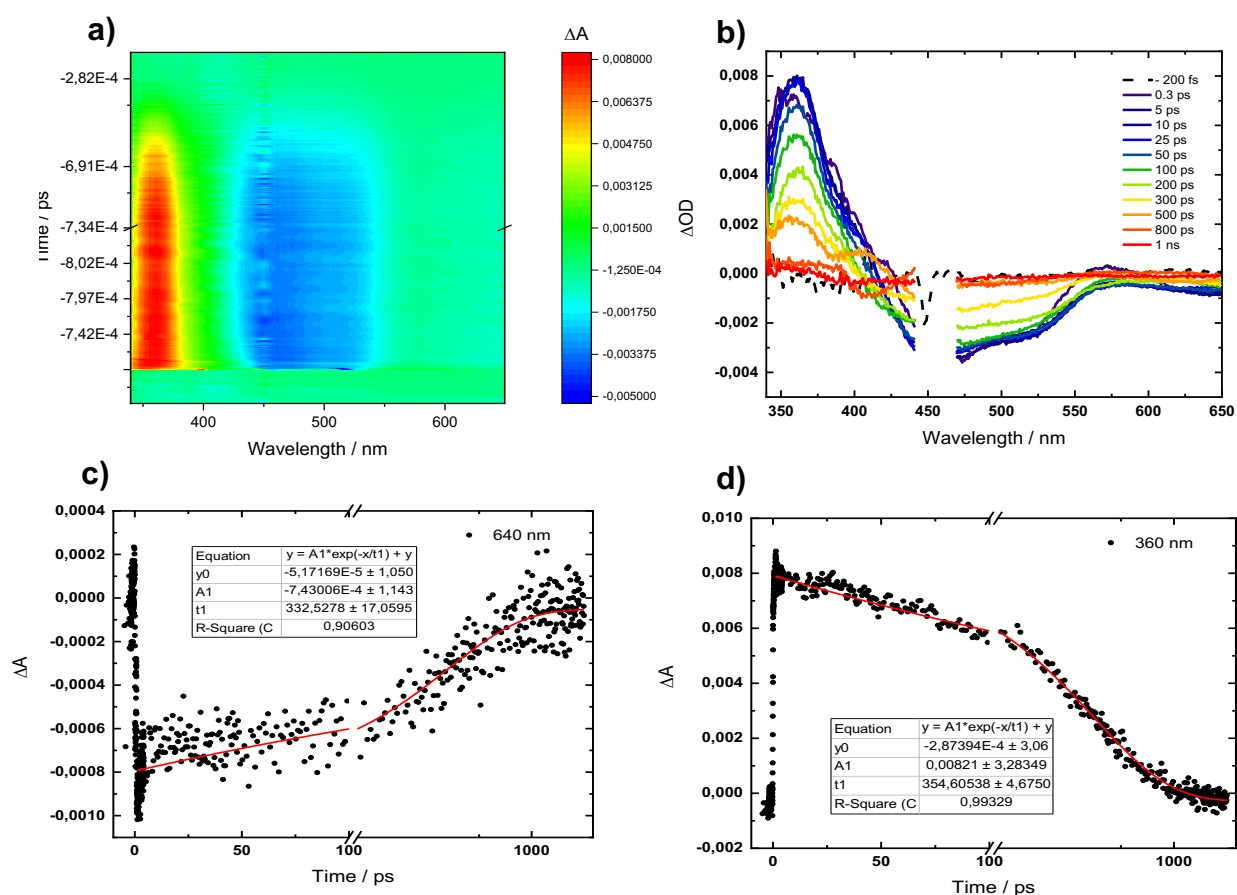


Figure S14: a) Contour graph and b) transient absorption spectra ($\lambda_{ex} = 440$ nm, 3.0 ± 0.4 mW, 10 scans averaged) of $[\text{Fe(II)(btz)}_3](\text{PF}_6)_2$ **2** in MeCN:MeOH (4:3); c) & d) kinetics selected at 640 nm and 360 nm (black dots) with corresponding fits (red lines), respectively.

Excited state reactivity of $[\text{Fe(III)(btz)}_3]^{3+}$ and $[\text{Fe(II)(btz)}_3]^{2+}$

The reactivity of the emissive $[\text{Fe(III)(btz)}_3]^{3+}$ towards the different reactants was inferred from steady state emission quenching. Stock solutions (25 mL) of $[\text{Fe(btz)}_3](\text{PF}_6)_3$ were prepared in either a solvent mixture of acetonitrile (spectroscopic grade Uvasol[®], $\geq 99.9\%$, from Merck) and methanol (ACS spectroscopic grade, $\geq 99.9\%$, from Merck) (volume ratio 4:3) or in neat acetonitrile, with concentrations that gave a UV-vis absorption of around 0.075 ± 0.005 at the excitation wavelength (525 nm). 1.5–2 mL of the solution was then transferred to a cuvette and

the quenchers were added straight into the cuvette with varying concentrations. UV-vis absorption and two emission spectra were taken for each quencher concentration and emission intensities were corrected for minor differences in absorbance at the excitation wavelength. Background measurements were collected for solutions containing only the quenchers at the same concentrations. The shown emission spectra are all averages of two measurements taken for each quencher concentration minus the background spectra. Stern-Volmer plots were obtained by taking the emission values at 620 nm after correction for minor differences in absorbance and all data points and error bars result from the average of the two measurements. In MeCN:MeOH (4:3) only TEA was found to quench the emission from $[\text{Fe(III)(btz)}_3]^{3+}$ (Figure S15). From the slope of the Stern-Volmer plot $K_{\text{SV}} = 0.81 \text{ M}^{-1}$ and the excited state lifetime of $\tau_0 = 94 \text{ ps}$ a bimolecular rate constant of $k_q = 8.4 \times 10^9 \text{ M}^{-1}\text{s}^{-1}$ and a quenching yield of $\eta_q = 0.31$ with 0.5 M TEA was obtained. No quenching could be observed with any of the other reactants up to concentrations equal to or above those used for the PRC reactions ($[\text{5-hexen-1-ol}]_{\text{max}} = 0.14 \text{ M}$, $[\text{C}_8\text{F}_{17}\text{I}]_{\text{max}} = 0.45 \text{ M}$) thereby excluding competing excited state reactions under the relevant conditions.

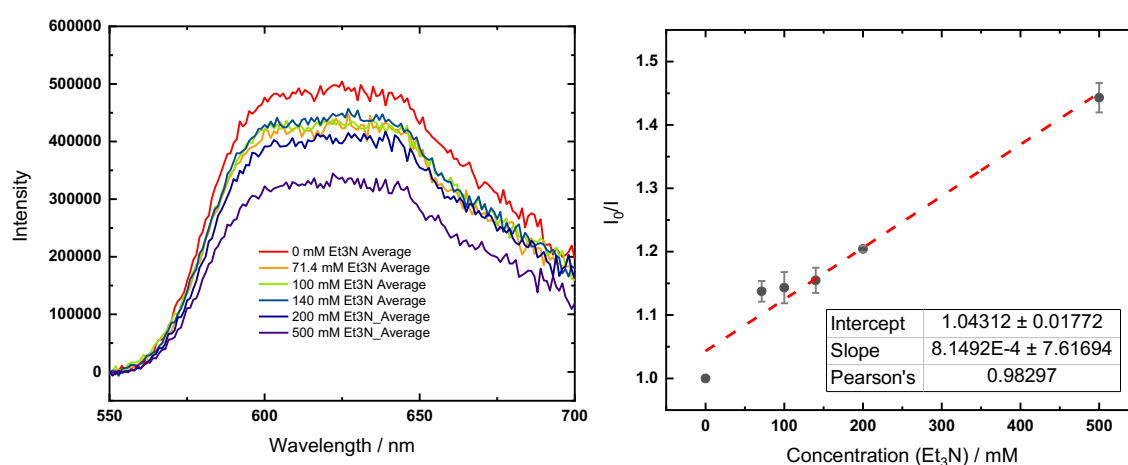


Figure S15: Quenching of $[\text{Fe(III)(btz)}_3]^{3+}$ by TEA in MeCN:MeOH (4:3).

In MeCN solution, the solvent used for the oxidative PRC reaction, very slight quenching of the excited $[\text{Fe(III)(btz)}_3]^{3+}$ by $\text{C}_8\text{F}_{17}\text{I}$ was observed for concentrations approaching the solubility limit of ca. 150 mM. At this concentration about 5-10 % of the excited states are quenched and from the slope of the Stern-Volmer plot $K_{\text{SV}} \approx 0.6 \text{ M}^{-1}$ and the excited state lifetime of $\tau_0 = 101 \text{ ps}$ a bimolecular rate constant of $k_q \approx 6 \times 10^9 \text{ M}^{-1}\text{s}^{-1}$ can be estimated. Like in MeCN:MeOH (4:3), 5-hexen-1-ol, did not quench the emission from $[\text{Fe(III)(btz)}_3]^{3+}$ in neat MeCN ($[\text{5-hexen-1-ol}]_{\text{max}} = 0.14 \text{ M}$).

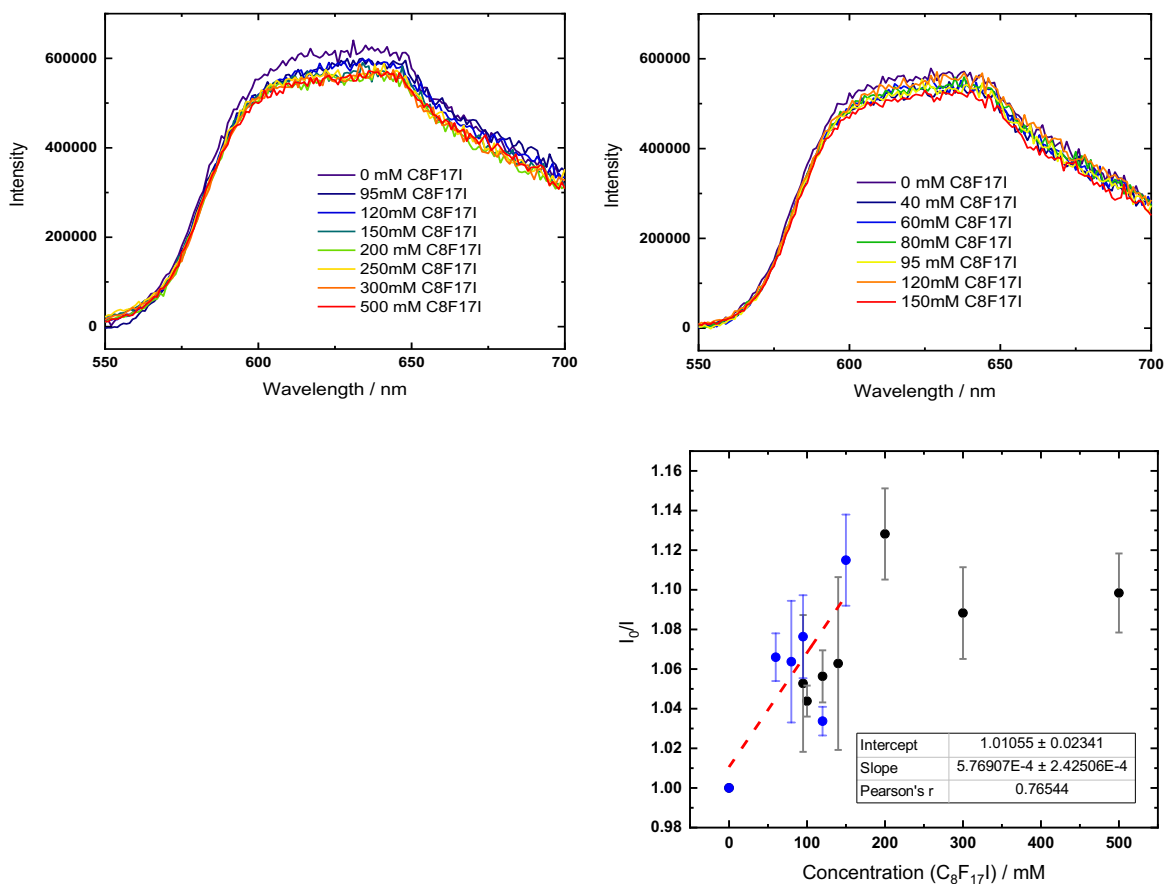


Figure S16: Quenching of $[\text{Fe}(\text{III})(\text{btz})_3]^{3+}$ by $\text{C}_8\text{F}_{17}\text{I}$ in MeCN.

The reactivity of the non-luminescent $[\text{Fe}(\text{II})(\text{btz})_3]^{2+}$ was inferred from laser flash photolysis experiments. In presence of $\text{C}_8\text{F}_{17}\text{I}$ (0.45 M) excitation with a ns laser pulse (650 nm or 465 nm) lead to instantaneous and irreversible transient absorption features that could be attributed to oxidative quenching (see Cage Escape Yields below and **Figure 4**).

Extended light exposure of $[\text{Fe}(\text{II})(\text{btz})_3]^{2+}$ in presence of $\text{C}_8\text{F}_{17}\text{I}$ led to quantitative conversion to $[\text{Fe}(\text{III})(\text{btz})_3]^{3+}$ (**Figure S17**). In control experiments, exposing a solution of $[\text{Fe}(\text{II})(\text{btz})_3]^{2+}$ to light without the electron acceptor or keeping a solution of $[\text{Fe}(\text{II})(\text{btz})_3]^{2+}$ and $\text{C}_8\text{F}_{17}\text{I}$ in the dark, no conversion of $[\text{Fe}(\text{II})(\text{btz})_3]^{2+}$ was observed.

Laser flash excitation of $[\text{Fe}(\text{II})(\text{btz})_3]^{2+}$ (465 nm) in presence of TEA (0.50 M) or 5-hexen-1-ol (0.14 M) in MeCN:MeOH (4:3) did not result in any detectable transient absorption between 400 and 750 nm. Any excited state reactions leading to products that could interfere with PRC reactions can therefore be excluded.

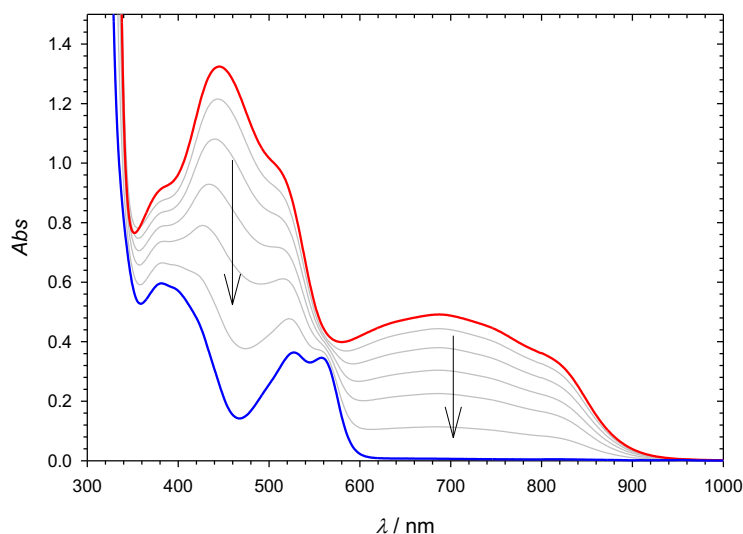


Figure S17: Oxidation of $[\text{Fe}(\text{II})(\text{btz})_3]^{2+}$ to $[\text{Fe}(\text{III})(\text{btz})_3]^{3+}$ with addition of 125 mM of $\text{C}_8\text{F}_{17}\text{I}$ in acetonitrile:methanol (4:3). Sample was prepared in a cuvette with 1 cm path length, left under room light and UV-vis absorption spectra were taken in time intervals, spanning 3.5 h.

Cage Escape Yields

Cage escape yields of quenching products were determined by laser flash photolysis from the magnitude of transient absorption after a ns laser flash. For those quenching reactions that lead to detectable transient absorption the electron transfer reactions were entirely irreversible and no charge recombination of the products was observable for at least 100 μs . As expected, no signs of absorption from the products of the sacrificial electron donor (TEA) or acceptor ($\text{C}_8\text{F}_{17}\text{I}$) was observed in the spectral range (400–750 nm) of the transient absorption data and quantification of the products could be based entirely on the well-established difference in extinction coefficients between the Fe(III) and Fe(II) states of the photocatalyst.

Due to the irreversible nature of the quenching reactions, care was taken to prepare the samples and perform all measurements with a minimum of light exposure. Transient absorption spectra were obtained after a single excitation pulse and the cuvette was thereafter purged with argon to ensure vigorous mixing of the sample before the next excitation. In this way, effects of sample depletion/product accumulation on the transient absorption spectra was avoided and the individual single shot spectra were finally averaged. $[\text{Ru}(\text{bpy})_3]^{2+}$ was used as actinometer to determine the number of photons absorbed by the sample and calculate the quantum yield of quenching products (**Table S16**).

Table S16: Cage escape yields of quenching products.^a

	$\lambda_{\text{ex}}/\text{nm}$	$A_{\text{Fe}}(\lambda_{\text{ex}})^{\text{d}}$	$\Delta A_{\text{Fe}}(452)^{\text{e}}$	$\Delta[\text{Fe}]/\text{M}^{\text{f}}$	$A_{\text{Ru}}(\lambda_{\text{ex}})^{\text{g}}$	$\Delta A_{\text{Ru}}(452)^{\text{h}}$	$\Delta[\text{Ru}]/\text{M}^{\text{i}}$	f^{j}	$\phi([\text{Q}]/\text{M})^{\text{k}}$	$\eta_{\text{q}}^{\text{l}}$	$\eta_{\text{ce}}^{\text{m}}$
Fe(III),^b TEA	490	0.55	0.0045	1.1×10^{-6}	0.58	-0.135	1.23×10^{-5}	1.03	0.09 (0.50)	0.31	0.29
Fe(II),^c C₈F₁₇I	465	0.85	-0.010	2.5×10^{-6}	0.61	-0.130	1.18×10^{-5}	0.87	0.18 (0.45)	$\leq 0.6^{\text{n}}$	≥ 0.3

^a In MeCN:MeOH (4:3)

^b Reductive quenching of $[\text{Fe(III)(btz)}_3]^{3+}$

^c Oxidative quenching of $[\text{Fe(II)(btz)}_3]^{2+}$

^d Sample absorbance at the excitation wavelength

^e Photo induced absorbance change of the sample at 452 nm

^f Photo generated concentration of Fe(III/II) based on $\Delta\epsilon = \pm 4.0 \times 10^3 \text{ M}^{-1}\text{cm}^{-1}$ at 452 nm

^g Actinometer absorbance at the excitation wavelength

^h Photo induced absorbance change of the actinometer at 452 nm

ⁱ Photo generated concentration of $^*[\text{Ru(bpy)}_3]^{2+}$ based on $\Delta\epsilon = -1.1 \times 10^4 \text{ M}^{-1}\text{cm}^{-1}$ at 452 nm^[12]

^j Correction factor for absorbance difference between sample and actinometer $f = (1 - 10^{-A_{\text{Ru}}(\lambda_{\text{ex}})}) / (1 - 10^{-A_{\text{Fe}}(\lambda_{\text{ex}})})$

^k Quantum yield of electron transfer products $\phi = (\Delta[\text{Fe}]/\Delta[\text{Ru}])f$

^l Quenching yield from steady state emission quenching

^m Cage escape yield $\eta_{\text{ce}} = \phi / \eta_{\text{q}}$

ⁿ Not determined. Upper limit estimated with $k_{\text{q}} \leq 2 \times 10^{10} \text{ M}^{-1}\text{s}^{-1}$

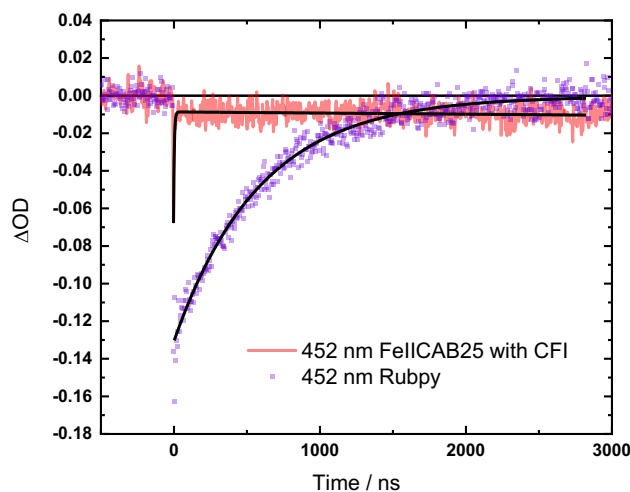


Figure S18: Transient absorption time traces (excitation wavelength 465 nm) monitoring the laser flash induced reaction of $[\text{Fe(II)(btz)}_3]^{2+}$ with $\text{C}_8\text{F}_{17}\text{I}$ (0.45 M) (ground state bleach at 452 nm) and the formation and decay of the $^3\text{MLCT}$ state of the $[\text{Ru(bpy)}_3]^{2+}$ actinometer (ground state bleach at 452 nm).

NMR Spectra

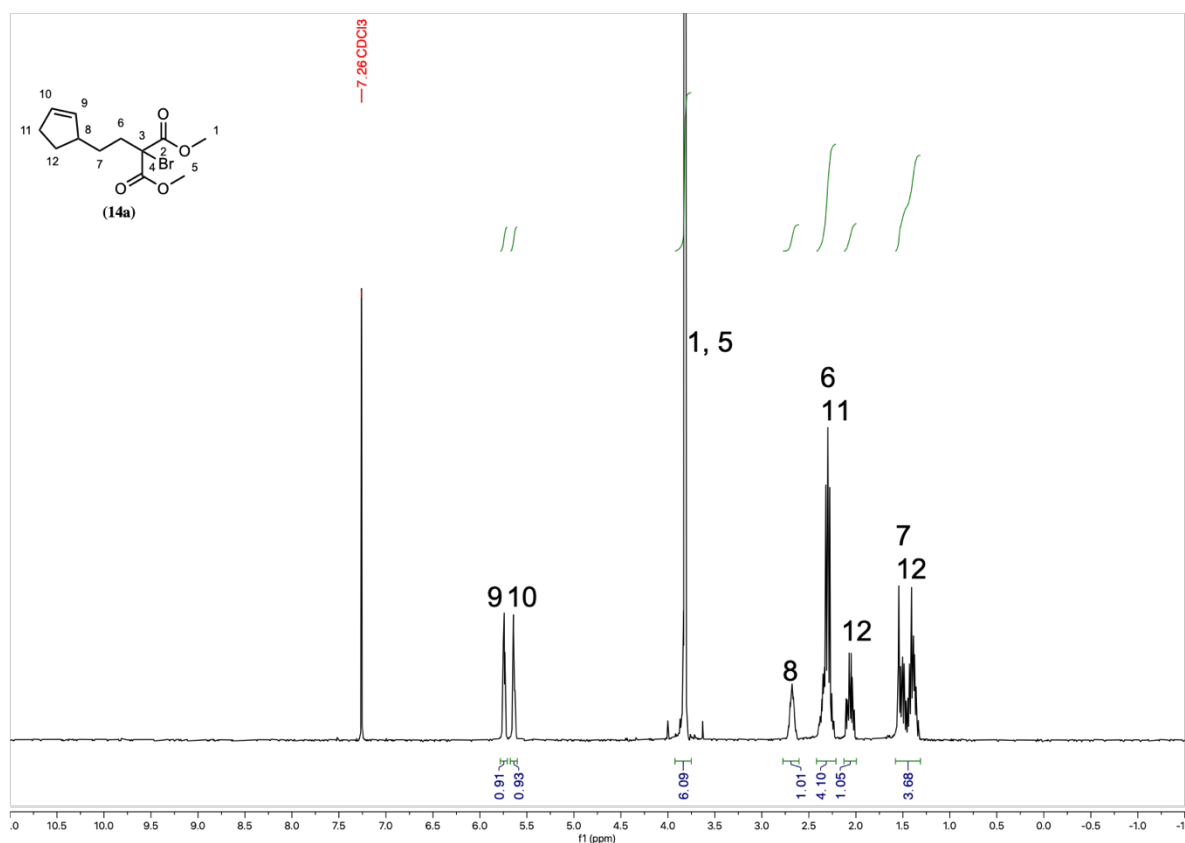


Figure S19: ^1H NMR spectrum (400 MHz) of (14a) in CDCl_3 .

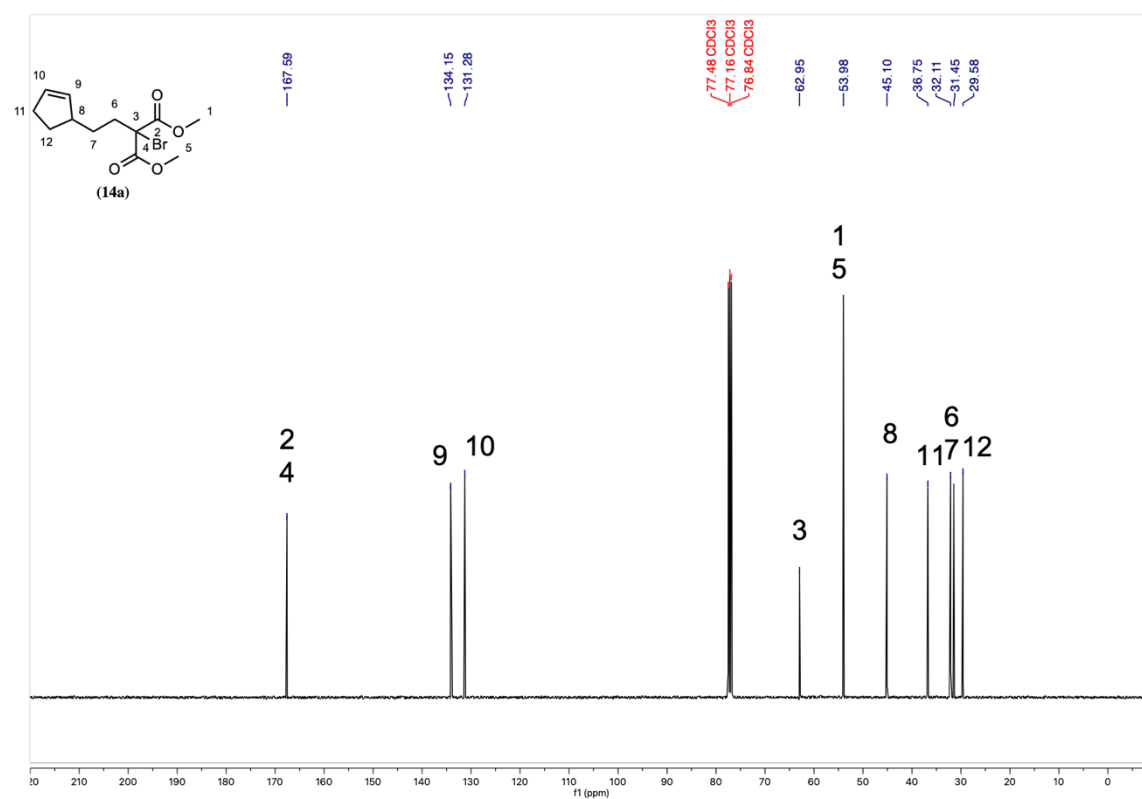


Figure S20: ^{13}C NMR spectrum (101 MHz) of (14a) in CDCl_3 .

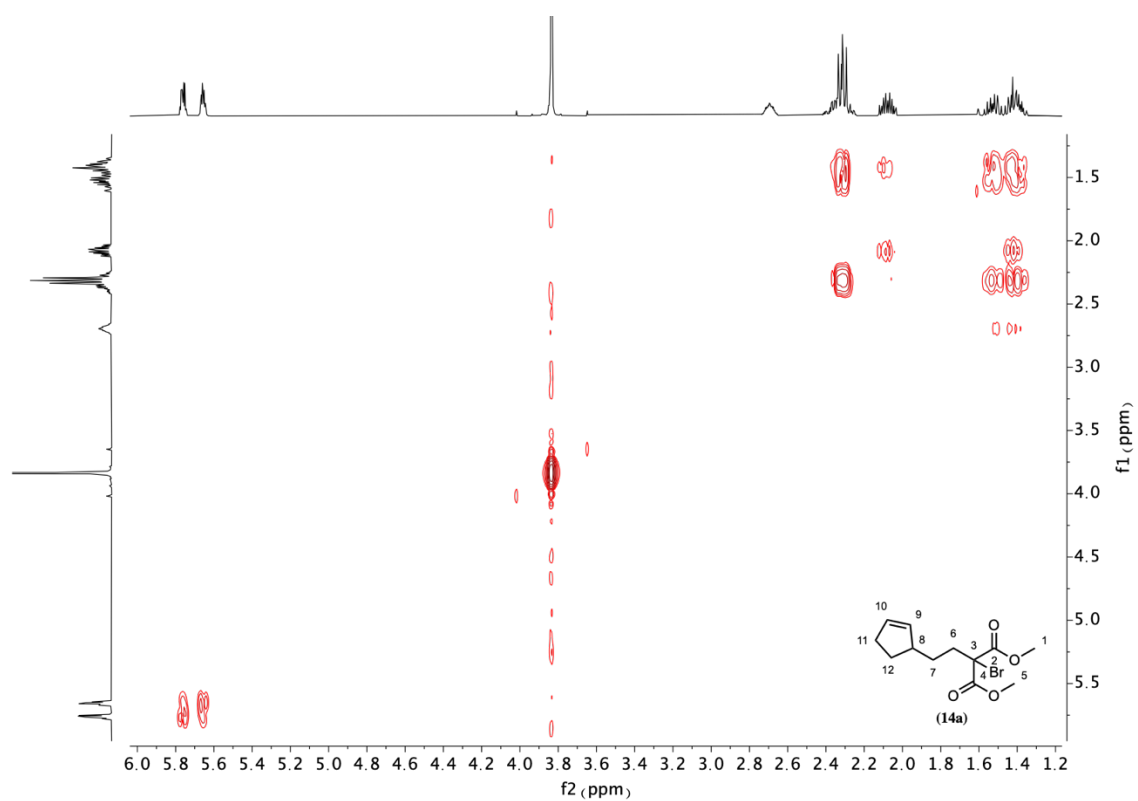


Figure S21: COSY spectrum (400 MHz) of **(14a)** in CDCl_3 .

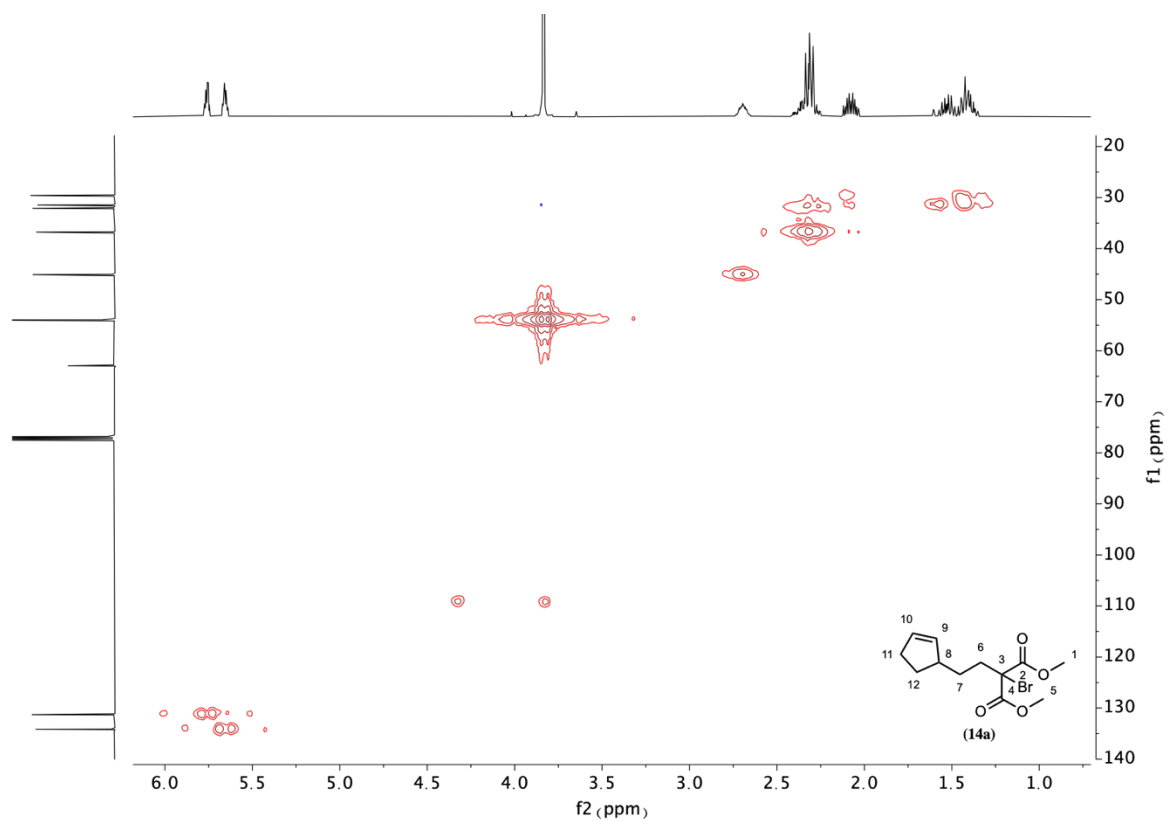


Figure S22: HMBC spectrum of **(14a)** in CDCl_3 .

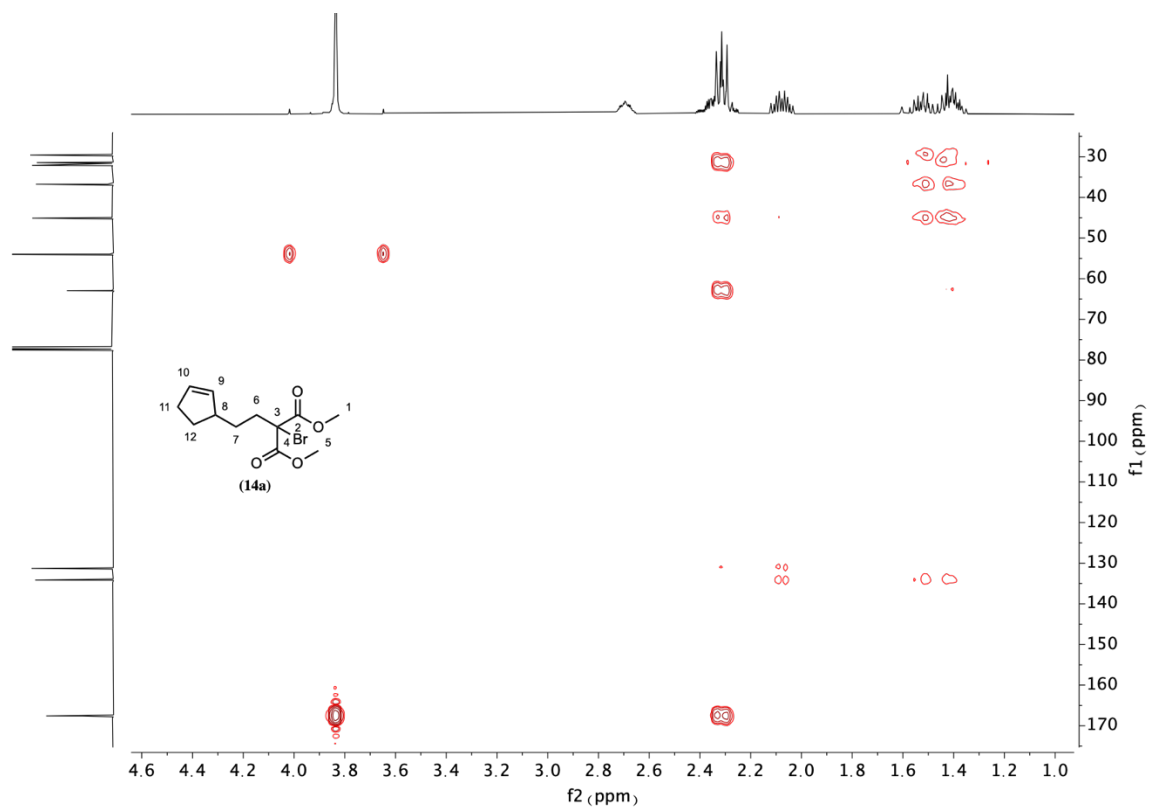


Figure S23: HMBC spectrum of (14a) in CDCl₃.

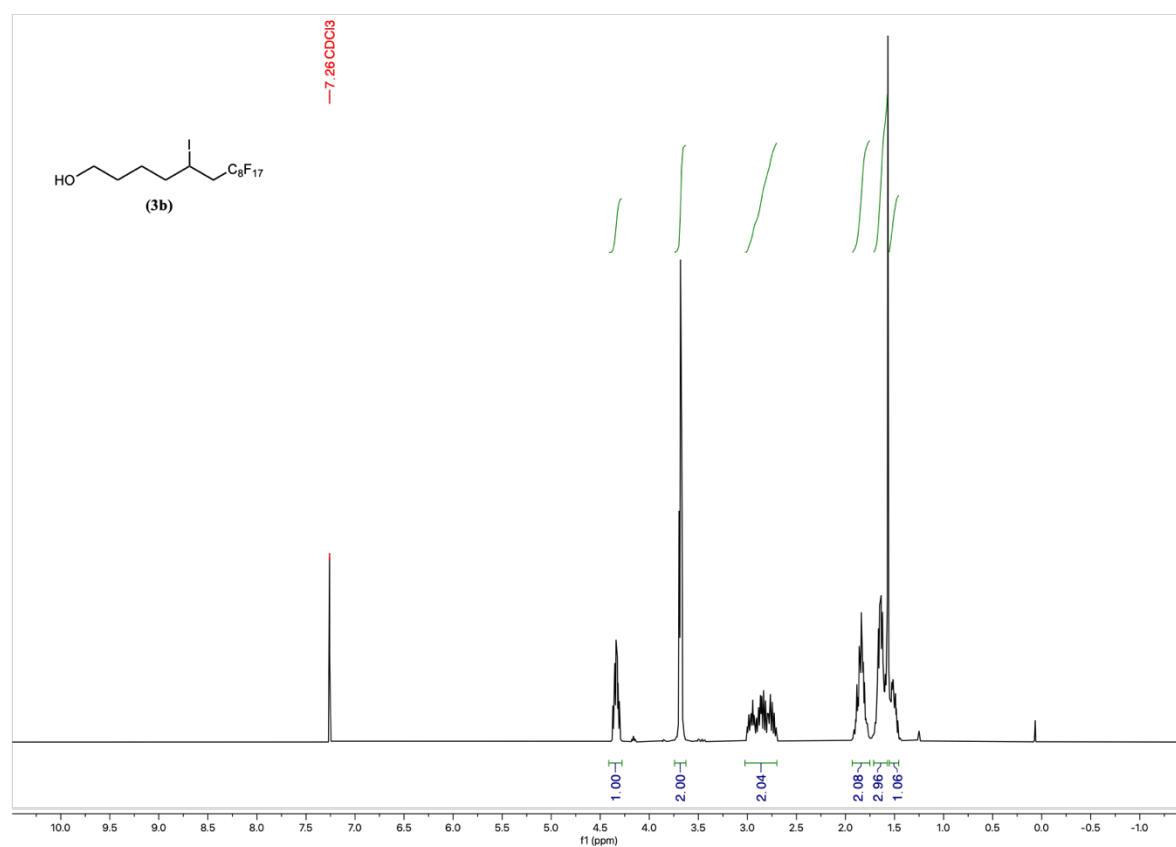


Figure S24: ¹H NMR spectrum (400 MHz) of (3b) in CDCl₃.

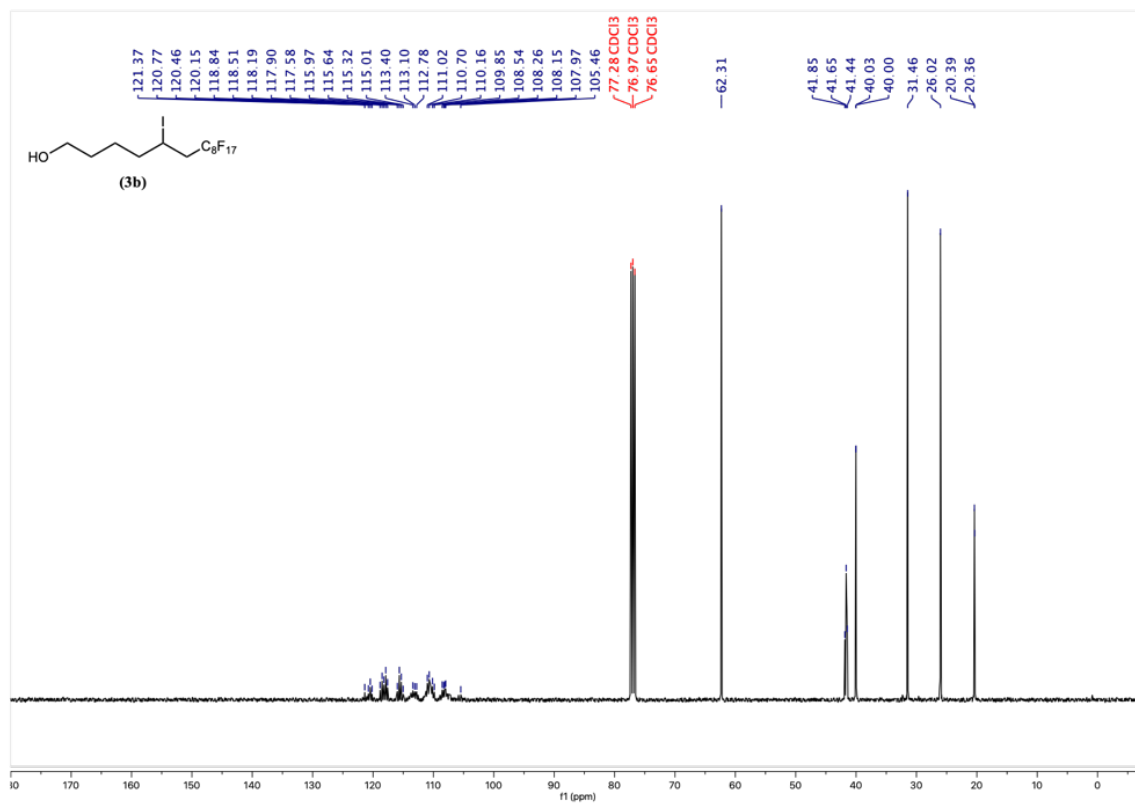


Figure S25: ¹³C NMR spectrum (101 MHz) of (3b) in CDCl₃.

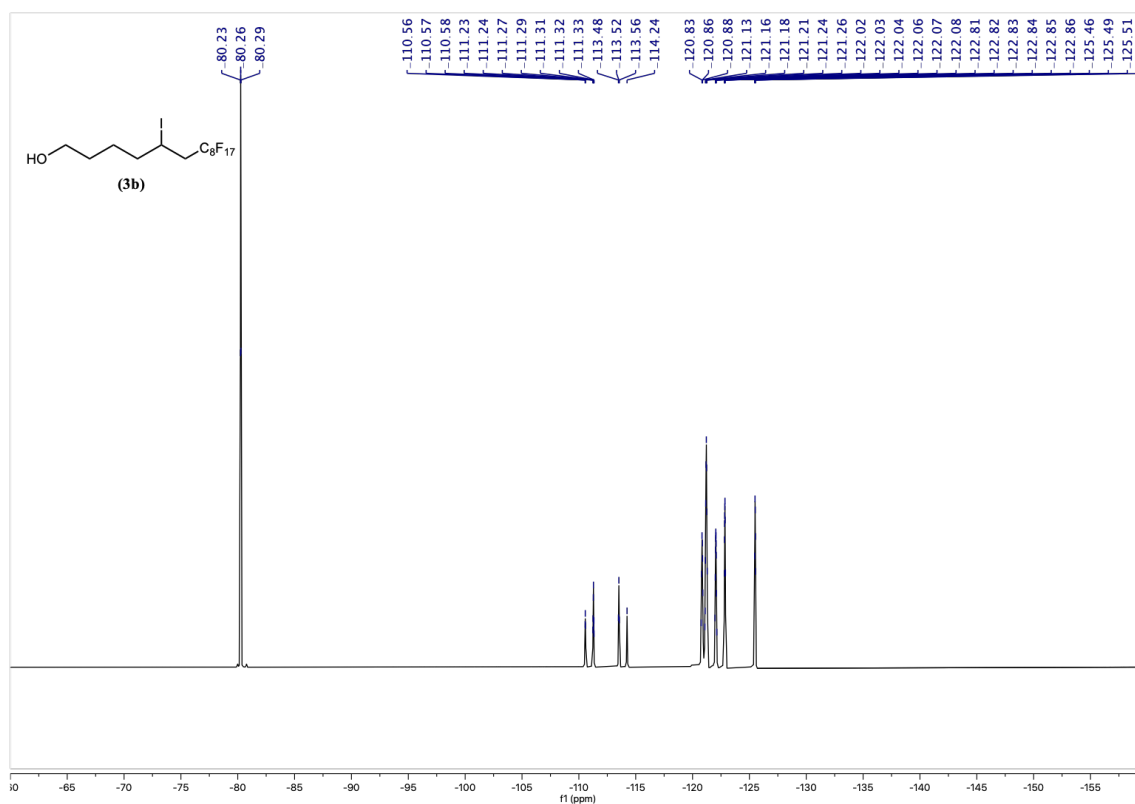


Figure S26: ¹⁹F NMR spectrum (376 MHz) of (3b) in CDCl₃.

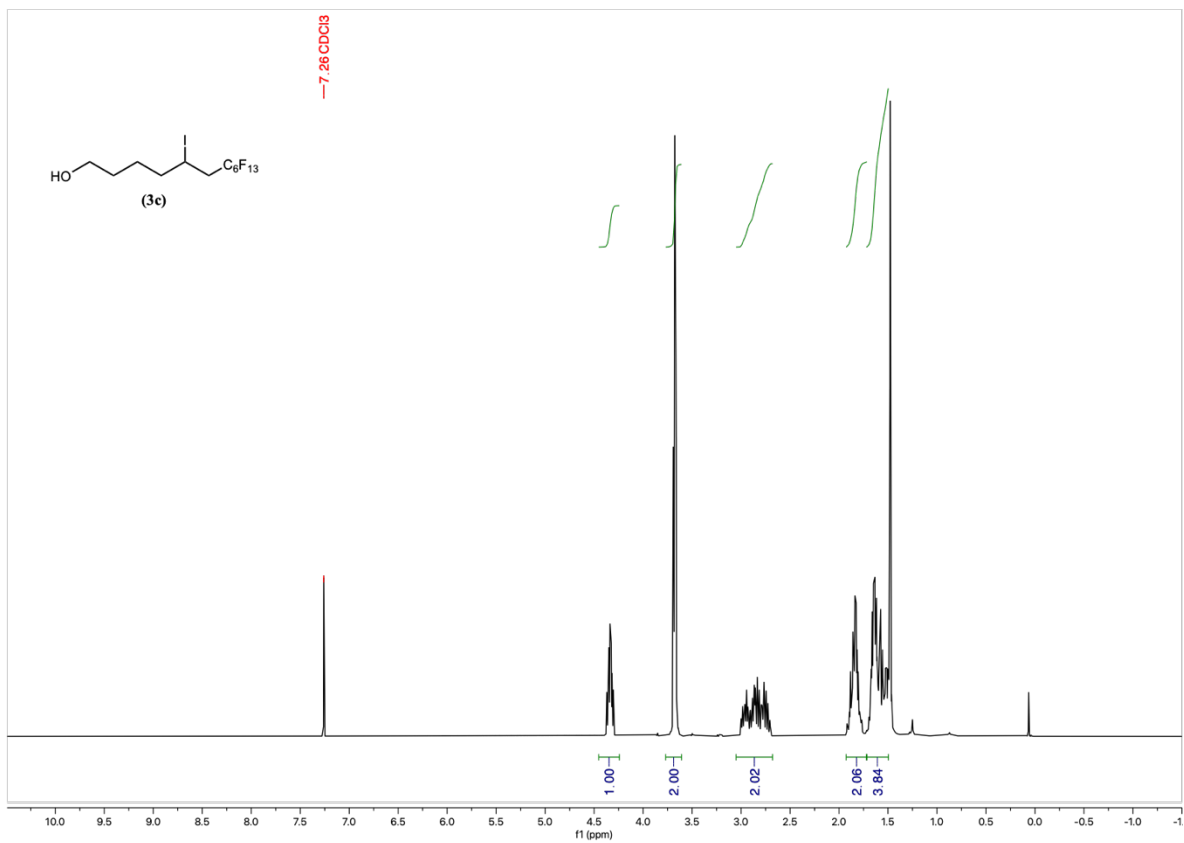


Figure S27: ¹H NMR spectrum (400 MHz) of (3c) in CDCl₃.

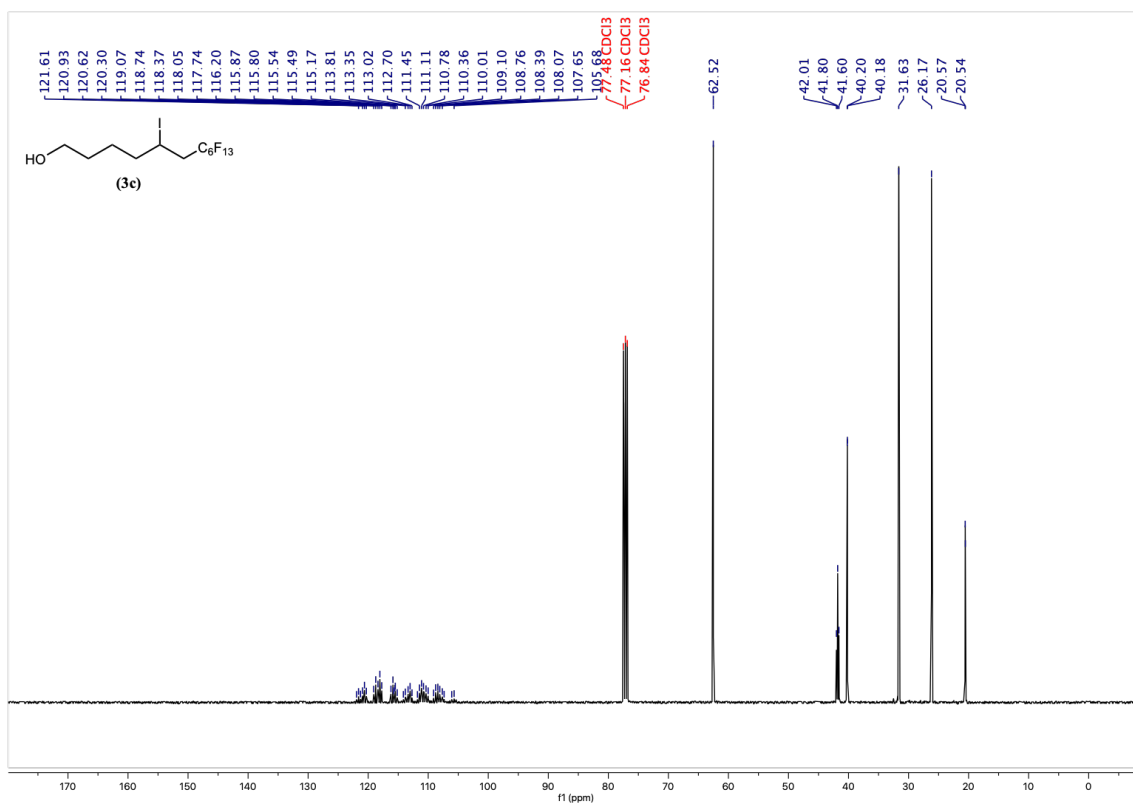


Figure S28: ¹³C NMR spectrum (101 MHz) of (3c) in CDCl₃.

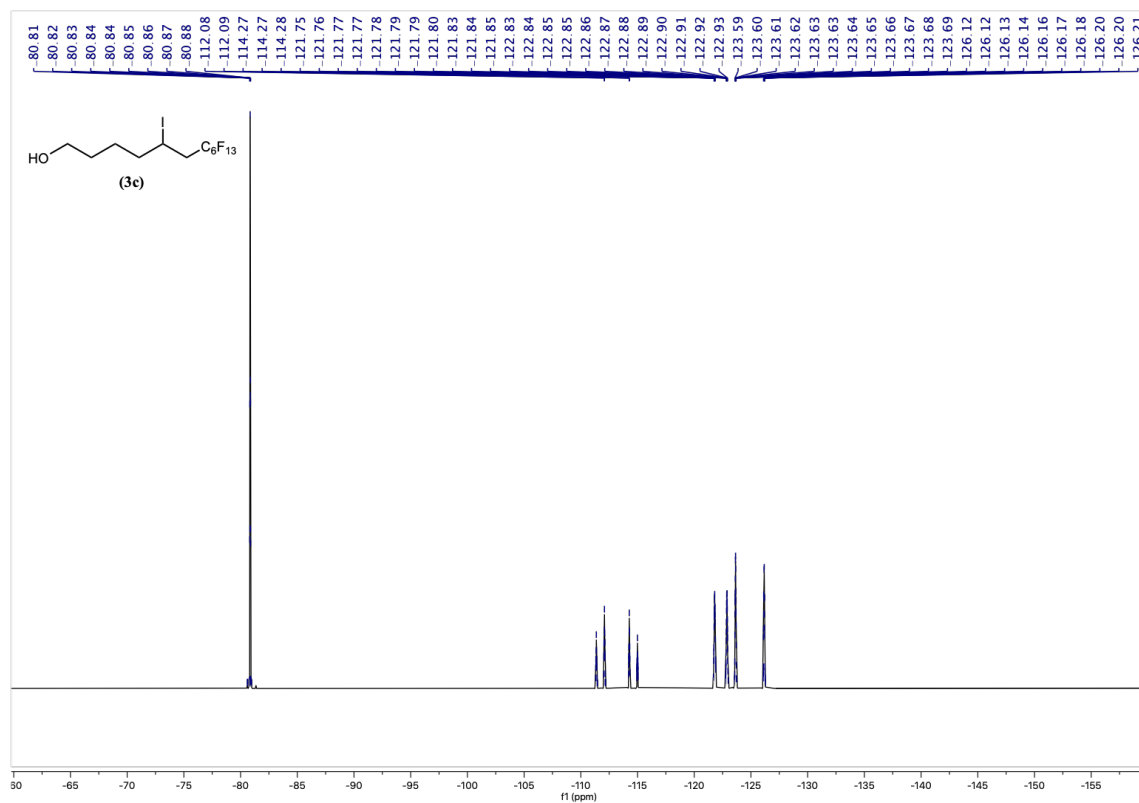


Figure S29: ^{19}F NMR spectrum (376 MHz) of (3c) in CDCl_3 .

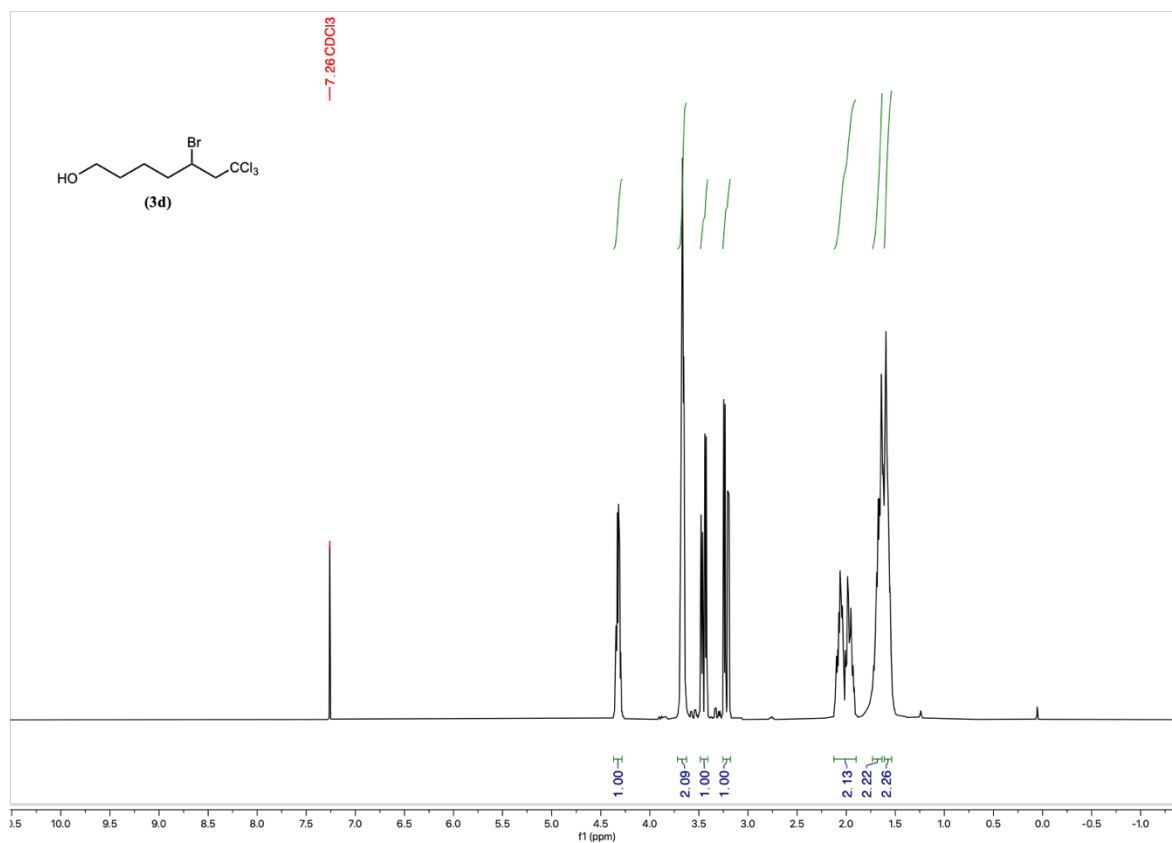


Figure S30: ¹H NMR spectrum (400 MHz) of (3d) in CDCl₃.

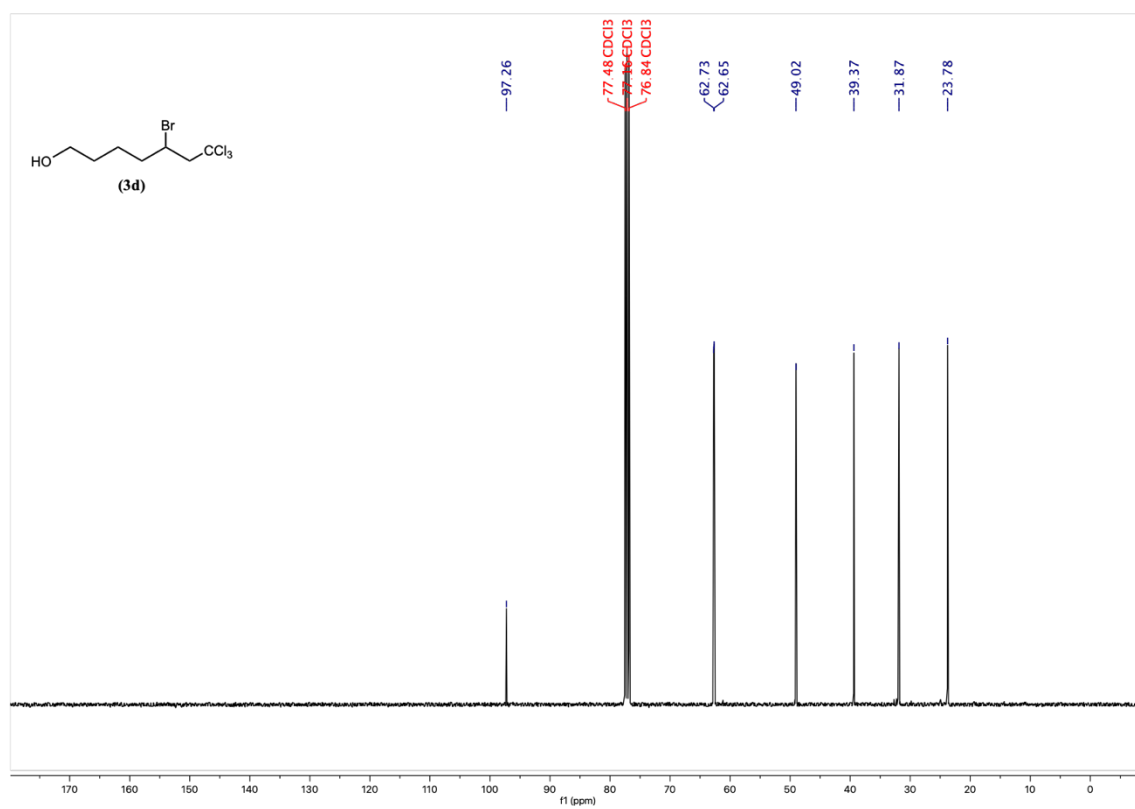


Figure S31: ¹³C NMR spectrum (101 MHz) of (3d) in CDCl₃.

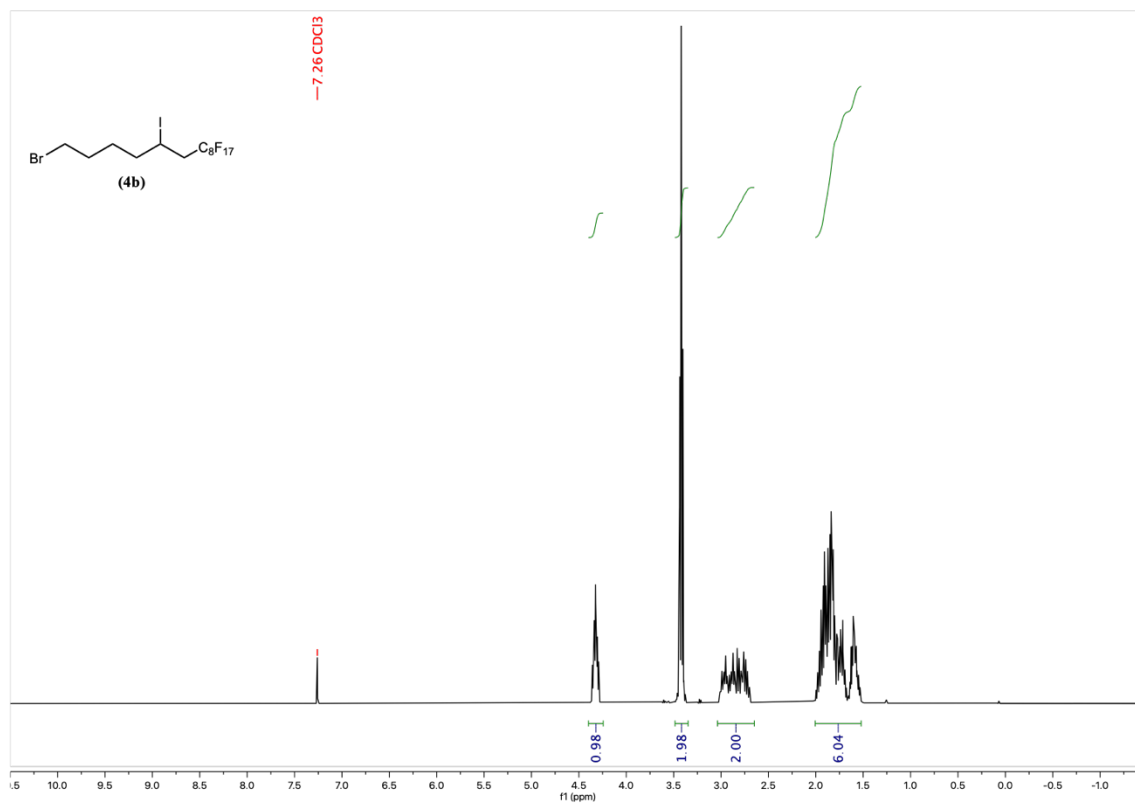


Figure S32: ¹H NMR spectrum (400 MHz) of (4b) in CDCl₃.

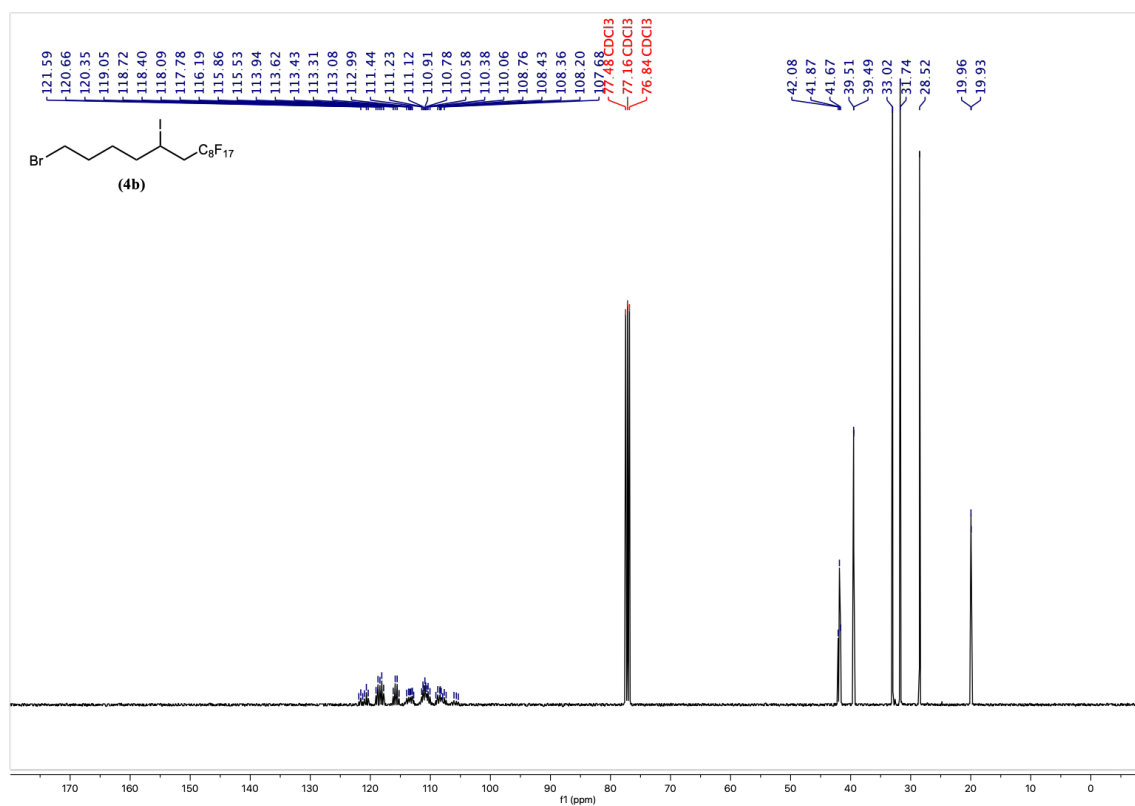


Figure S33: ¹³C NMR spectrum (101 MHz) of (4b) in CDCl₃.

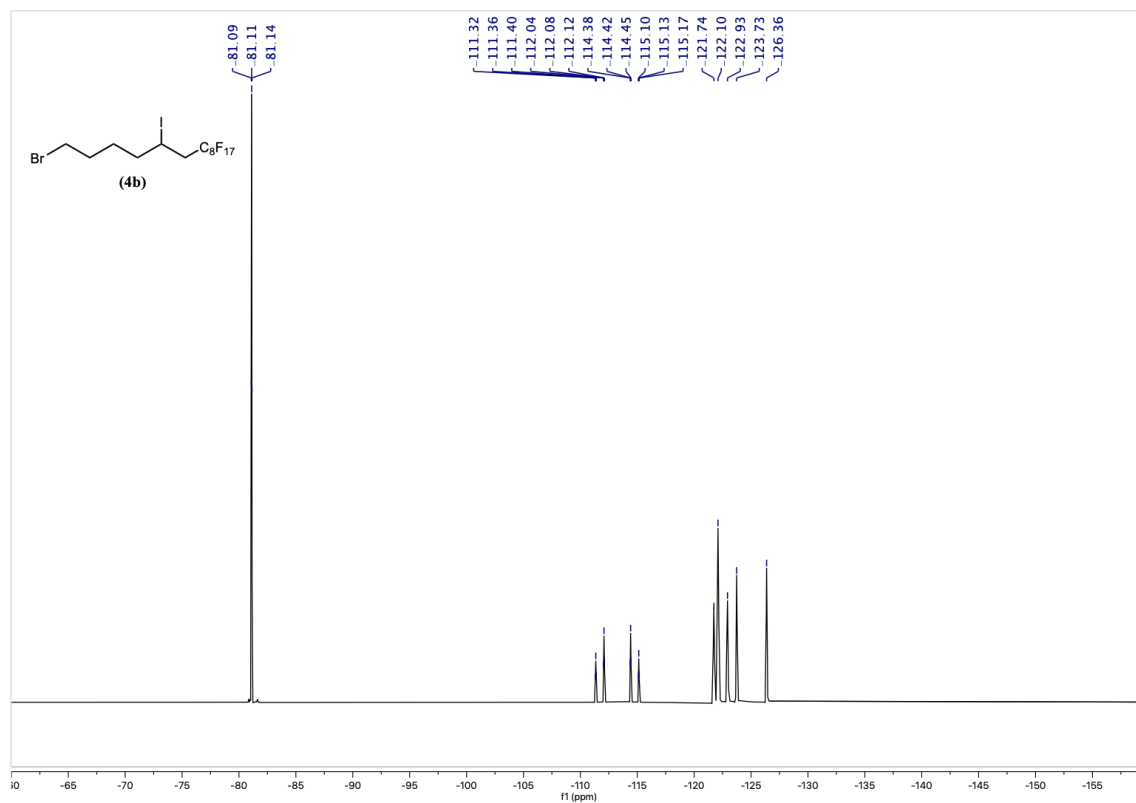


Figure S34: ¹⁹F NMR spectrum (376 MHz) of (4b) in CDCl₃.

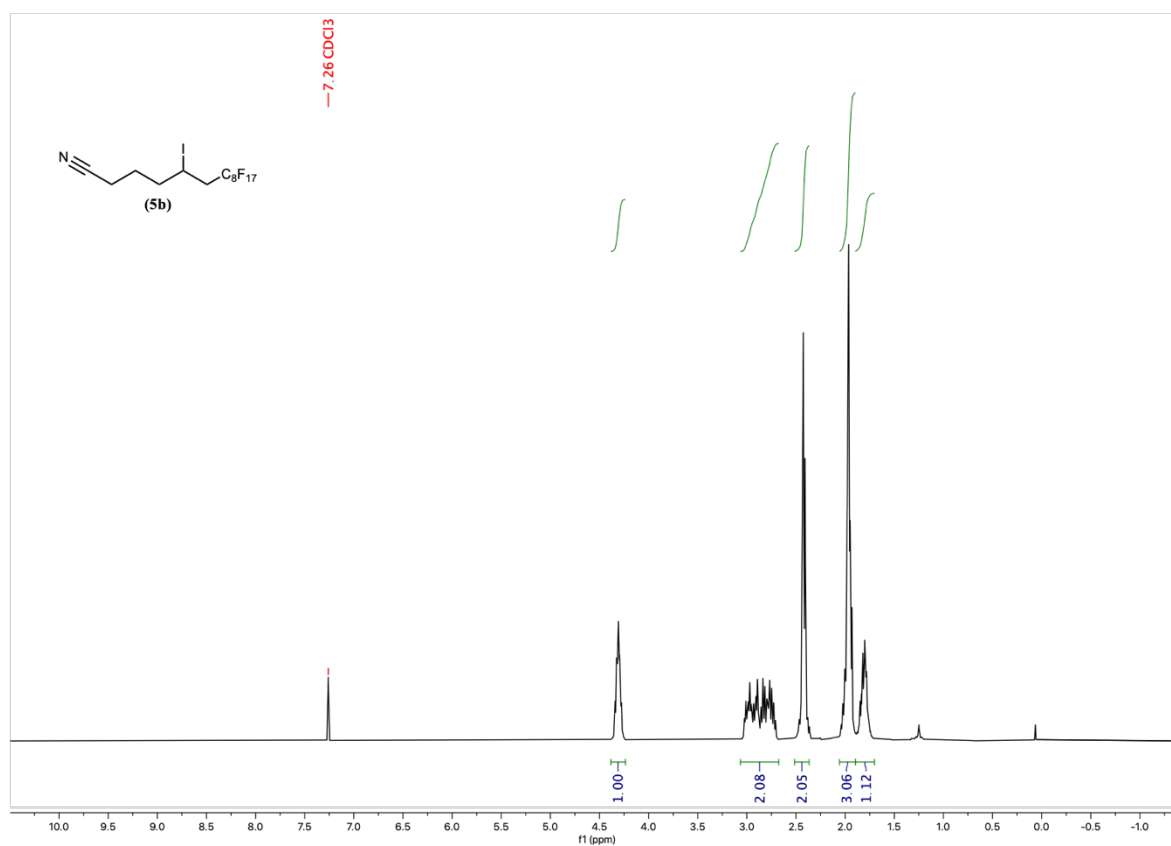


Figure S35: ¹H NMR spectrum (400 MHz) of (5b) in CDCl₃.

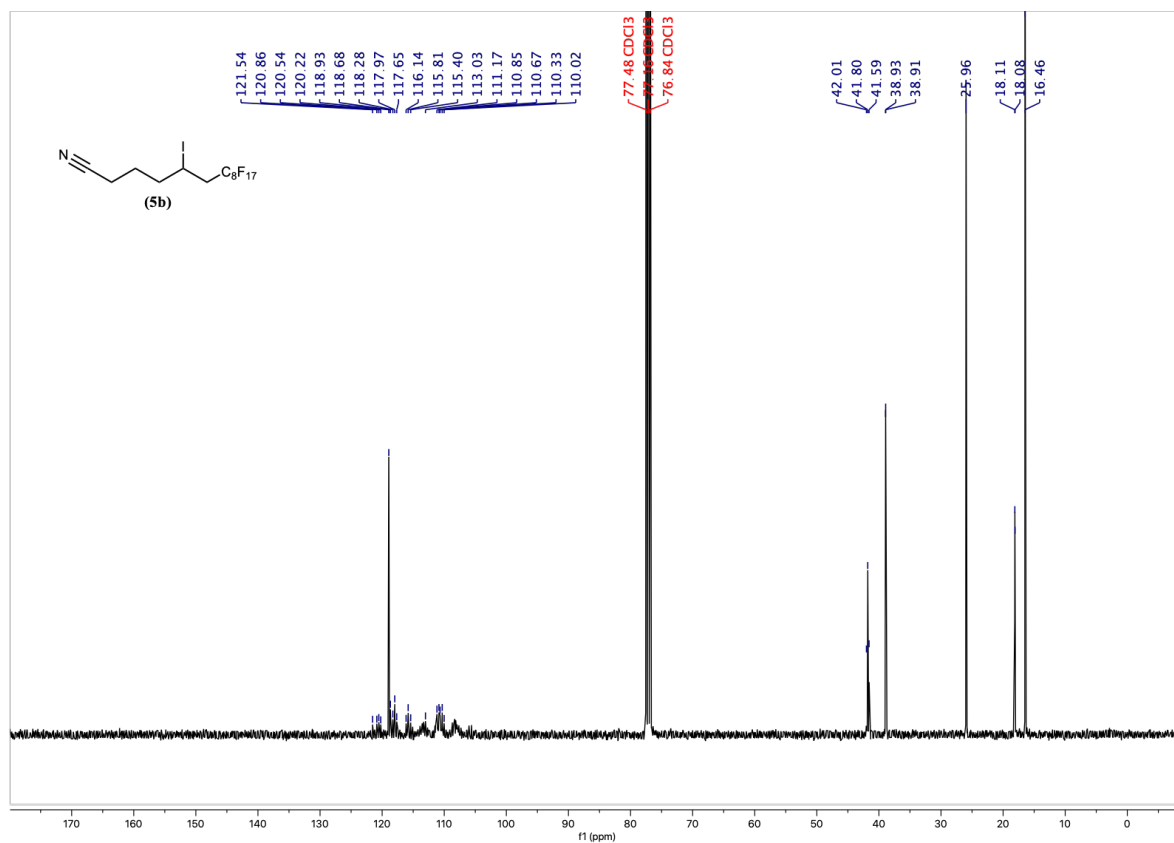


Figure S36: ¹³C NMR spectrum (101 MHz) of (5b) in CDCl₃.

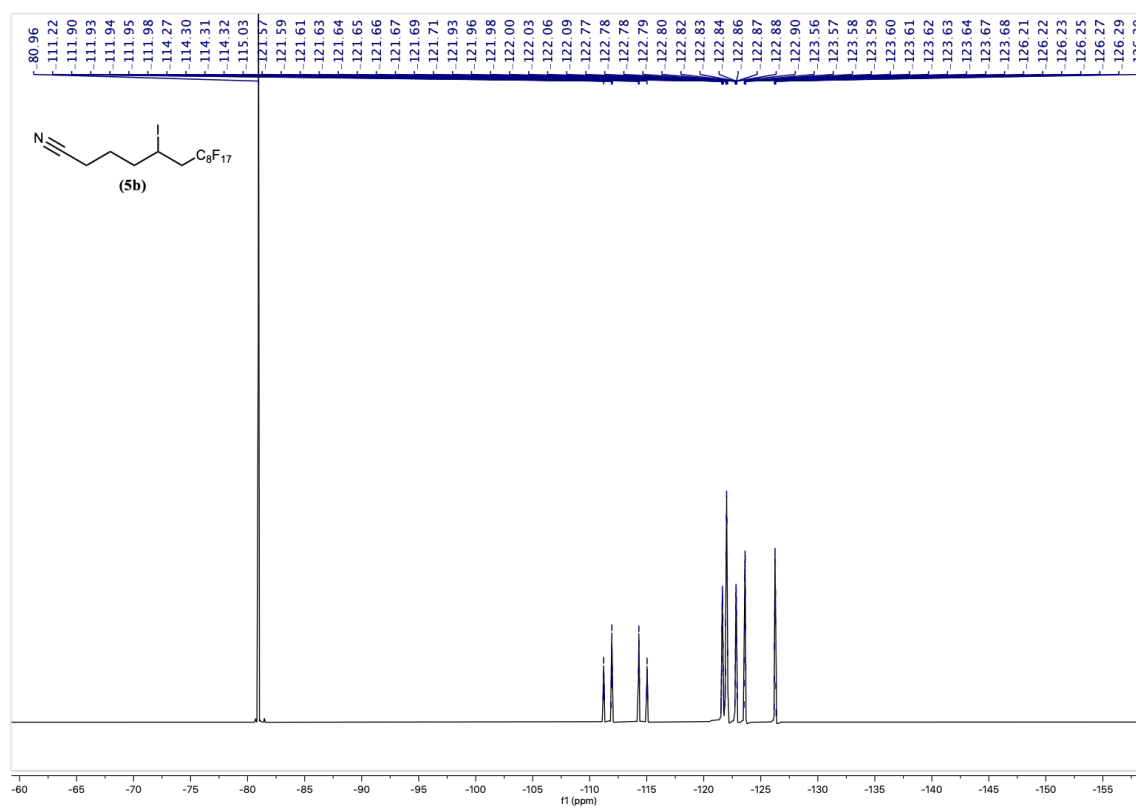


Figure S37: ¹⁹F NMR spectrum (376 MHz) of (5b) in CDCl₃.

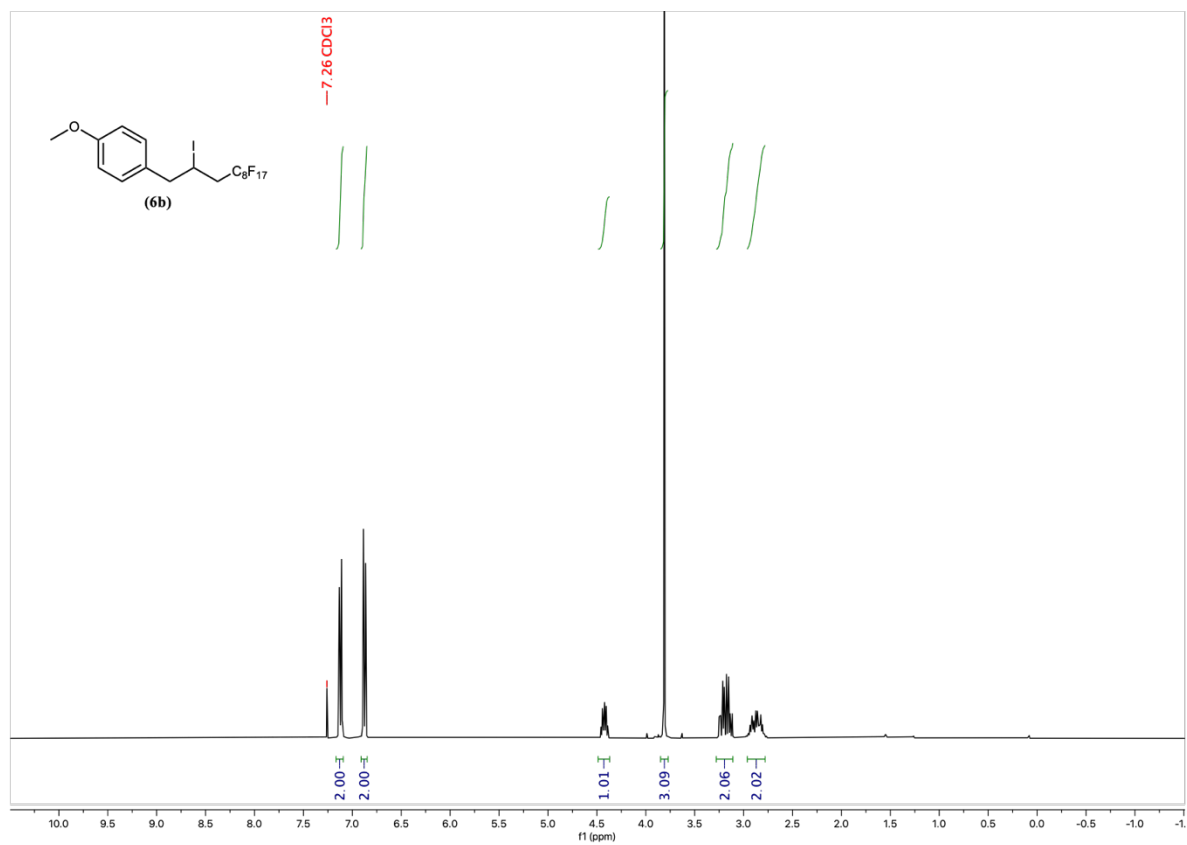


Figure S38: ¹H NMR spectrum (400 MHz) of (6b) in CDCl₃.

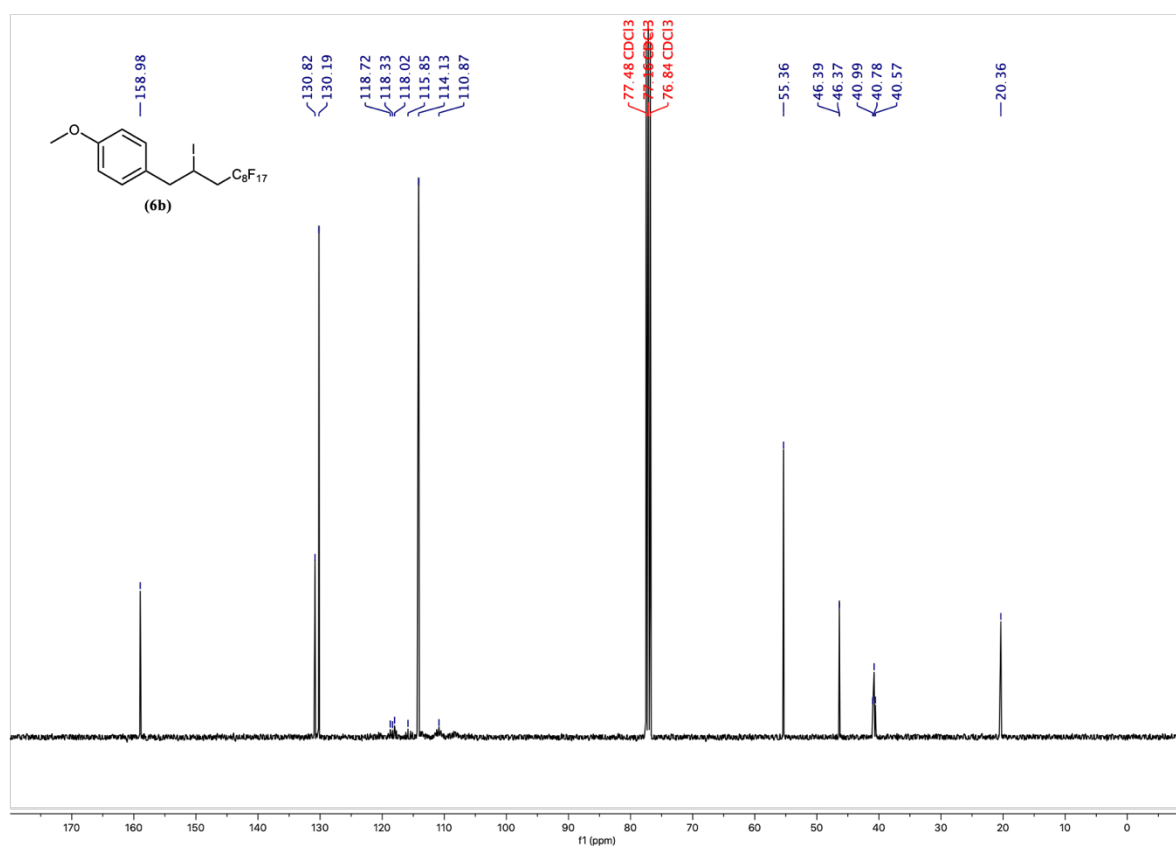


Figure S39: ¹³C NMR spectrum (101 MHz) of (6b) in CDCl₃.

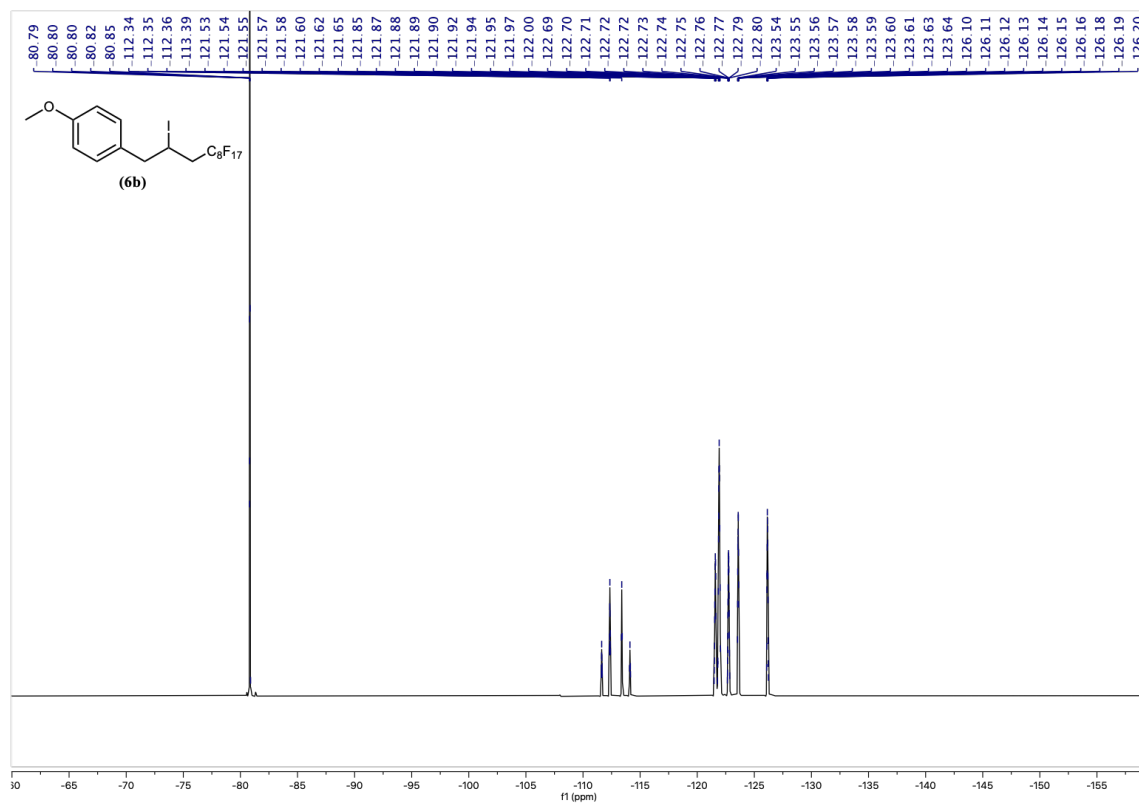


Figure S40: ^{19}F NMR spectrum (376 MHz) of **(6b)** in CDCl_3 .

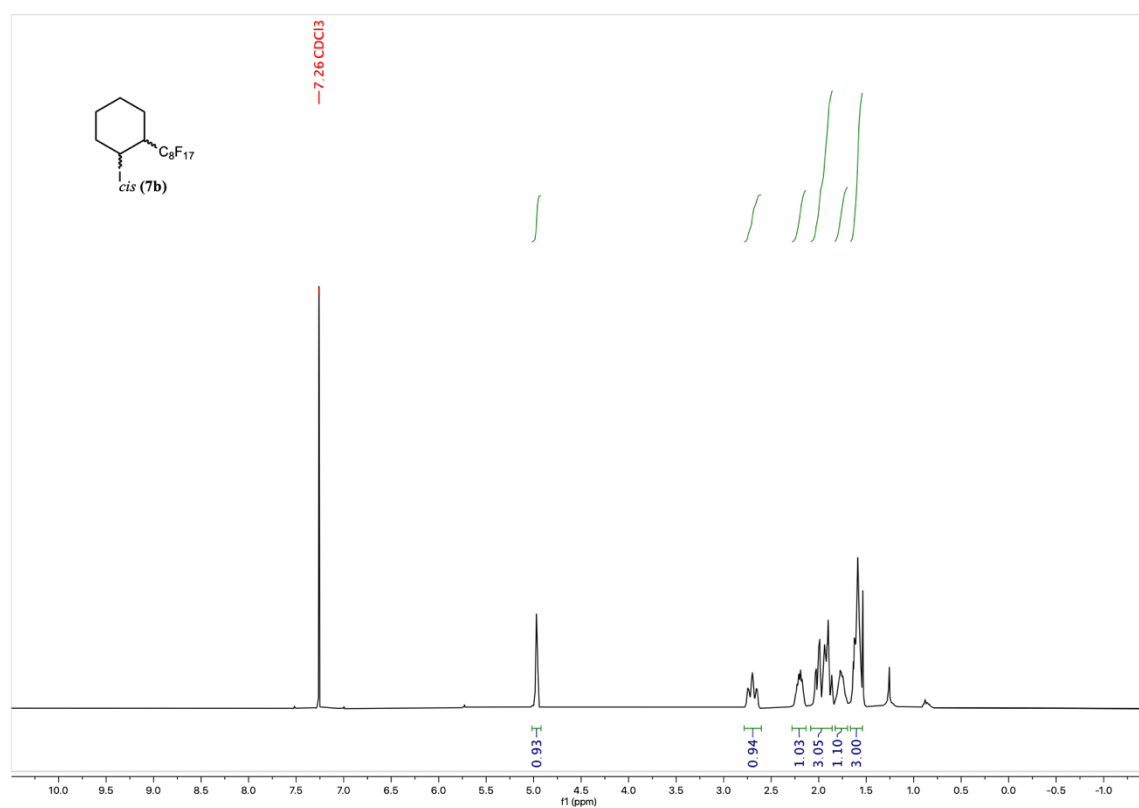


Figure S41: ^1H NMR spectrum (400 MHz) of **(7b)** in CDCl_3 .

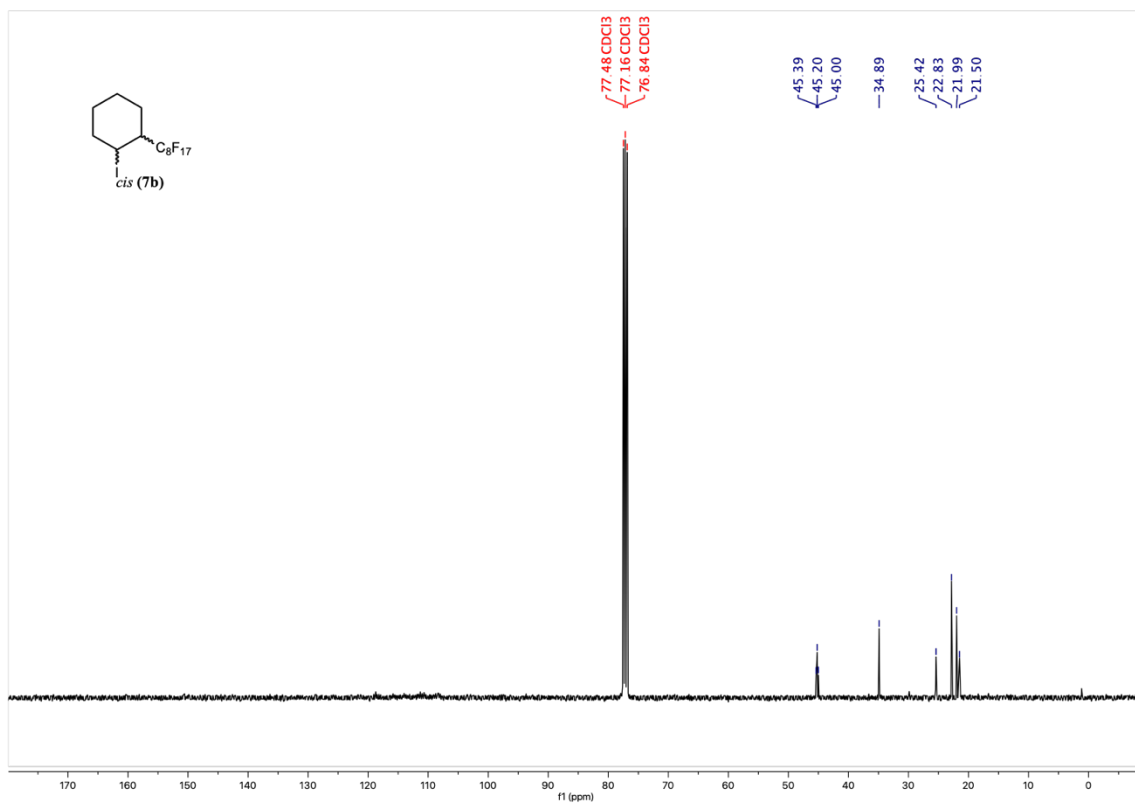


Figure S42: ¹³C NMR spectrum (101 MHz) of (7b) in CDCl₃.

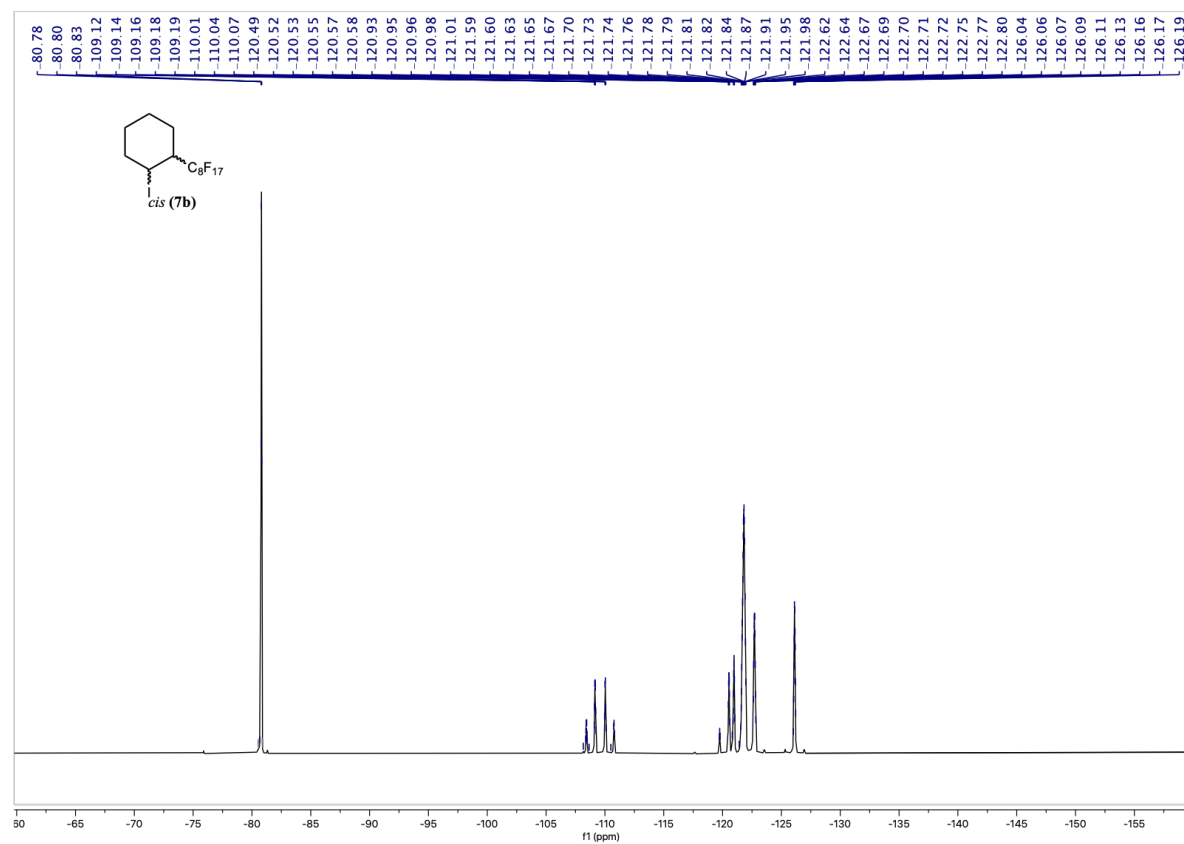


Figure S43: ¹⁹F NMR spectrum (376 MHz) of (7b) in CDCl₃.

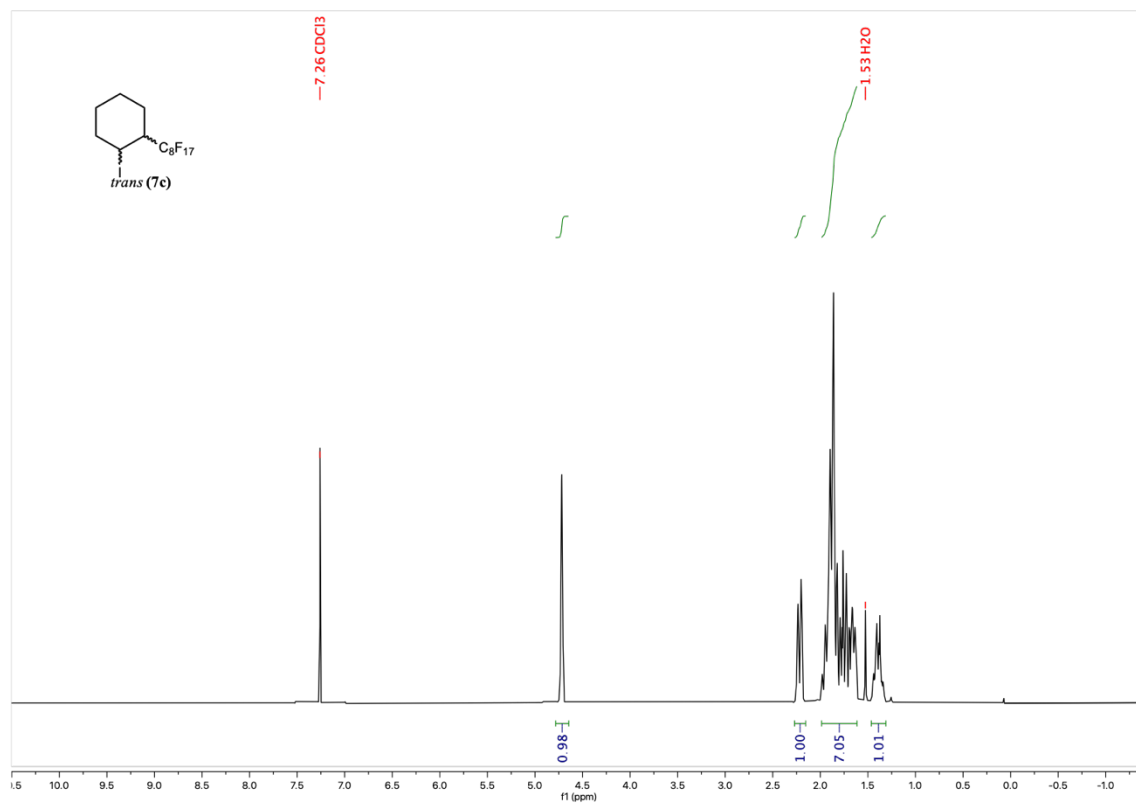


Figure S44: ^1H NMR spectrum (400 MHz) of (7c) in CDCl_3 .

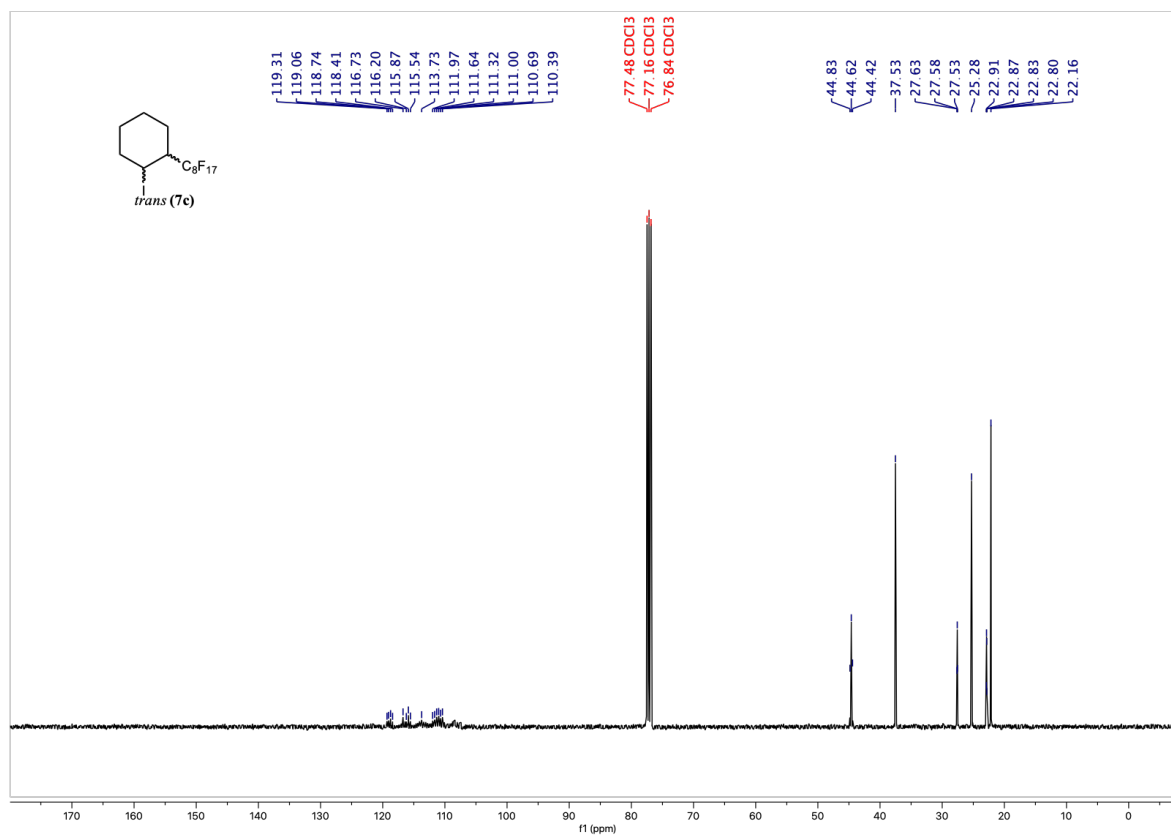


Figure S45: ^{13}C NMR spectrum (101 MHz) of (7c) in CDCl_3 .

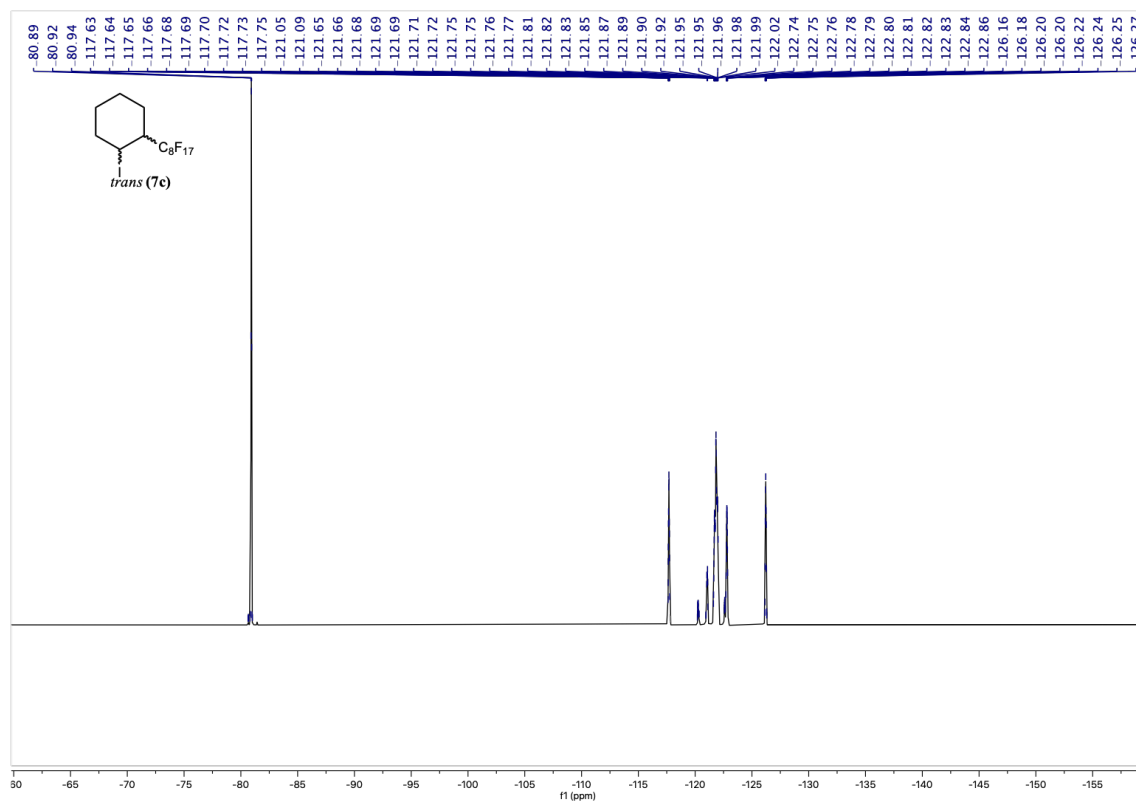


Figure S46: ¹⁹F NMR spectrum (376 MHz) of (7c) in CDCl₃.

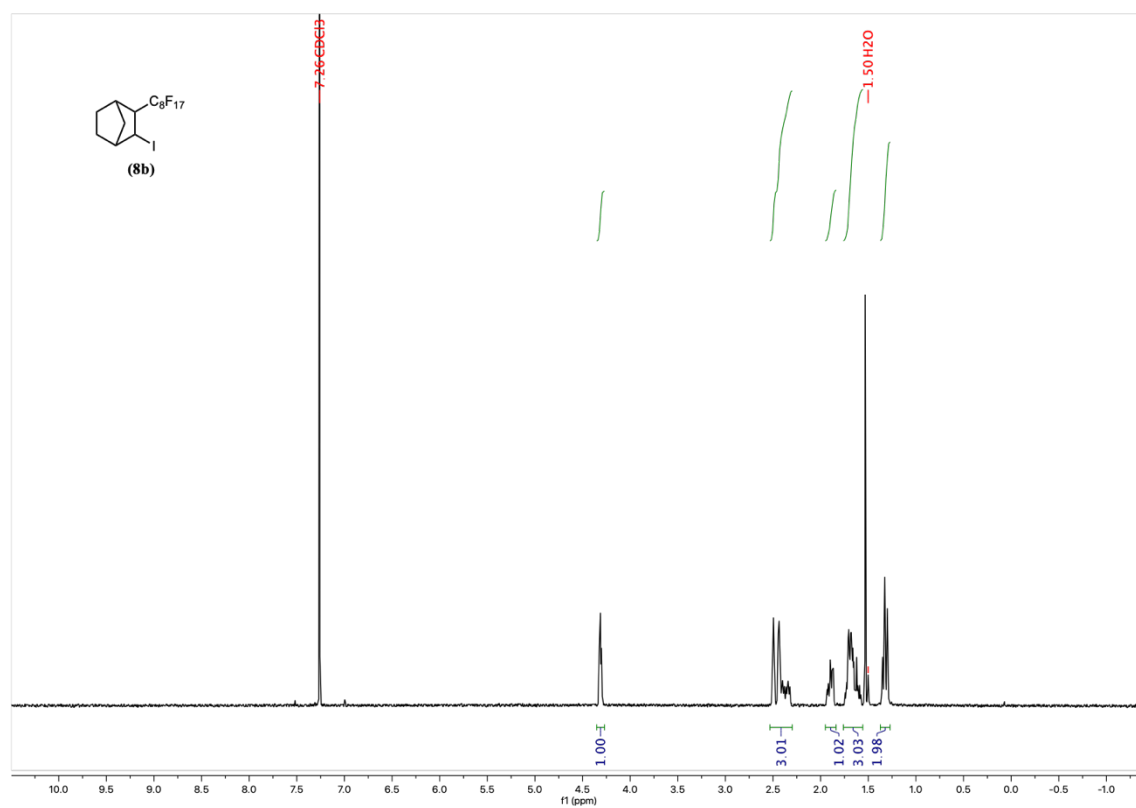


Figure S47: ¹H NMR spectrum (400 MHz) of (8b) in CDCl₃.

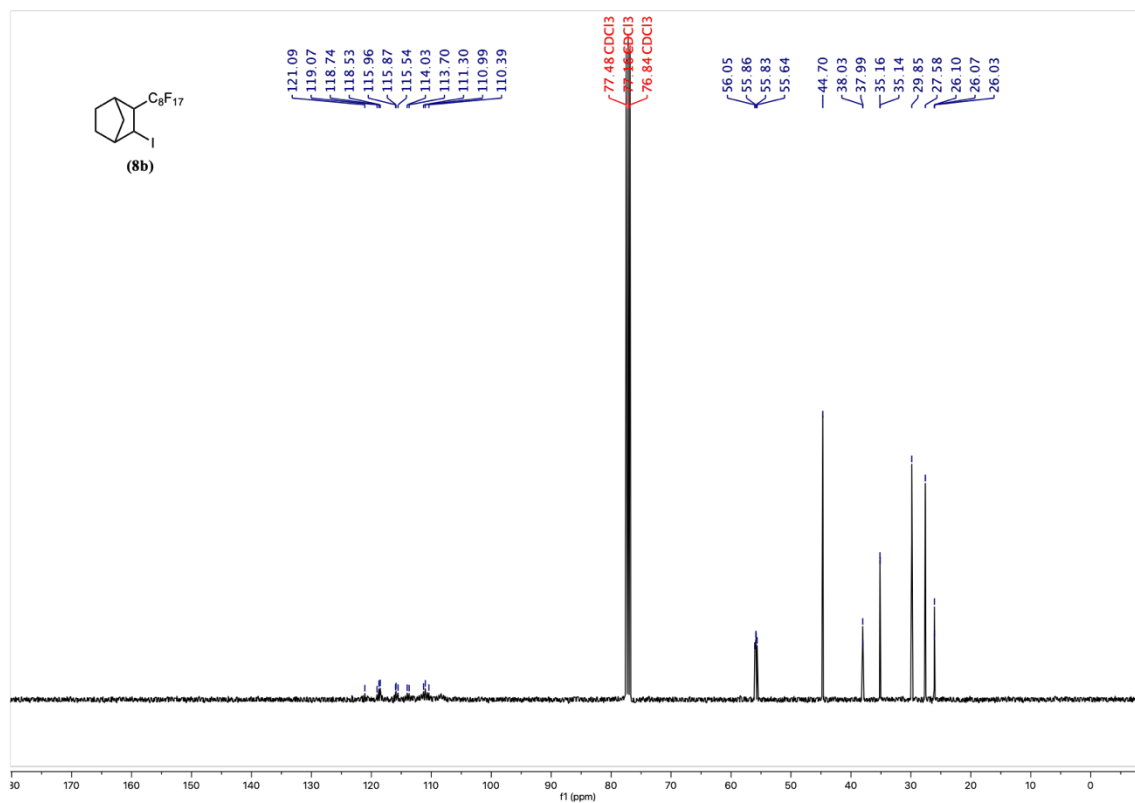


Figure S48: ¹³C NMR spectrum (101 MHz) of (8b) in CDCl₃.

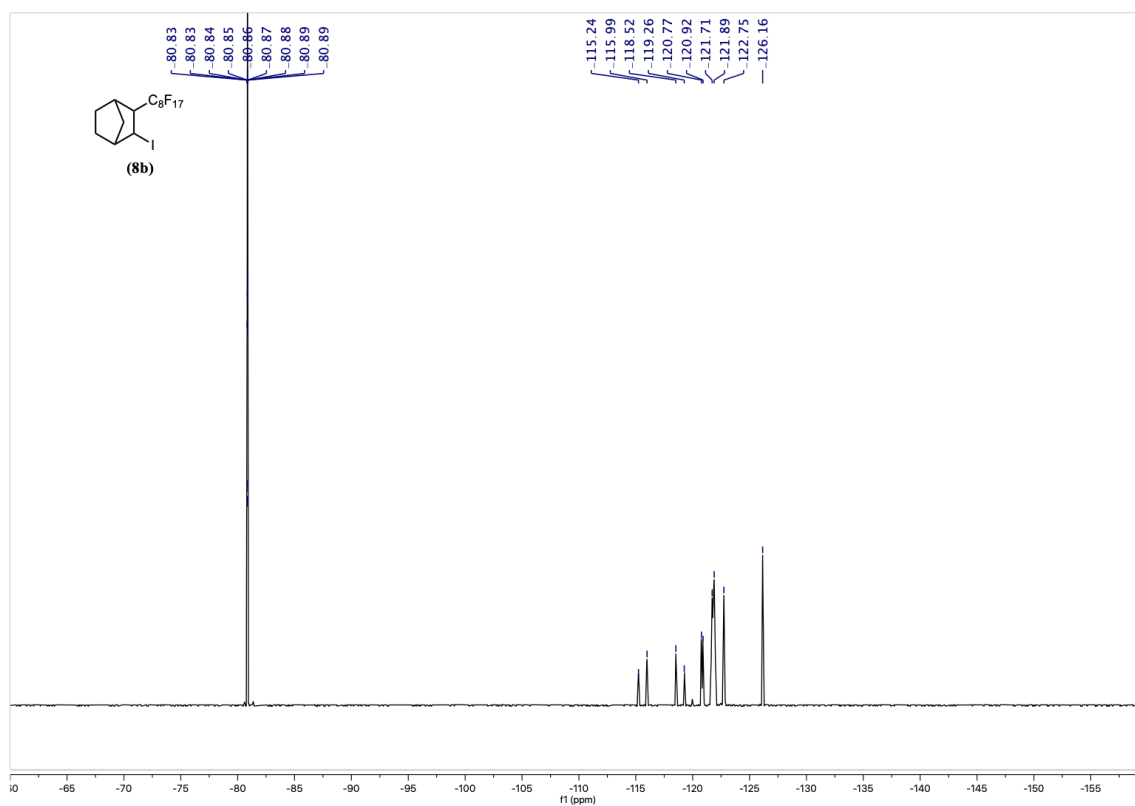


Figure S49: ¹⁹F NMR spectrum (376 MHz) of (8b) in CDCl₃.

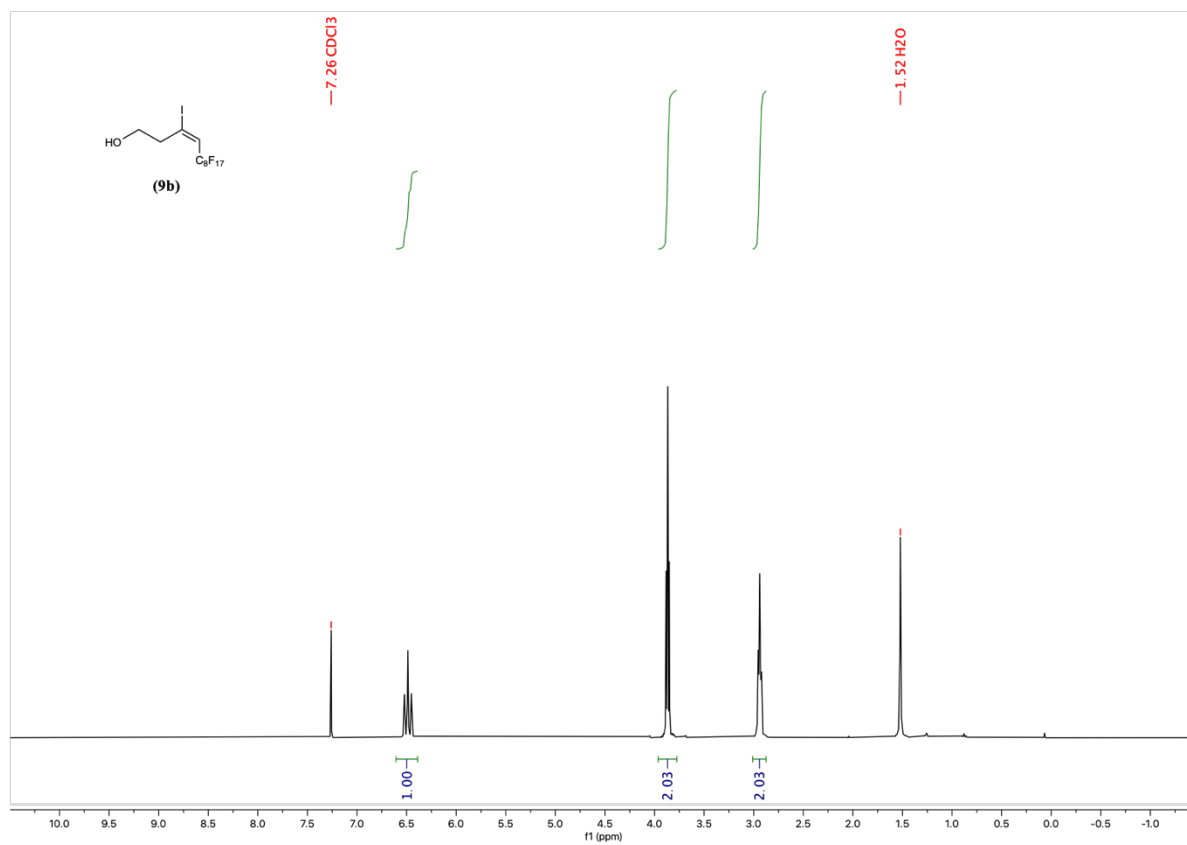


Figure S50: ¹H NMR spectrum (400 MHz) of (9b) in CDCl₃.

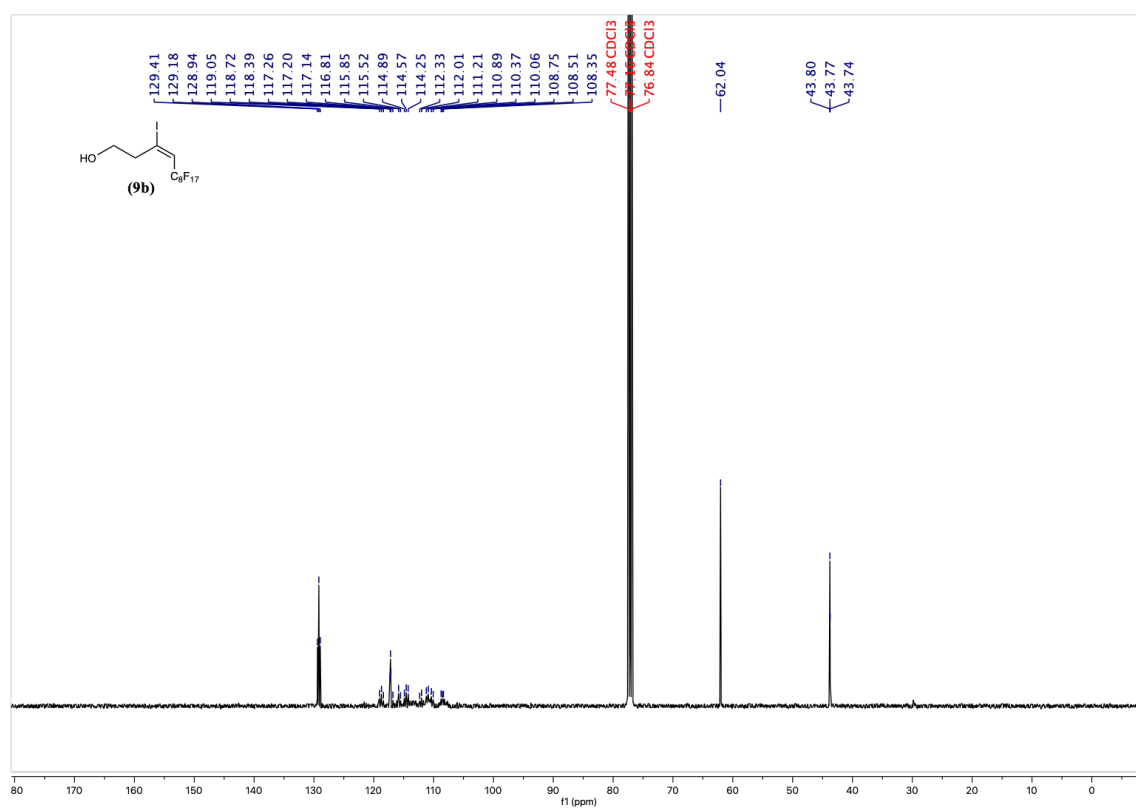


Figure S51: ¹³C NMR spectrum (101 MHz) of (9b) in CDCl₃.

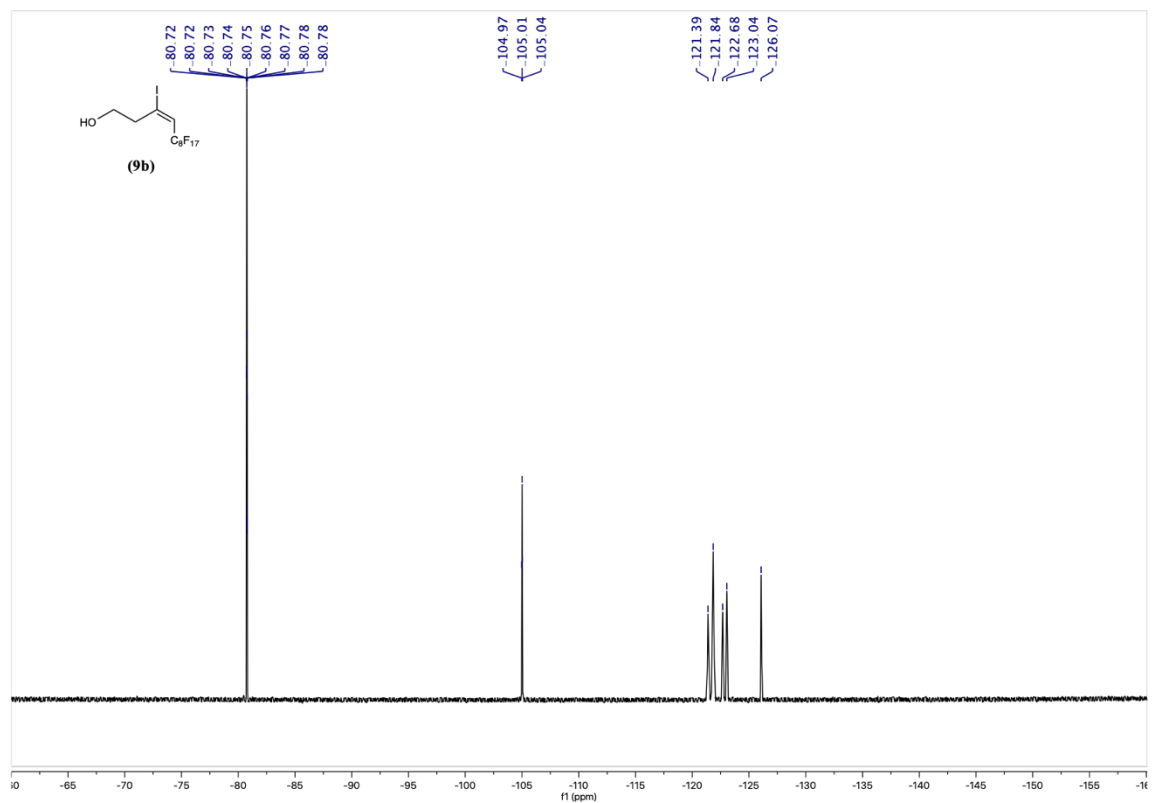


Figure S52: ¹⁹F NMR spectrum (376 MHz) of (9b) in CDCl₃.

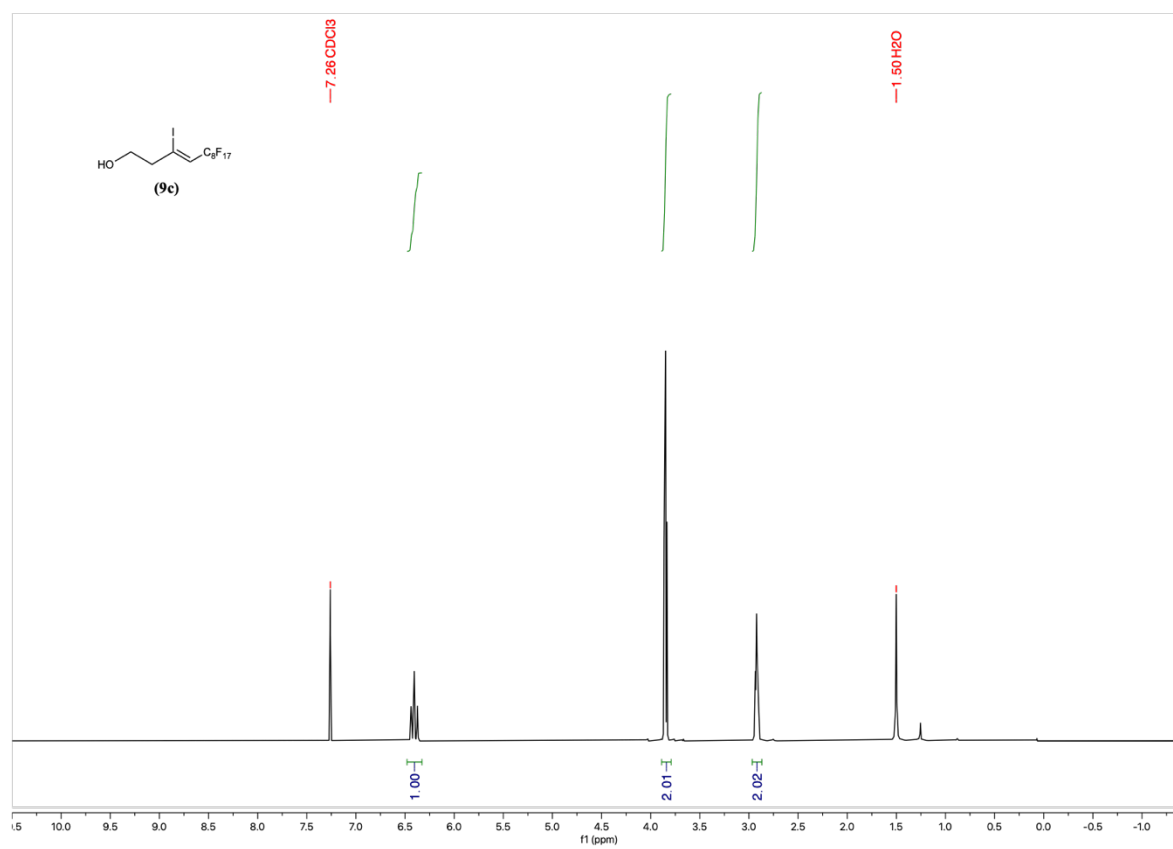


Figure S53: ¹H NMR spectrum (400 MHz) of (9c) in CDCl₃.

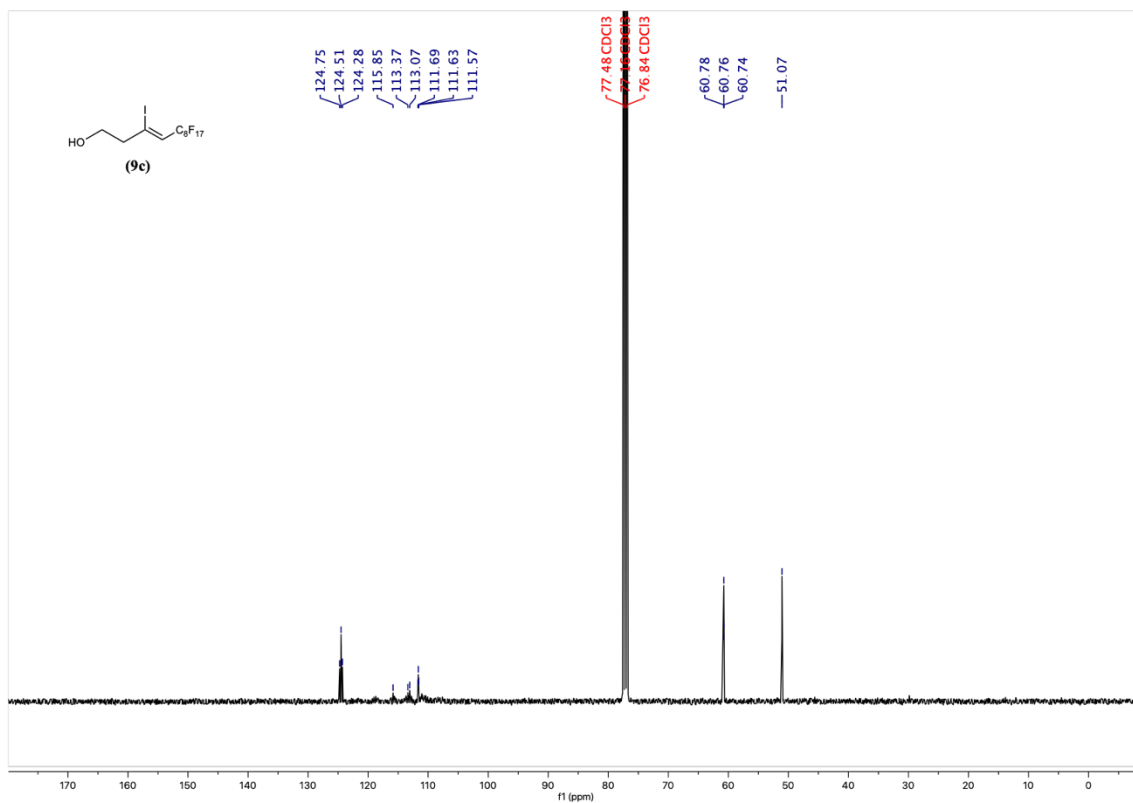


Figure S54: ¹³C NMR spectrum (101 MHz) of (9c) in CDCl₃.

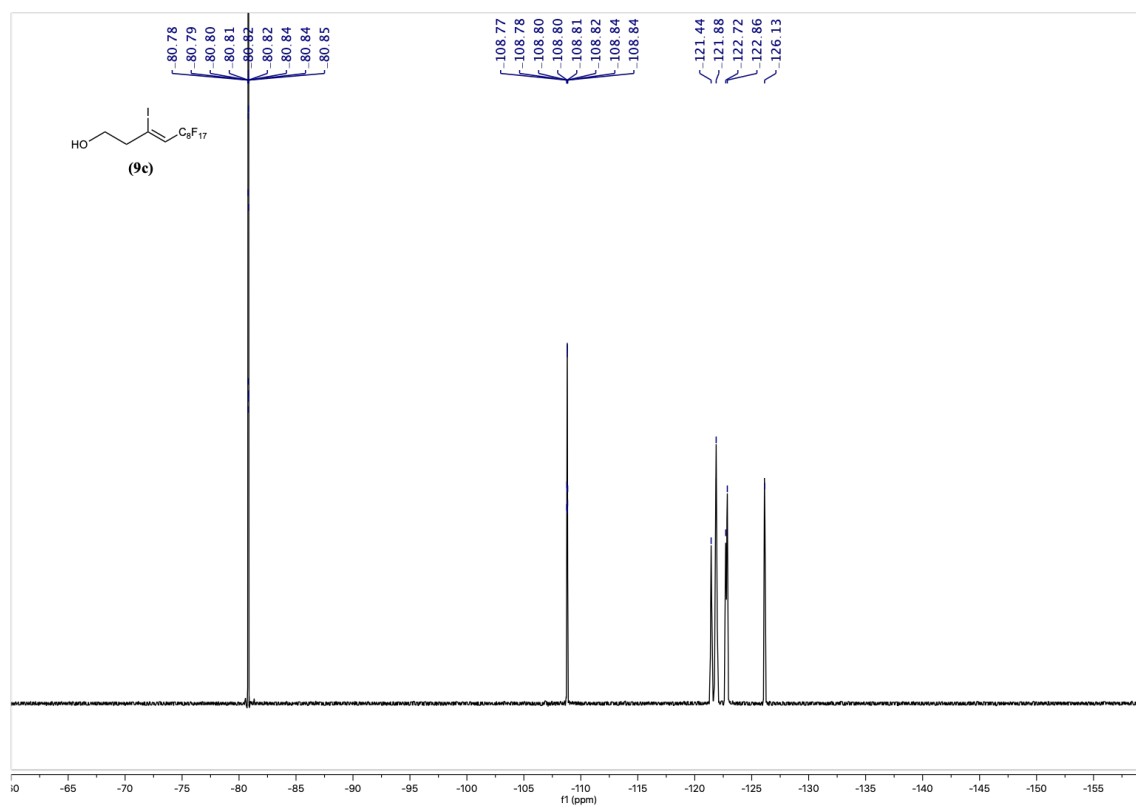


Figure S55: ¹⁹F NMR spectrum (376 MHz) of (9c) in CDCl₃.

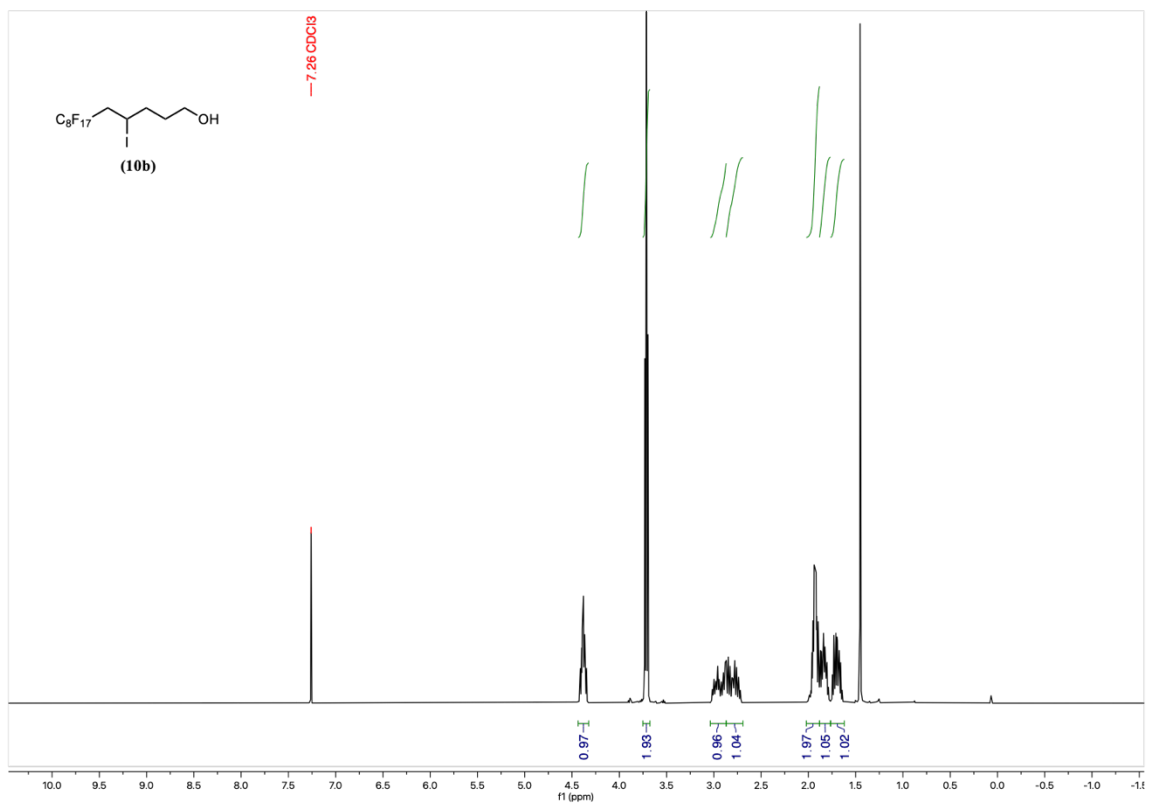


Figure S56: ¹H NMR spectrum (400 MHz) of (10b) in CDCl₃.

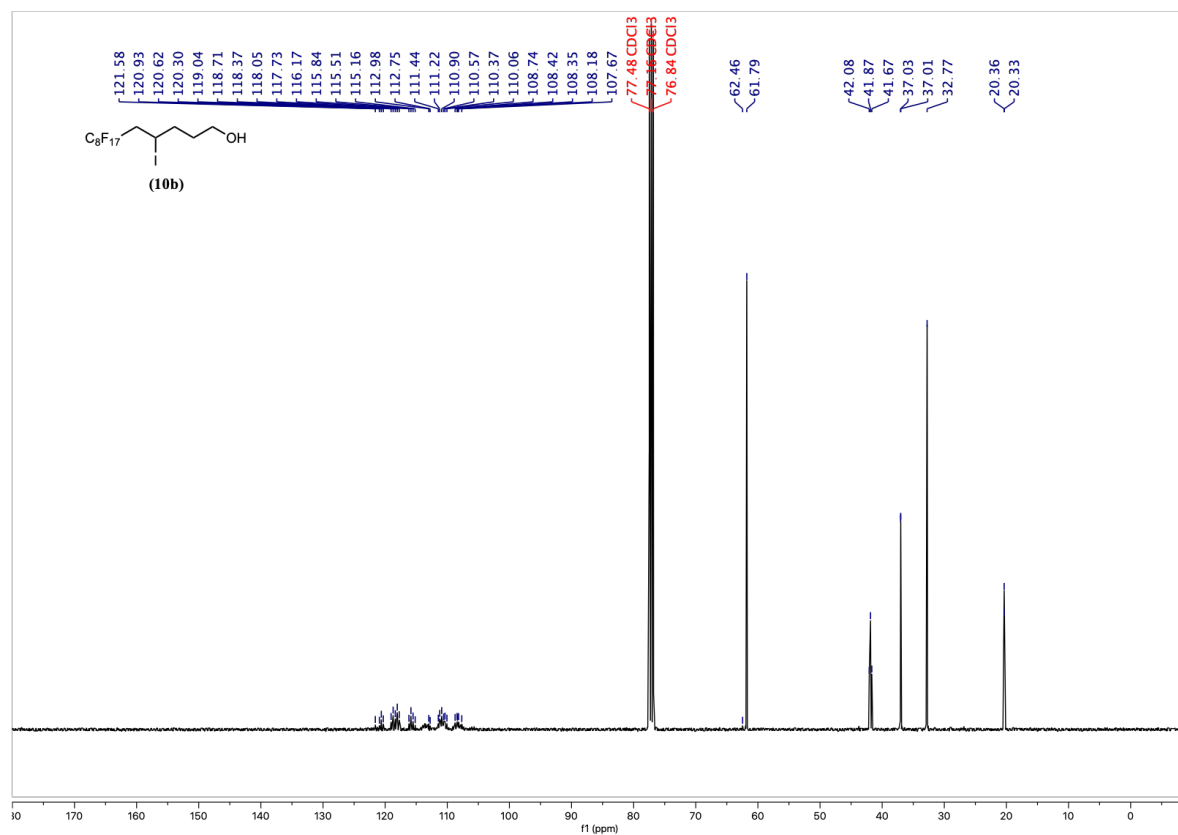


Figure S57: ¹³C NMR spectrum (101 MHz) of (10b) in CDCl₃.

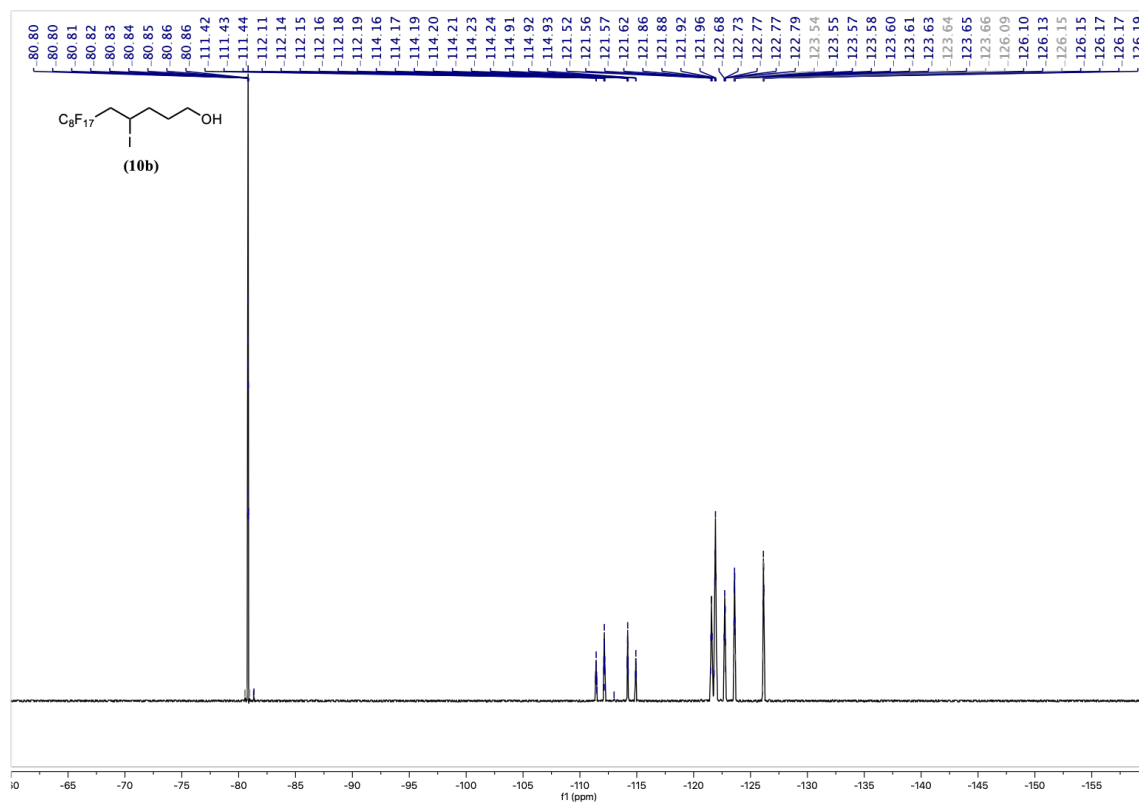


Figure S58: ¹⁹F NMR spectrum (376 MHz) of (10b) in CDCl₃.

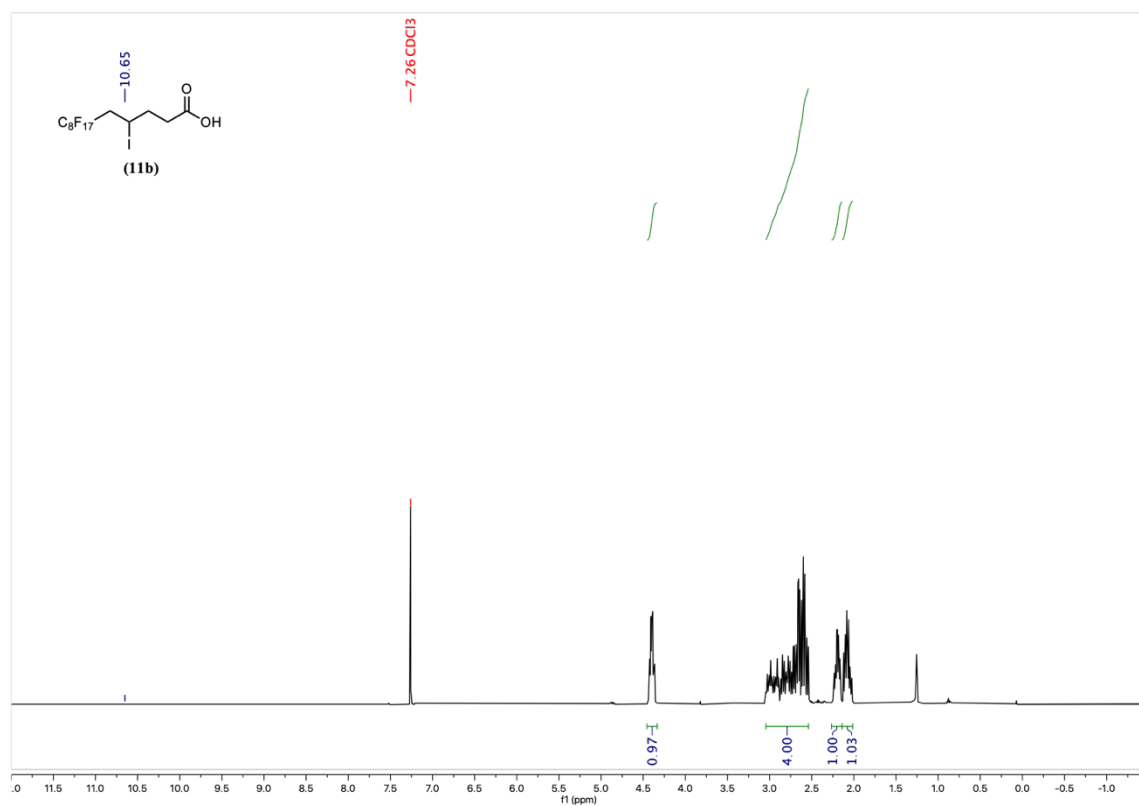


Figure S59: ¹H NMR spectrum (400 MHz) of (11b) in CDCl₃.

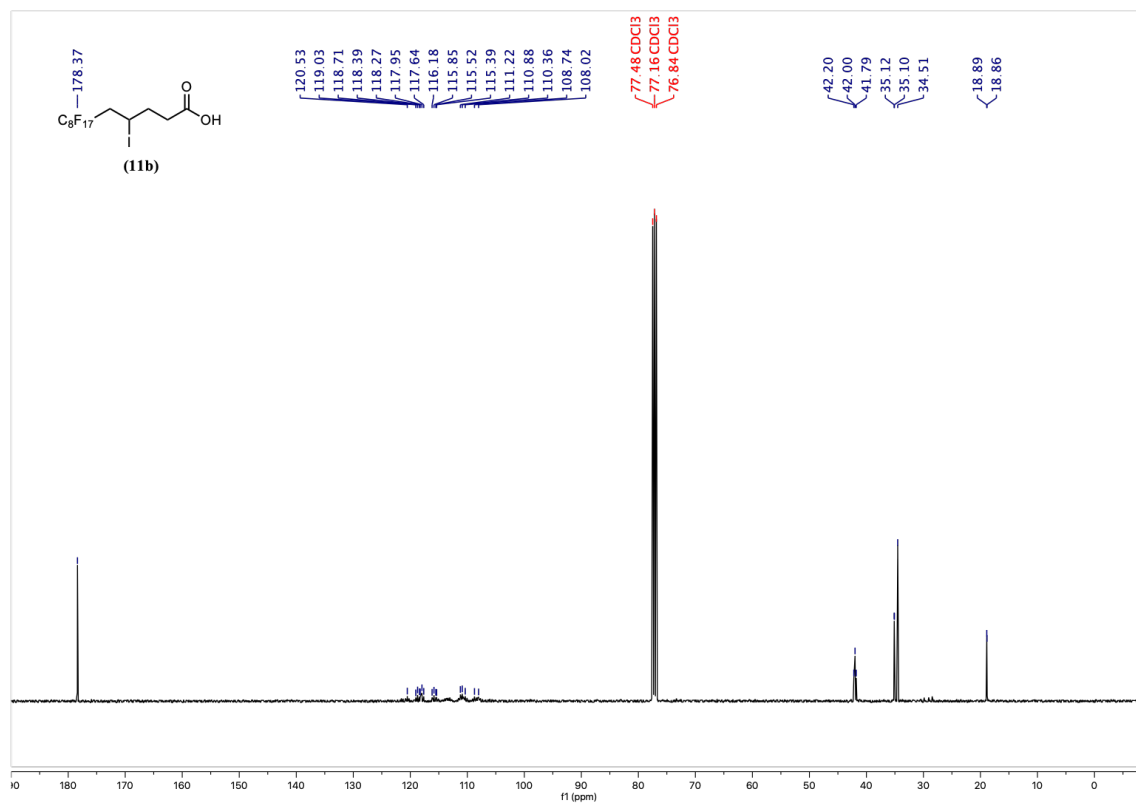


Figure S60: ¹³C NMR spectrum (101 MHz) of (11b) in CDCl₃.

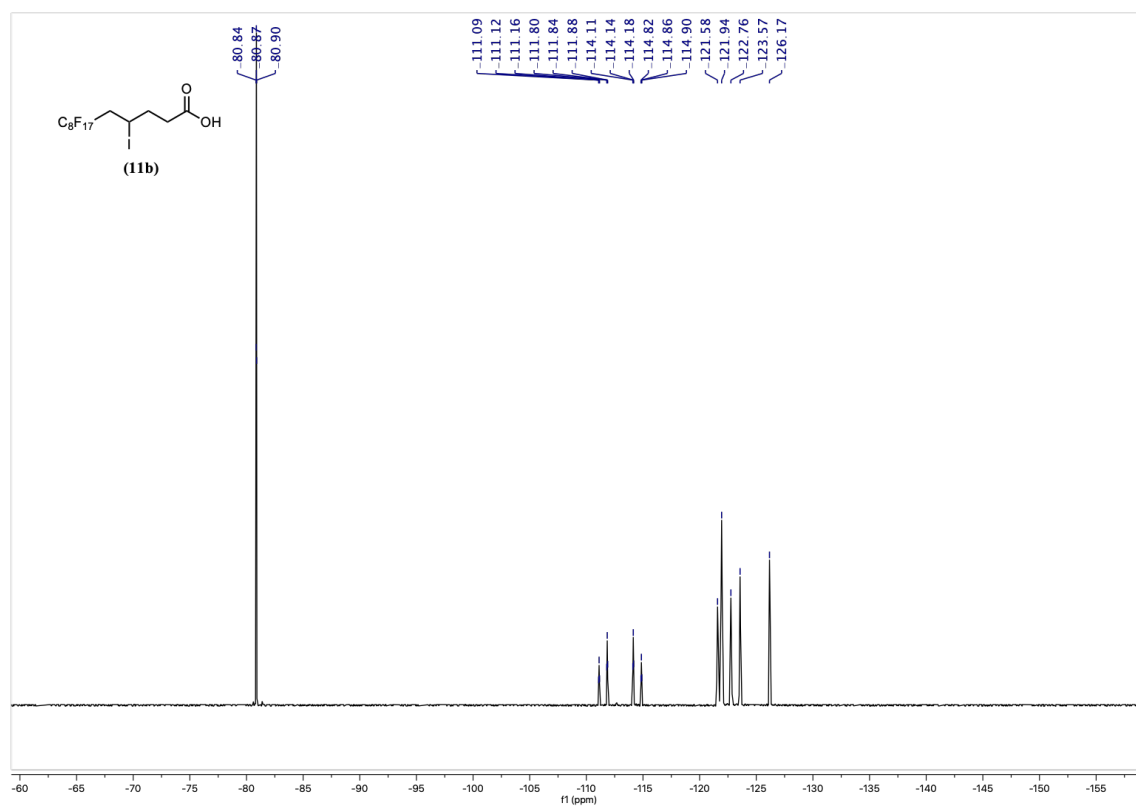


Figure S61: ¹⁹F NMR spectrum (376 MHz) of (11b) in CDCl₃.

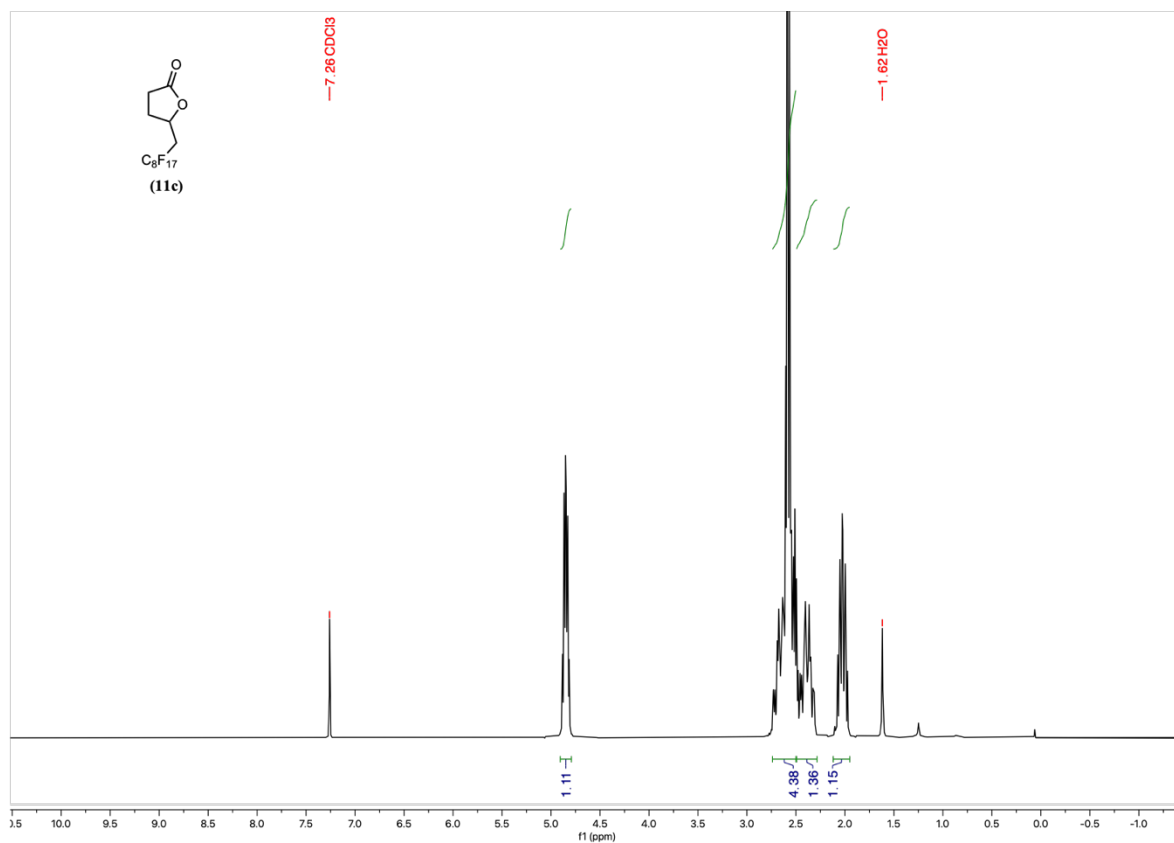


Figure S62: ¹H NMR spectrum (400 MHz) of **(11c)** in CDCl₃.

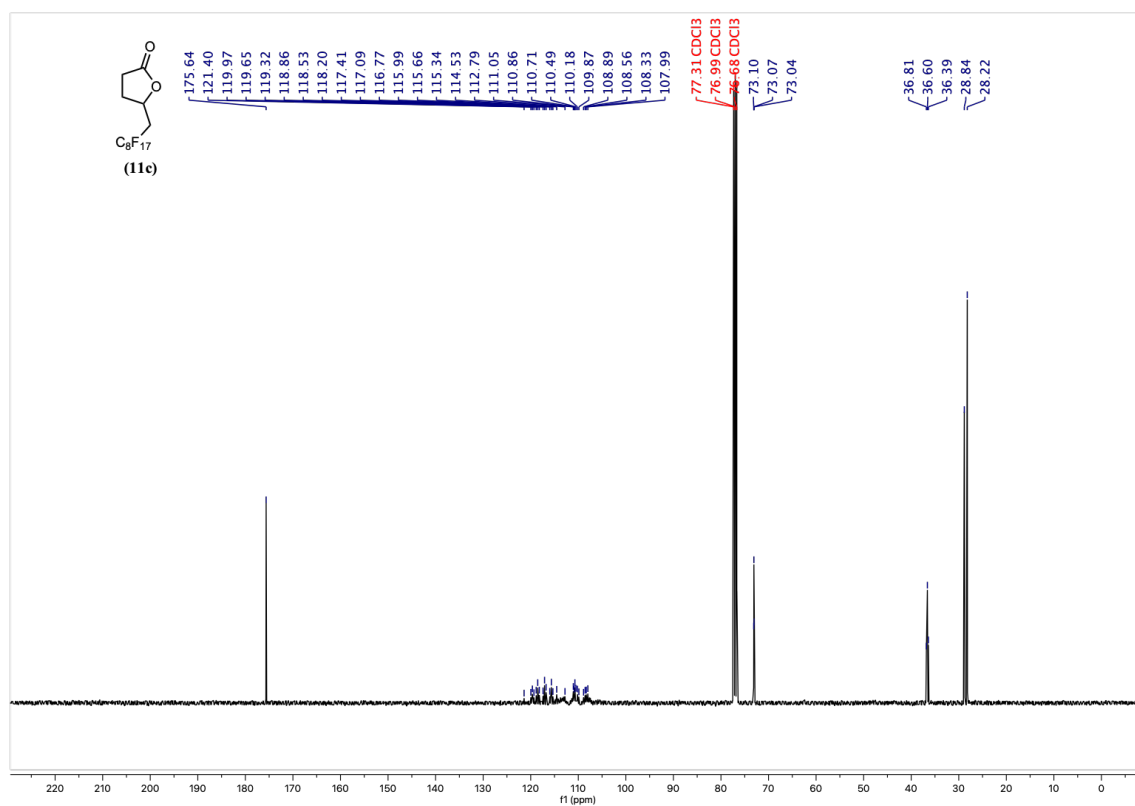


Figure S63: ¹³C NMR spectrum (101 MHz) of **(11c)** in CDCl₃.

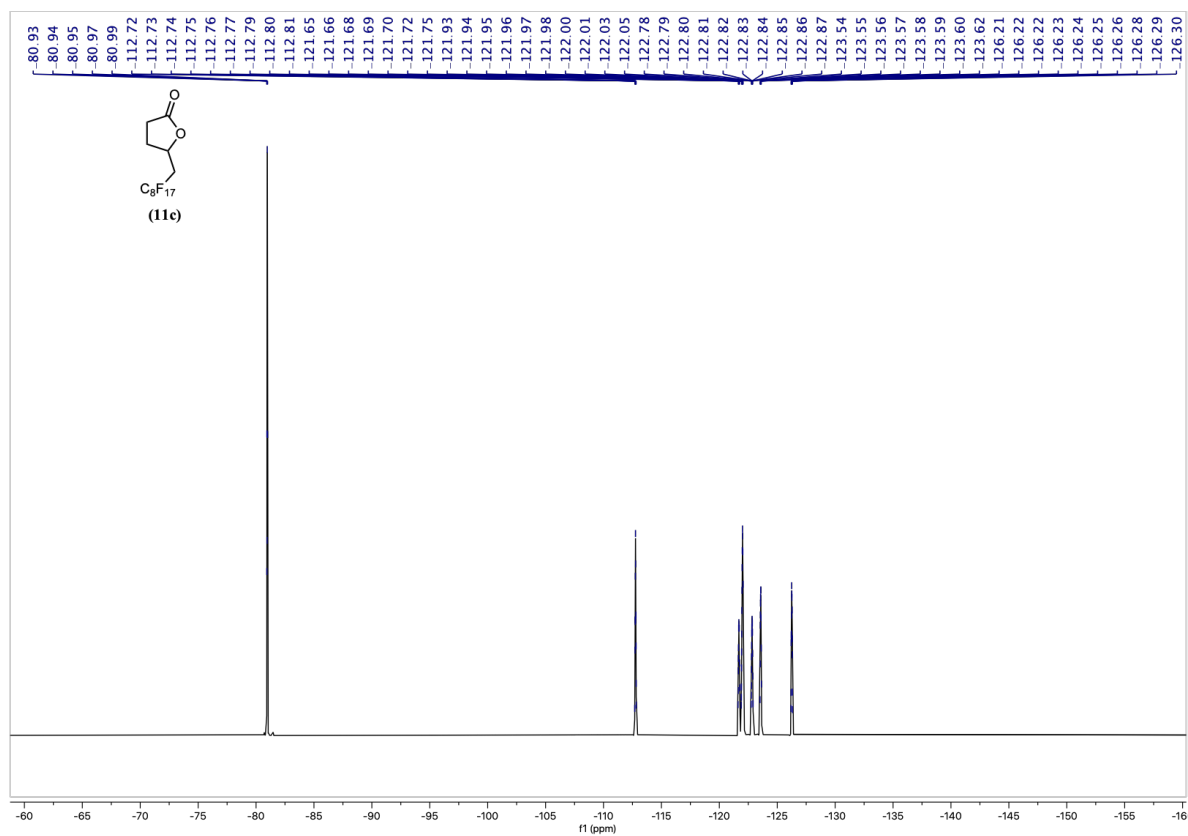


Figure S64: ¹⁹F NMR spectrum (376 MHz) of (11c) in CDCl₃.

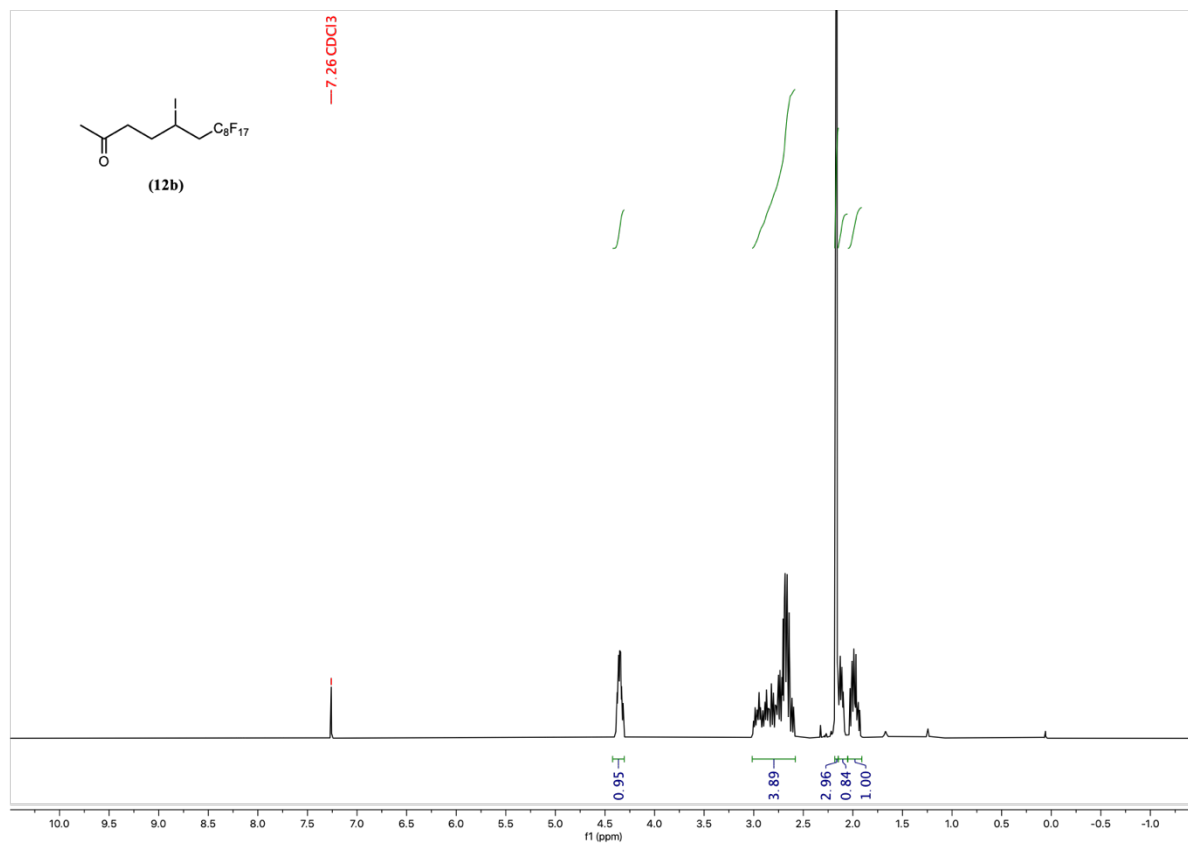


Figure S65: ¹H NMR spectrum (400 MHz) of (12b) in CDCl₃.

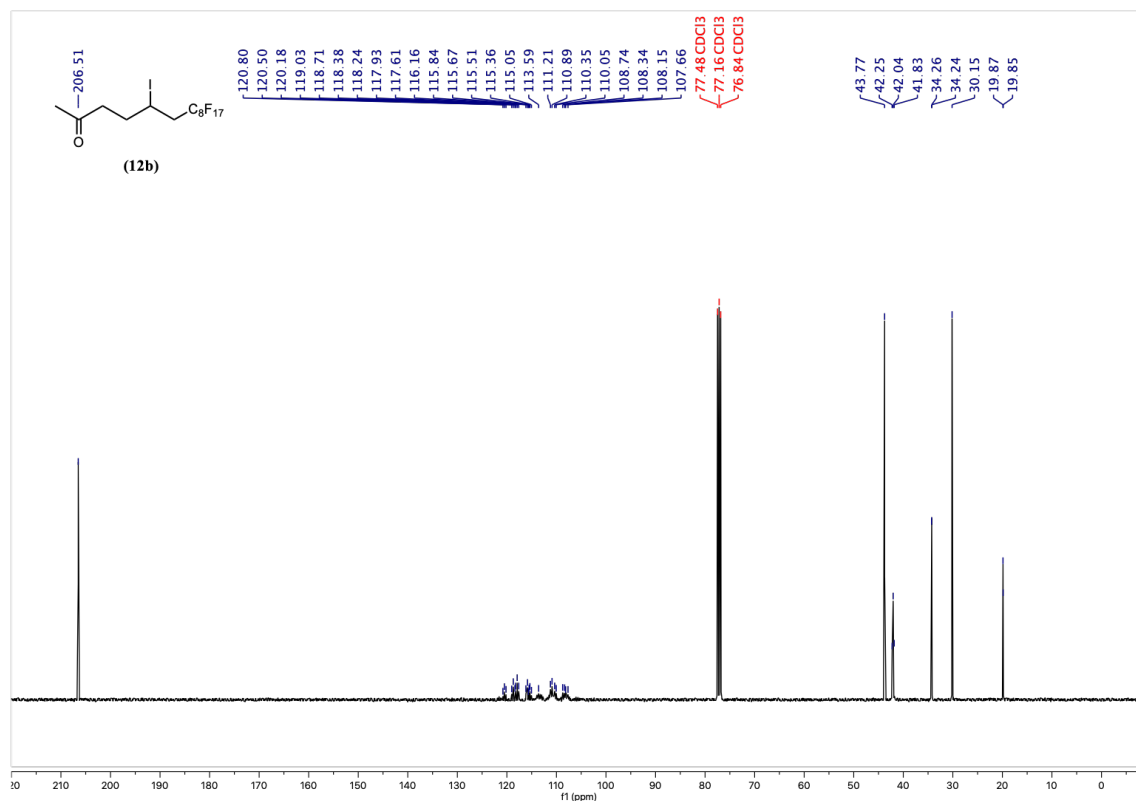


Figure S66: ¹³C NMR spectrum (101 MHz) of (12b) in CDCl₃.

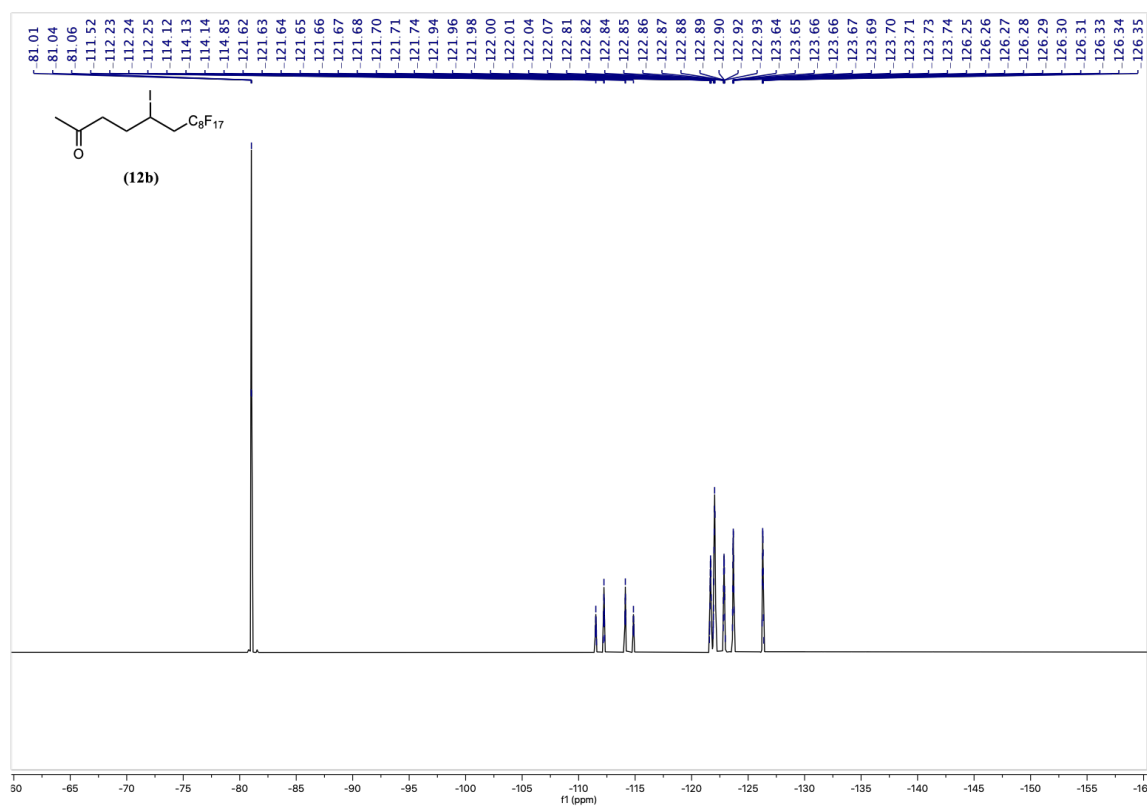


Figure S67: ¹⁹F NMR spectrum (376 MHz) of (12b) in CDCl₃.

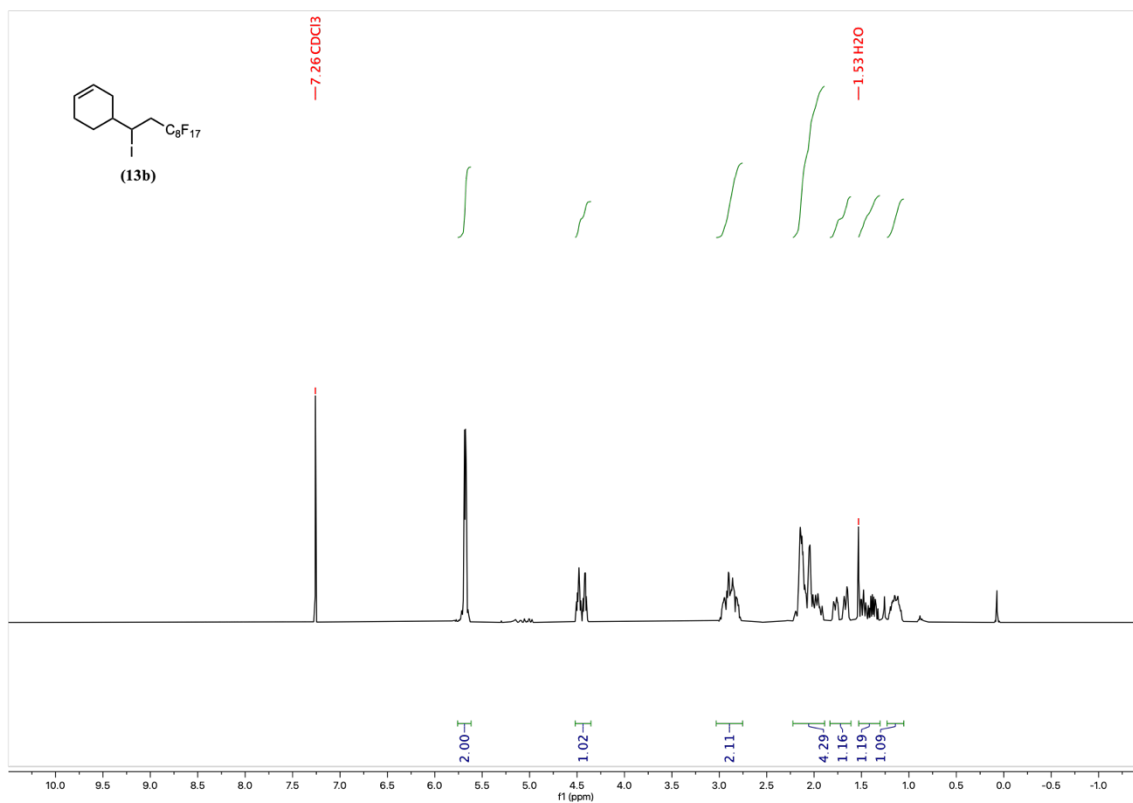


Figure S68: ¹H NMR spectrum (400 MHz) of (13b) in CDCl₃.

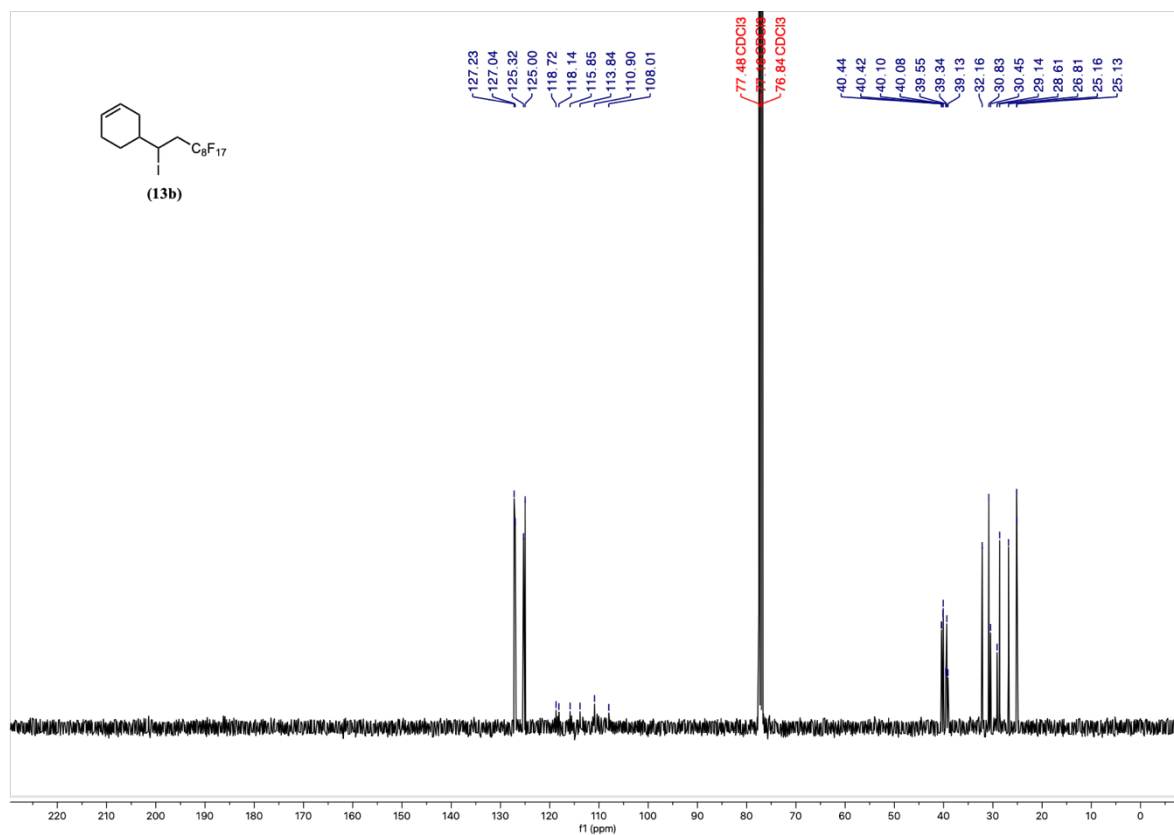


Figure S69: ¹³C NMR spectrum (101 MHz) of (13b) in CDCl₃.

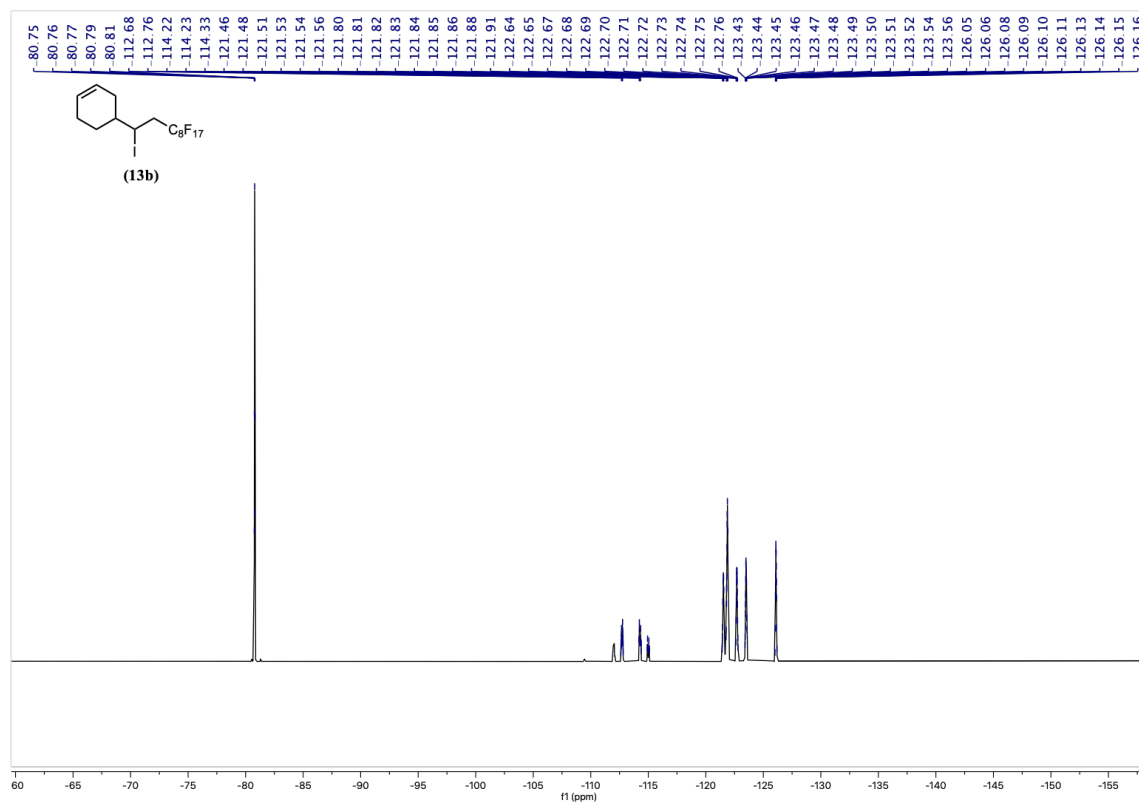


Figure S70: ¹⁹F NMR spectrum (376 MHz) of (13b) in CDCl₃.

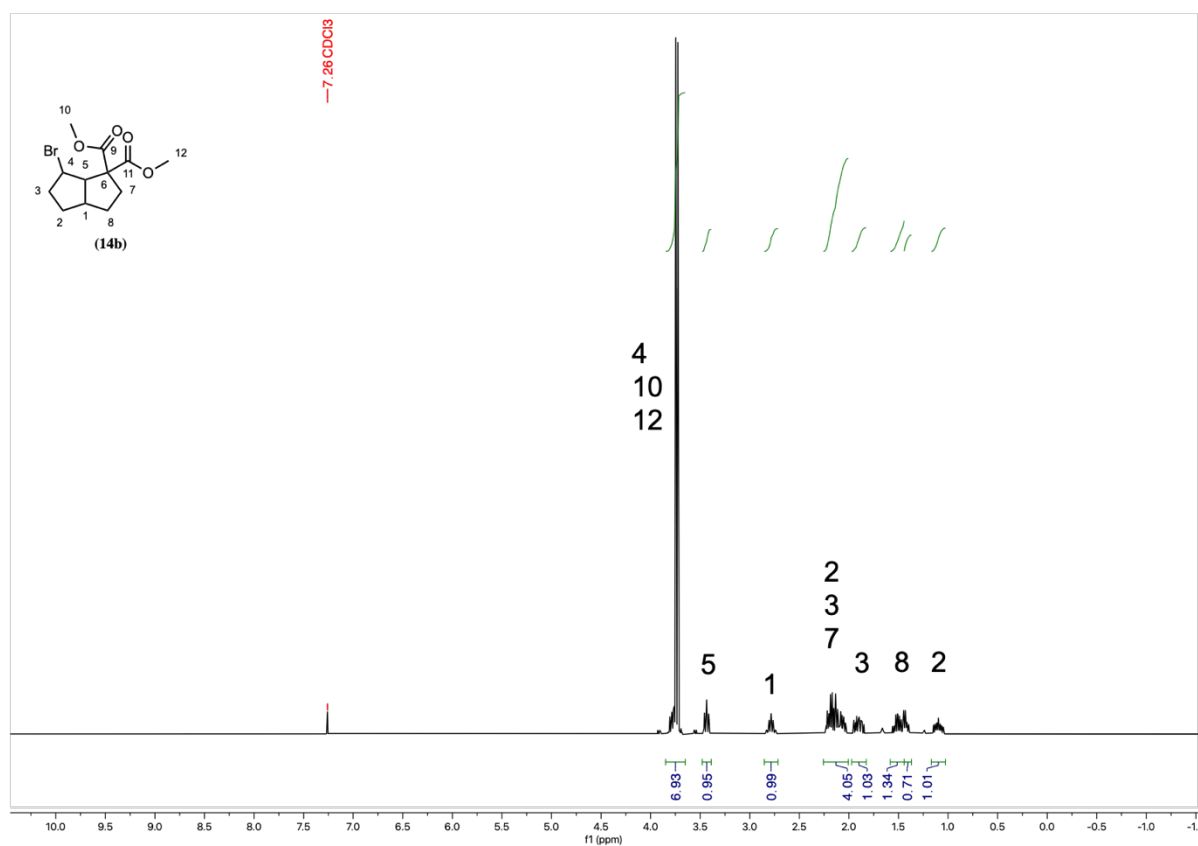


Figure S71: ¹H NMR spectrum (400 MHz) of (14b) in CDCl₃.

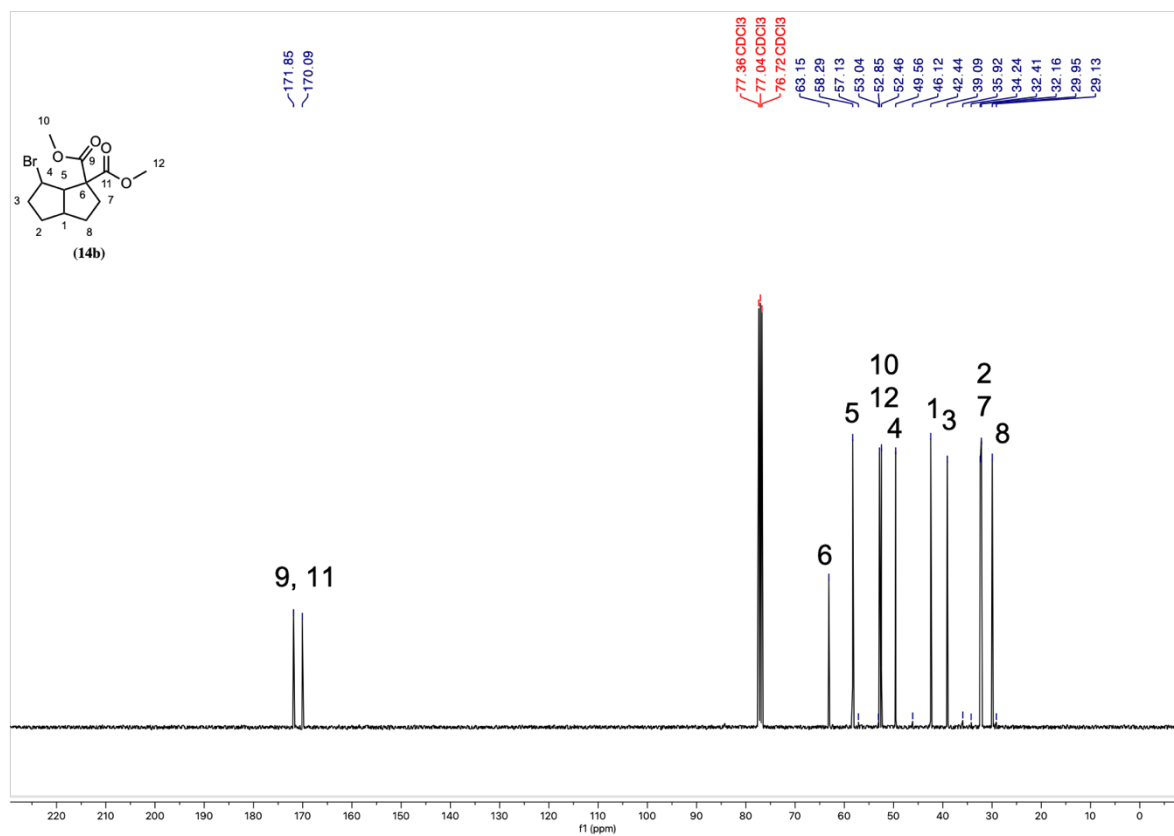


Figure S72: ^{13}C NMR spectrum (101 MHz) of (14b) in CDCl_3 .

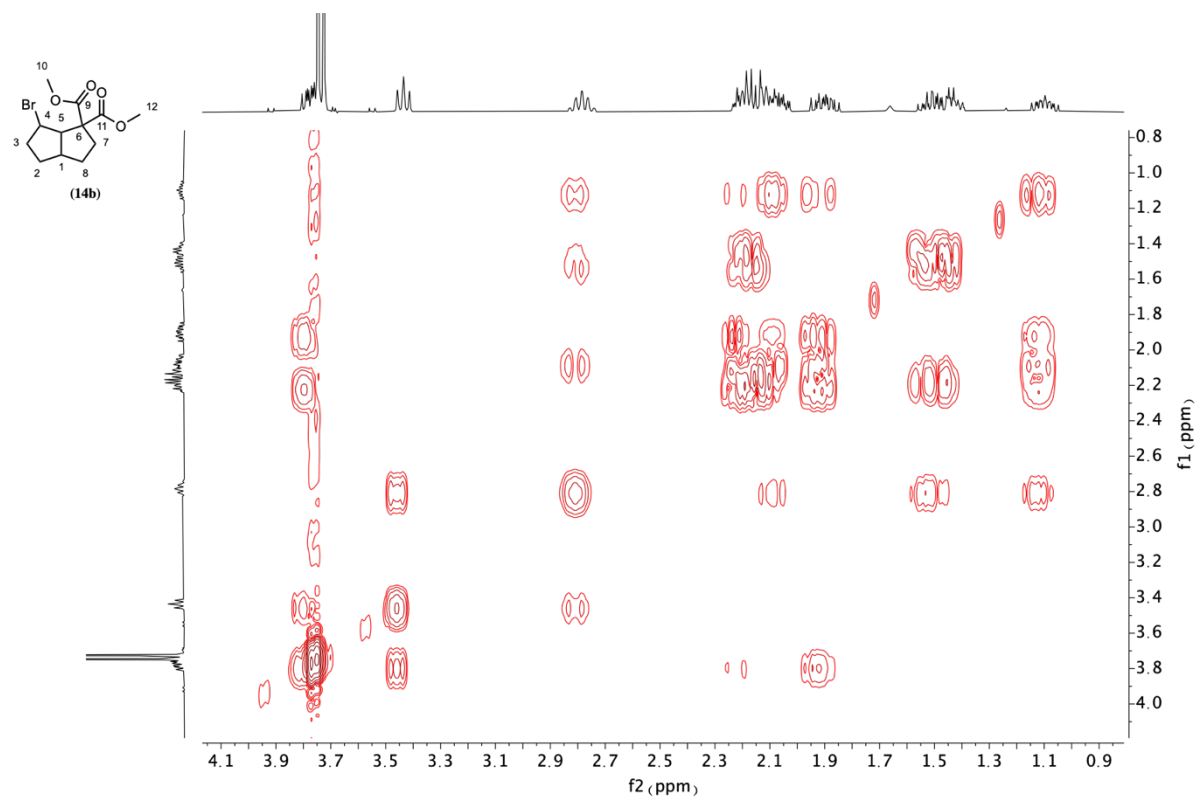


Figure S73: COSY spectrum (400 MHz) of (14b) in CDCl_3 .

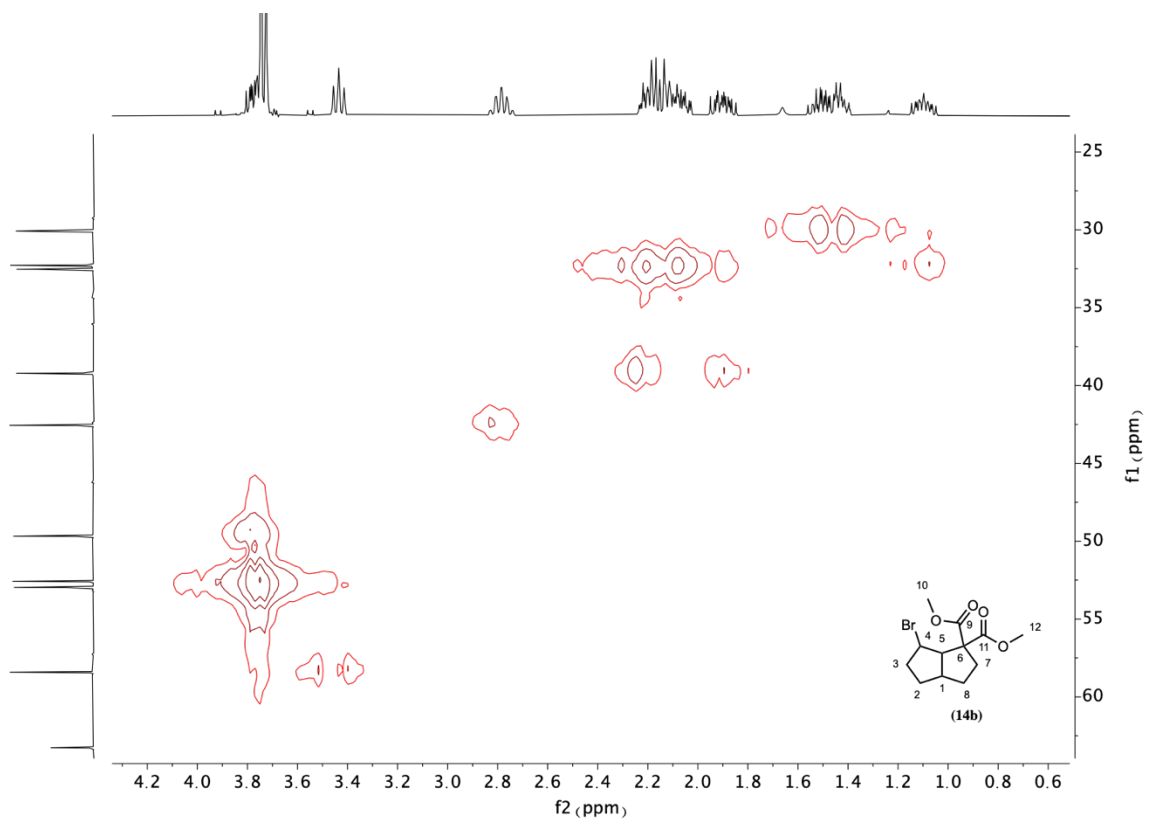


Figure S74: HMQC spectrum of (14b) in CDCl₃.

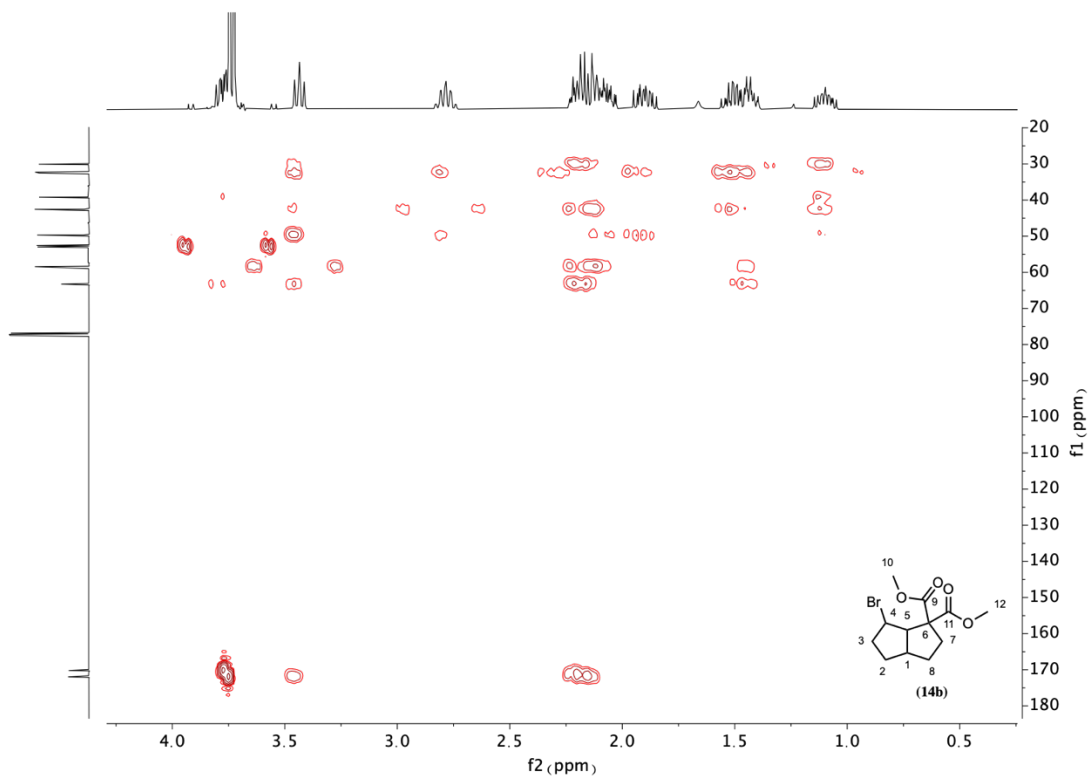


Figure S75: HMBC spectrum of (14b) in CDCl₃.

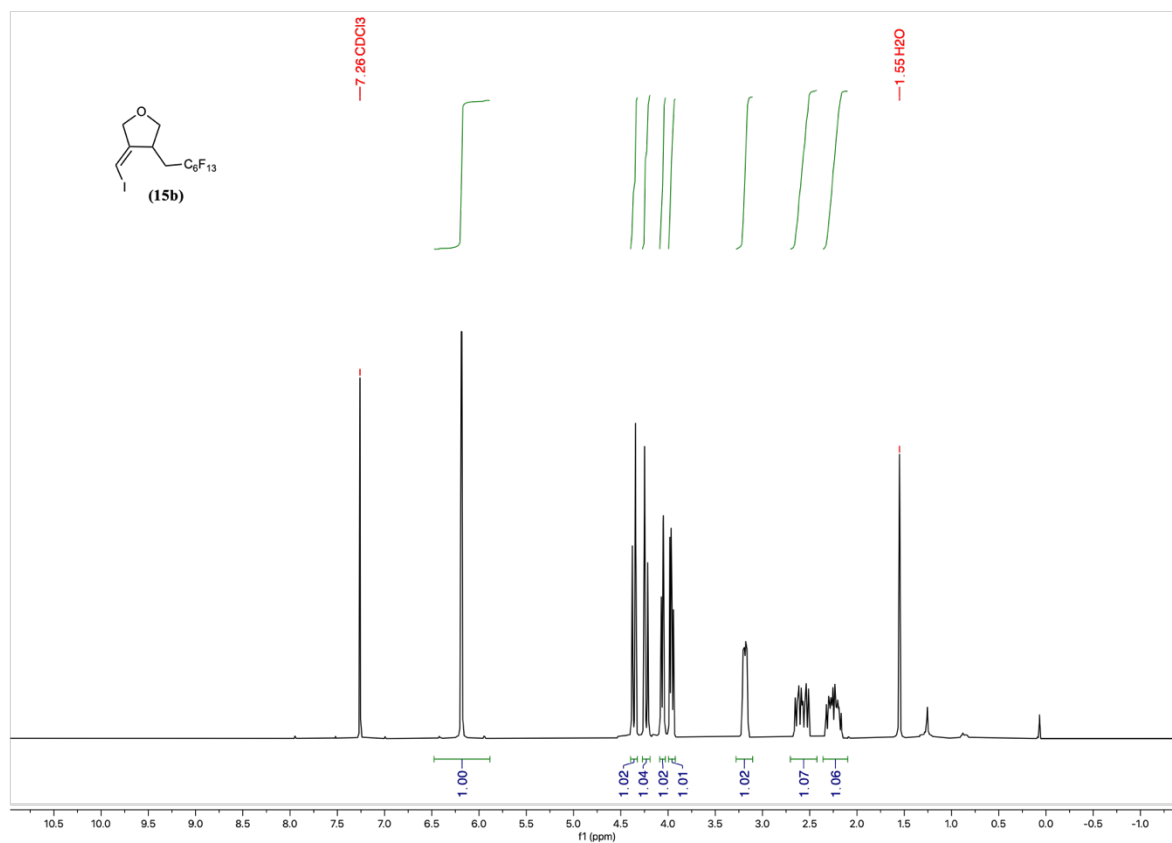


Figure S76: ¹H NMR spectrum (400 MHz) of (15b) in CDCl₃.

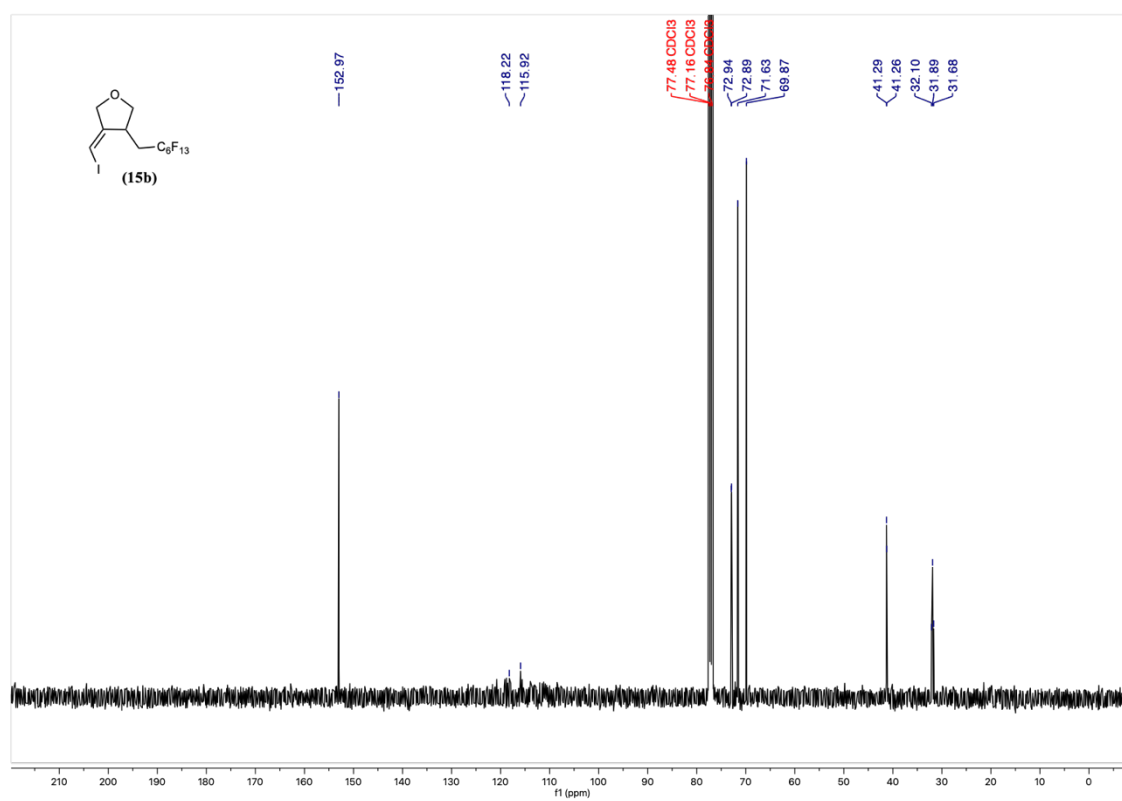
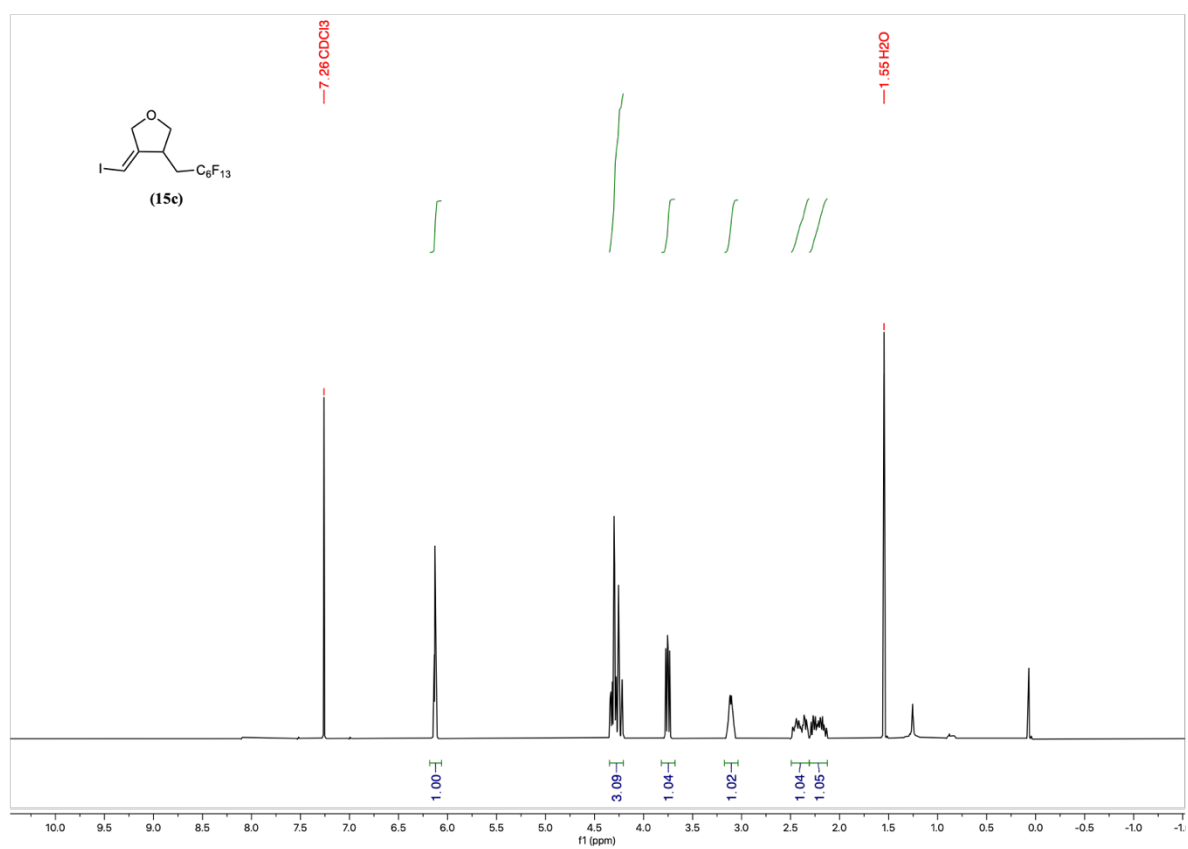
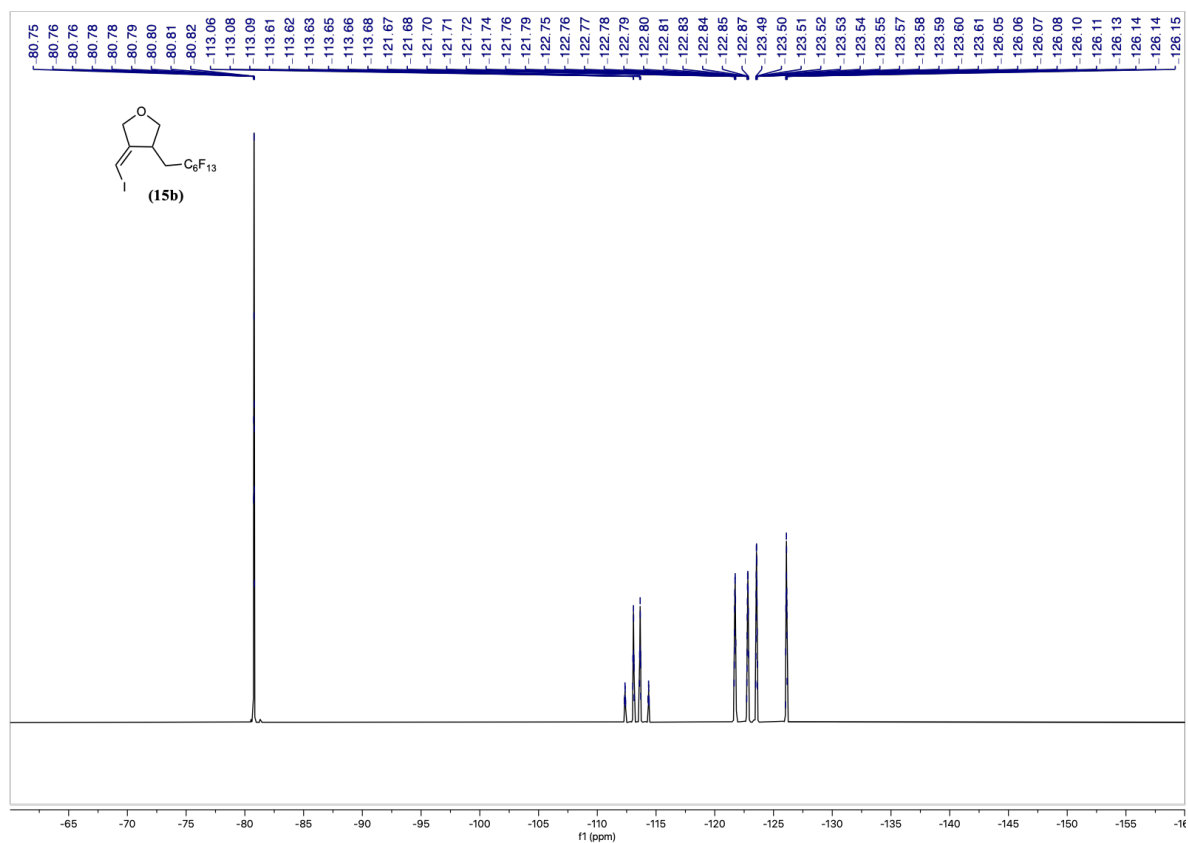


Figure S77: ¹³C NMR spectrum (101 MHz) of (15b) in CDCl₃.



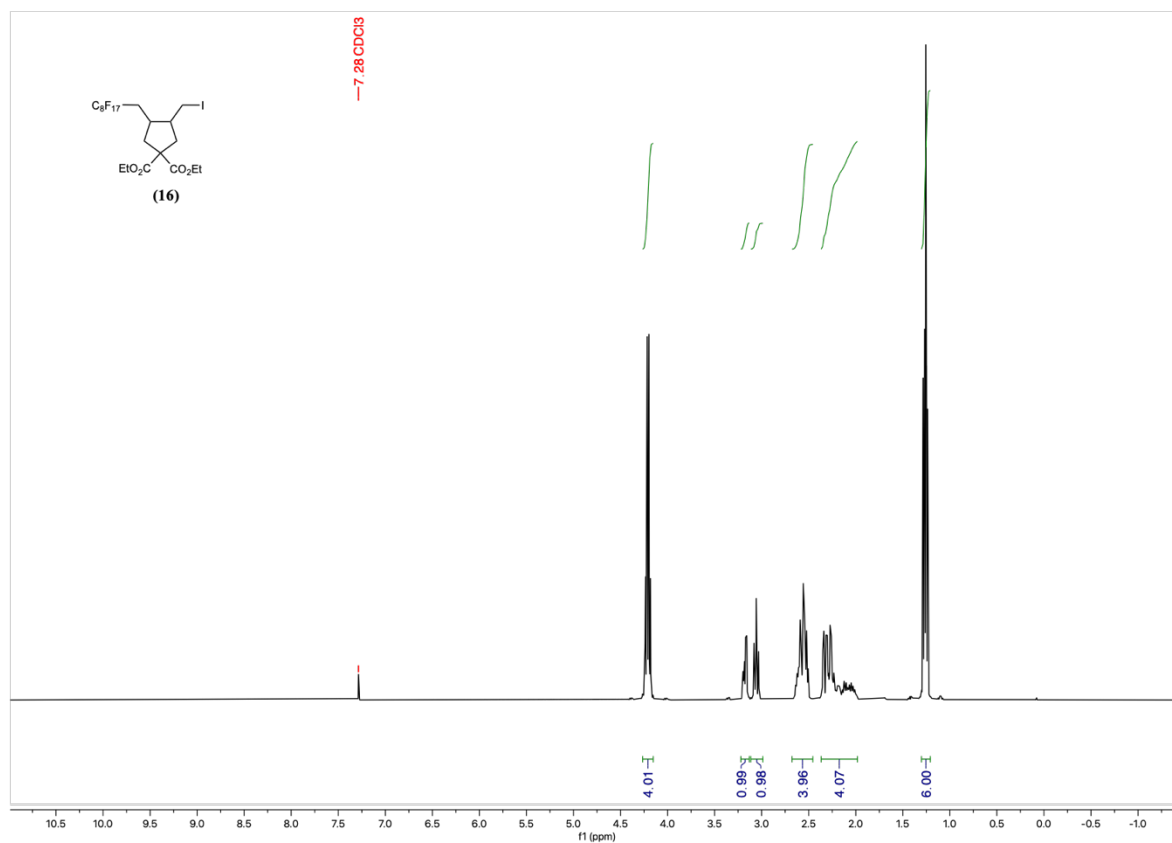


Figure S82: ¹H NMR spectrum (400 MHz) of (16) in CDCl₃.

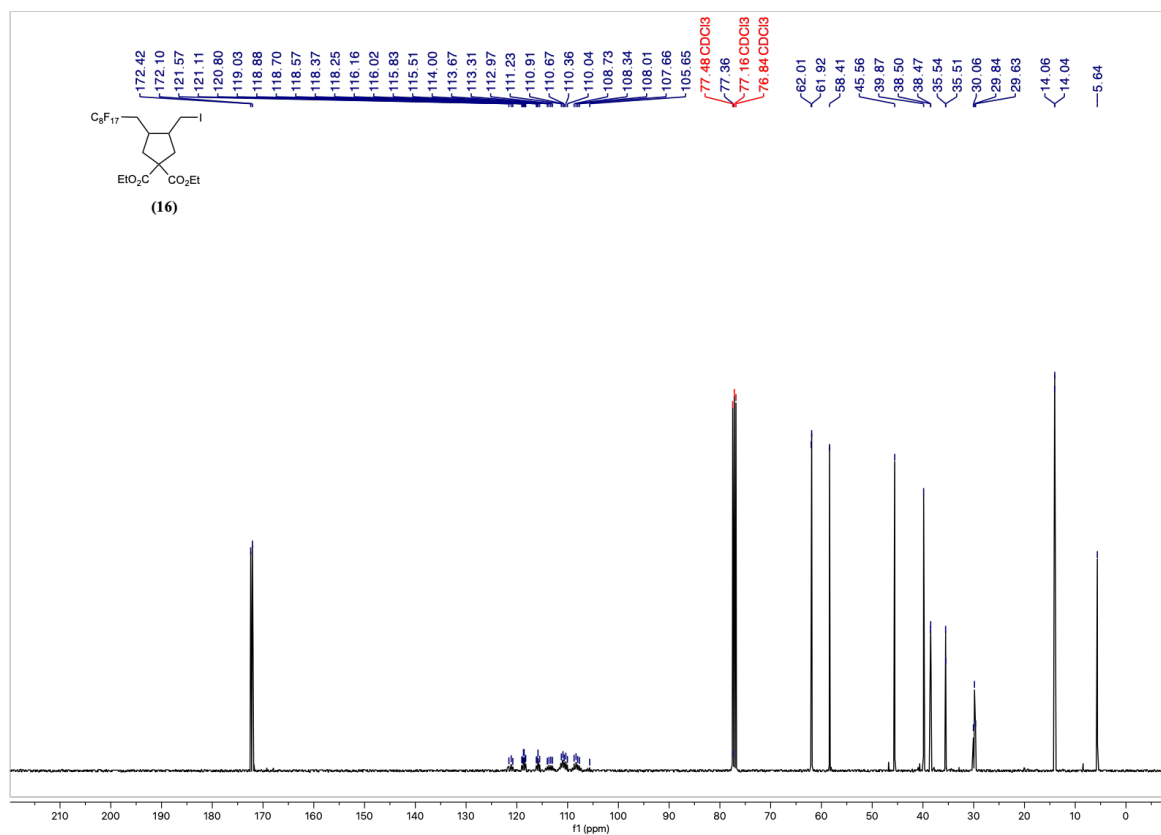


Figure S83: ¹³C NMR spectrum (101 MHz) of (16) in CDCl₃.

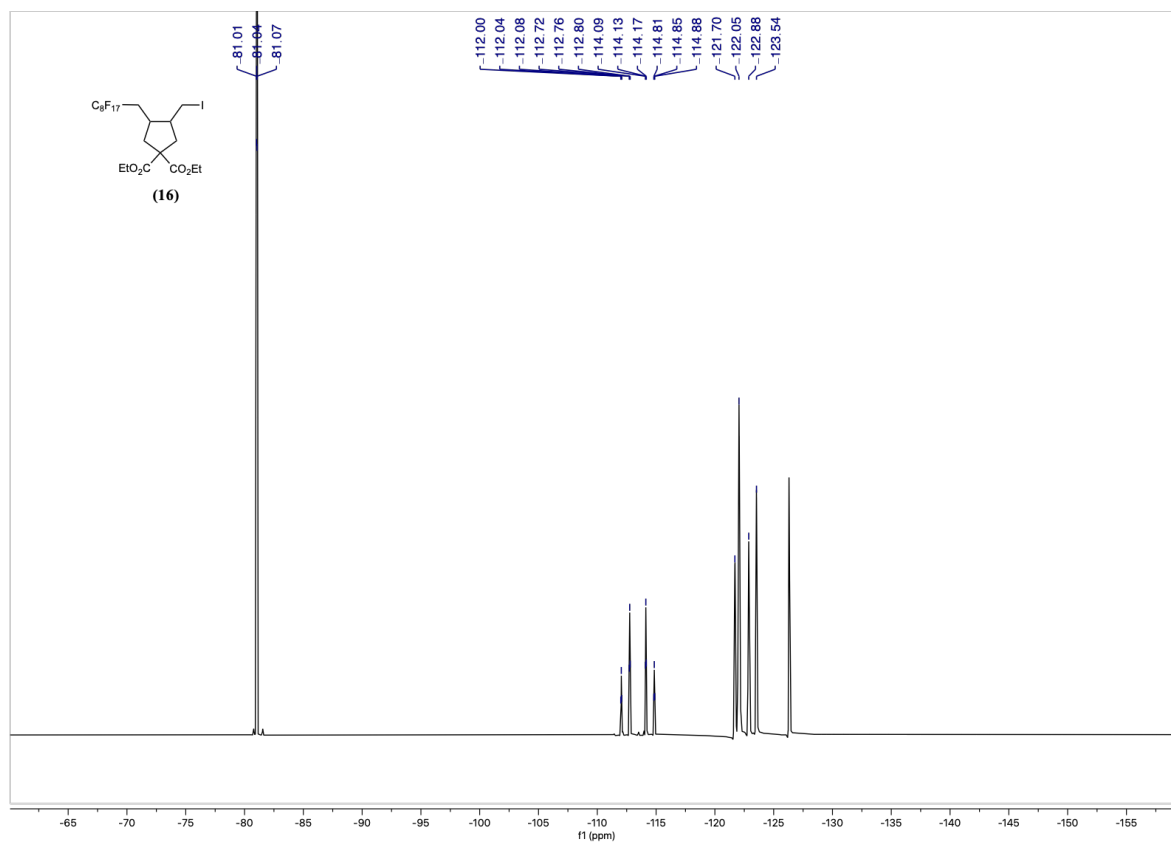


Figure S84: ¹⁹F NMR spectrum (376 MHz) of (16) in CDCl₃.

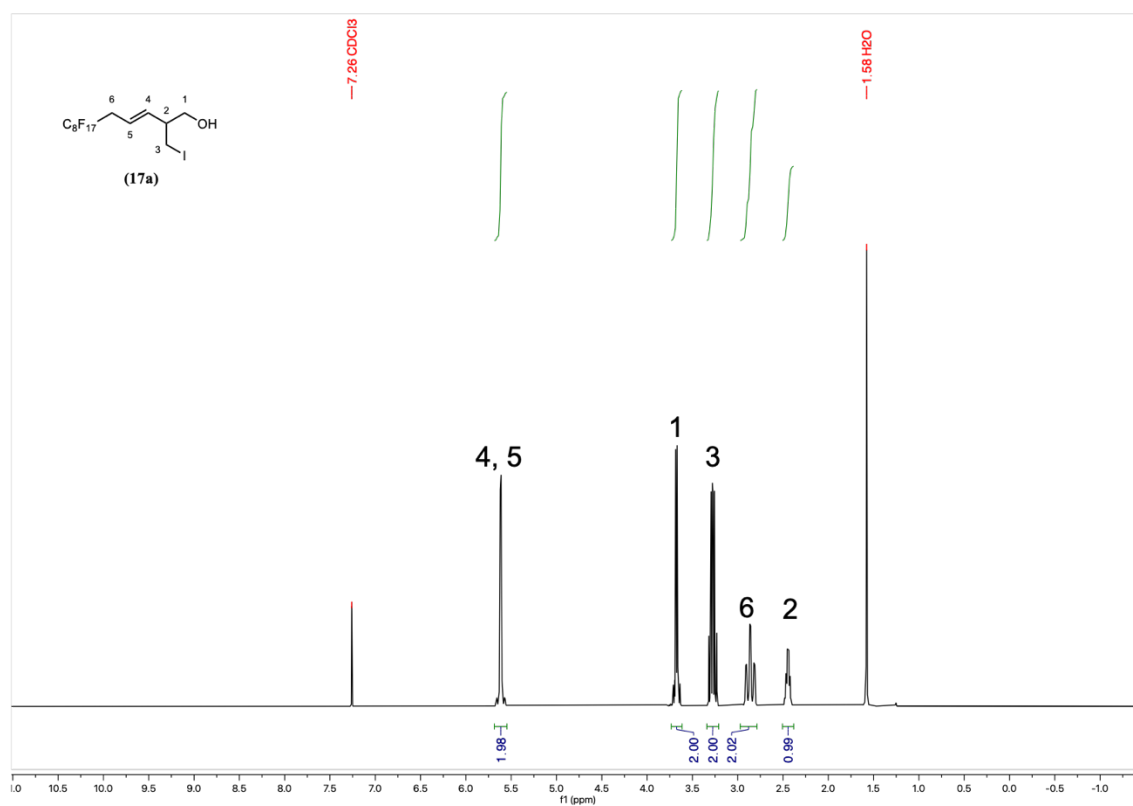


Figure S85: ¹H NMR spectrum (400 MHz) of (17a) in CDCl₃.

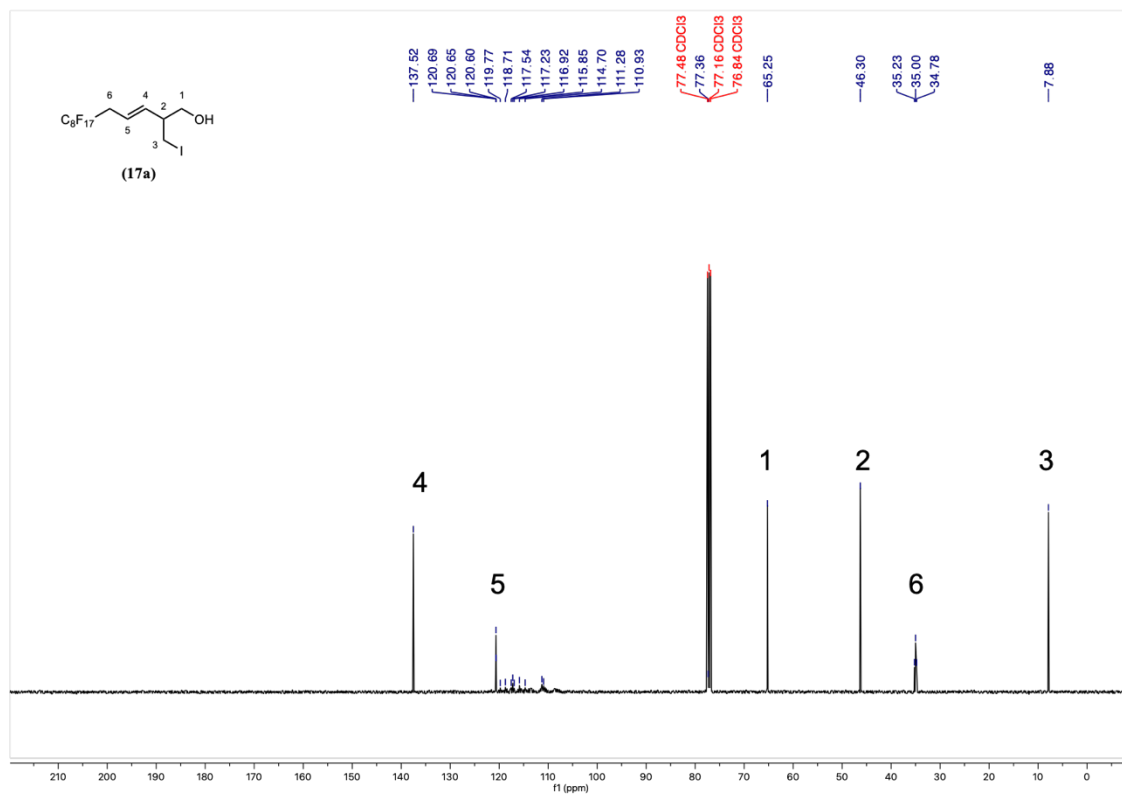


Figure S86: ¹³C NMR spectrum (101 MHz) of (17a) in CDCl₃.

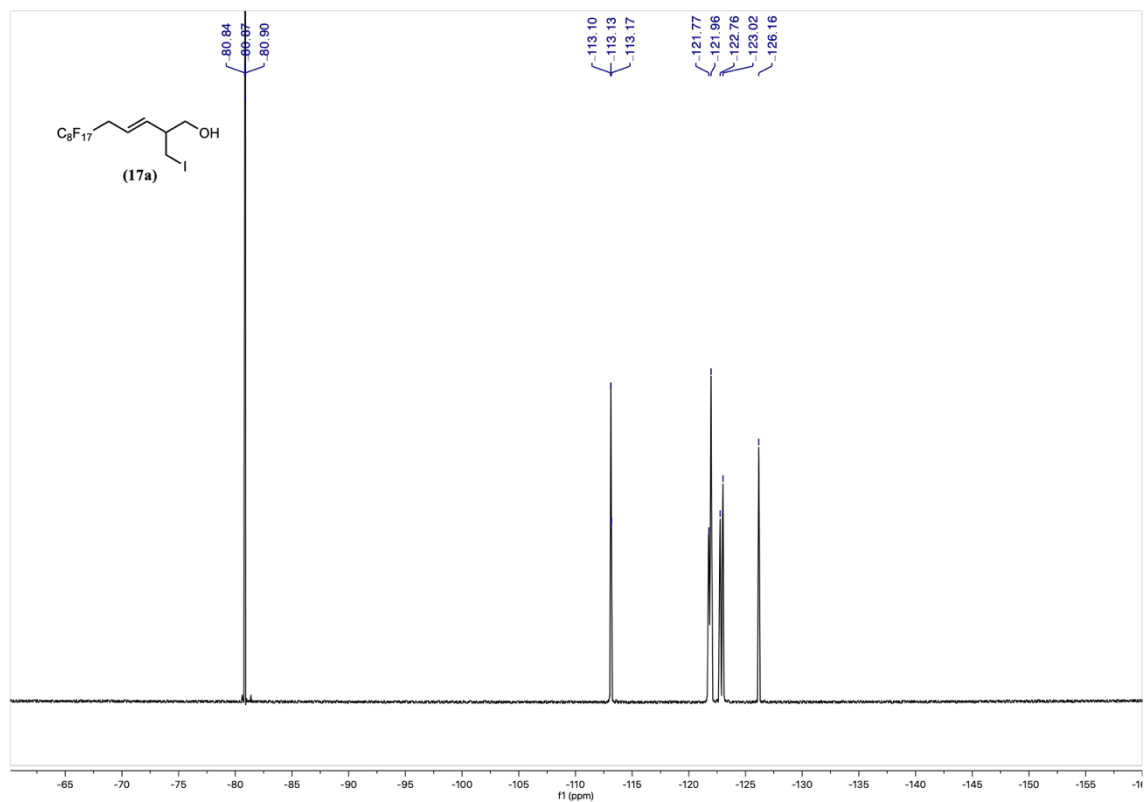


Figure S87: ¹⁹F NMR spectrum (376 MHz) of (17a) in CDCl₃.

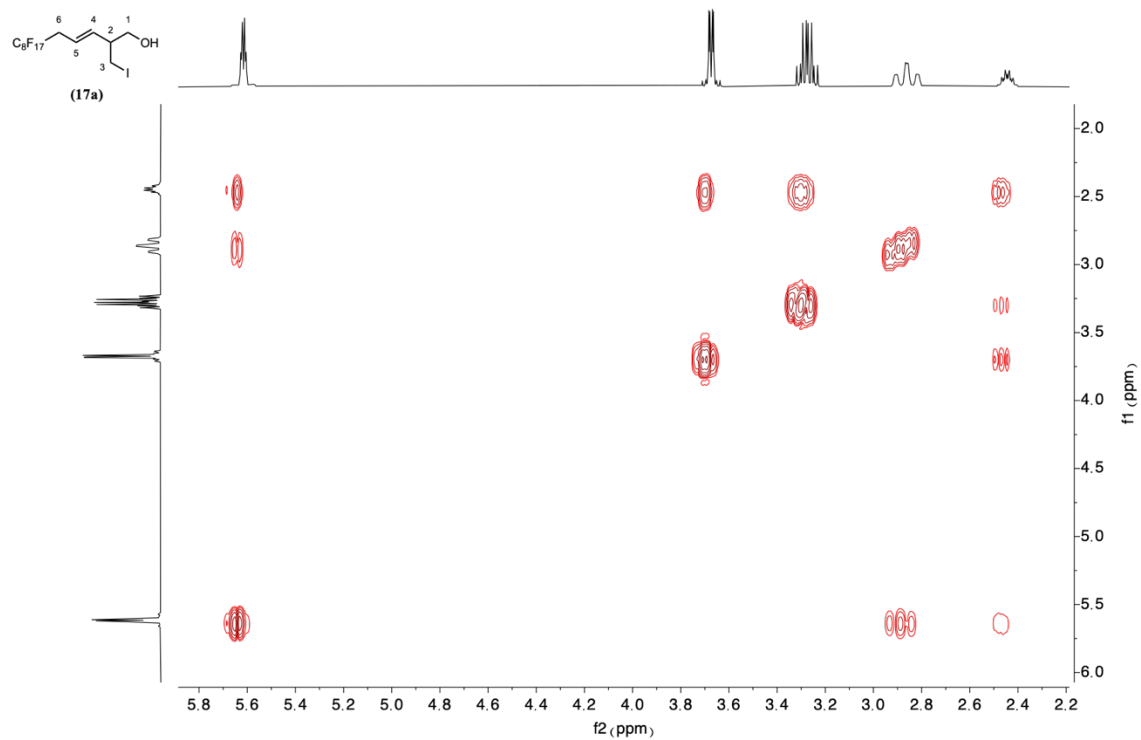


Figure S88: COSY spectrum (400 MHz) of **(17a)** in CDCl₃.

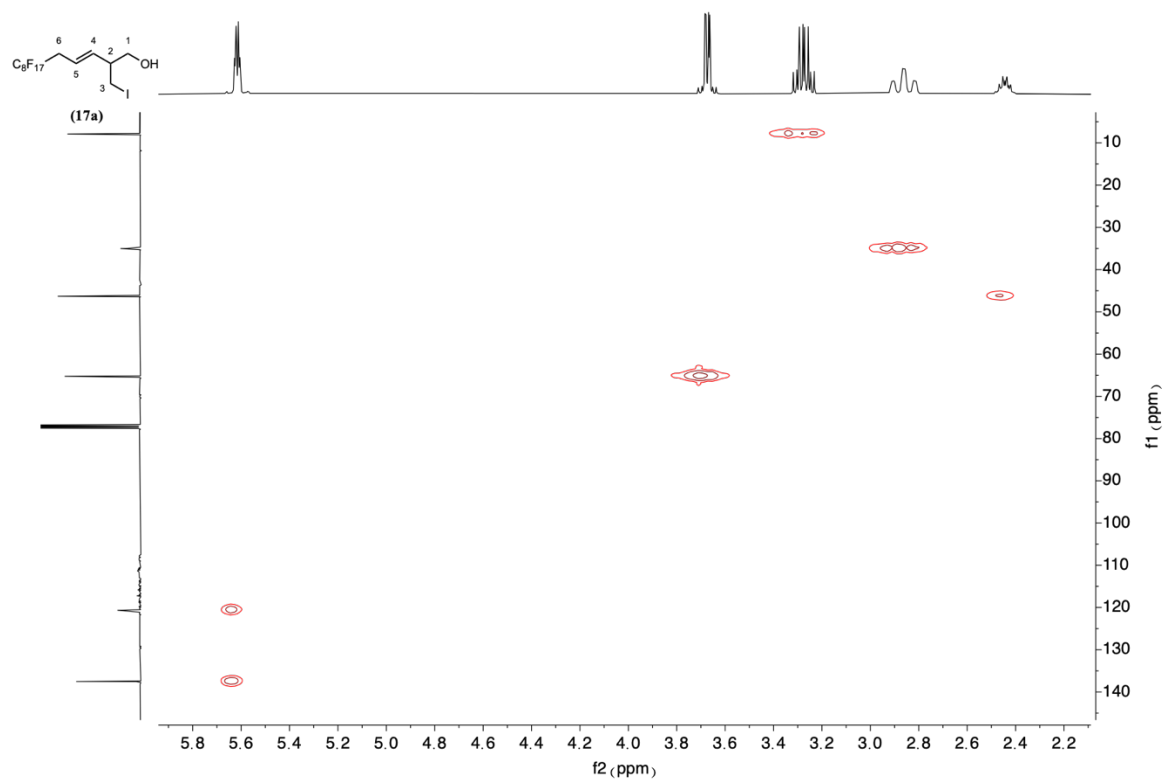


Figure S89: HMQC spectrum of **(17a)** in CDCl₃.

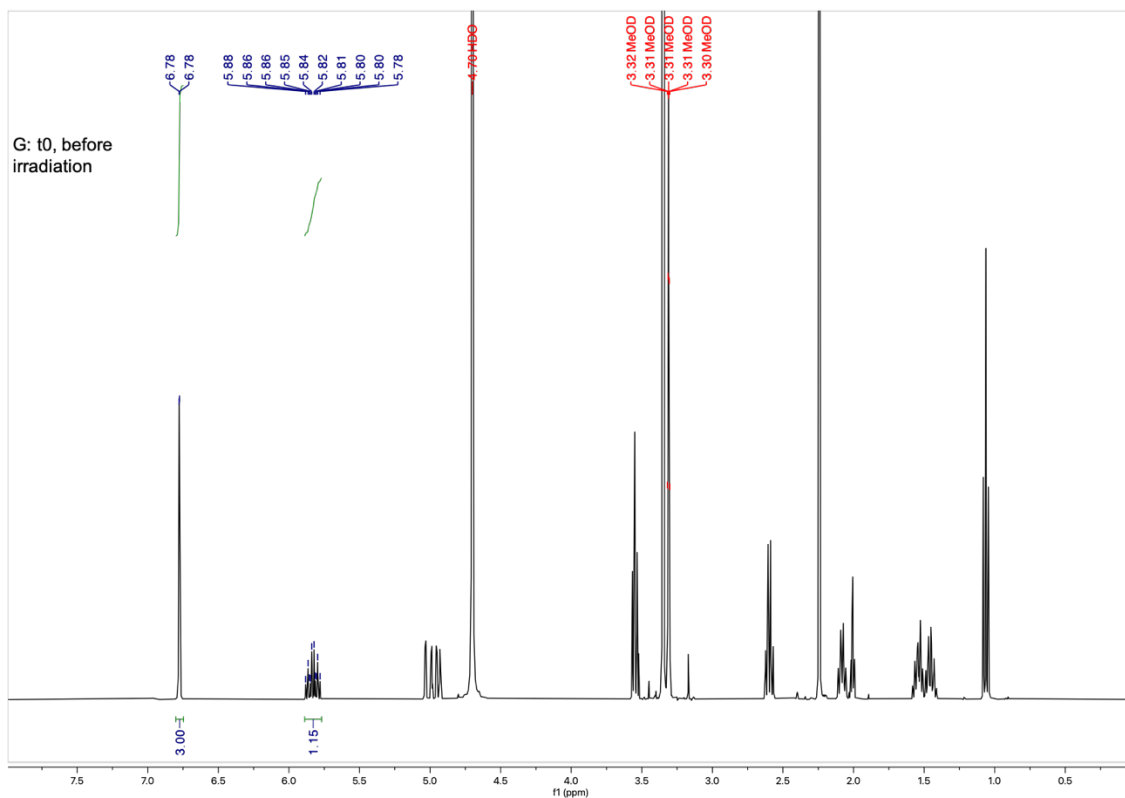


Figure S90: ^1H NMR spectrum (400 MHz) of Sample G (Wavelength-switching experiment) before irradiation (CD_3OD , integrated against internal standard ($3H$ (ArH)): mesitylene (15 μL)).

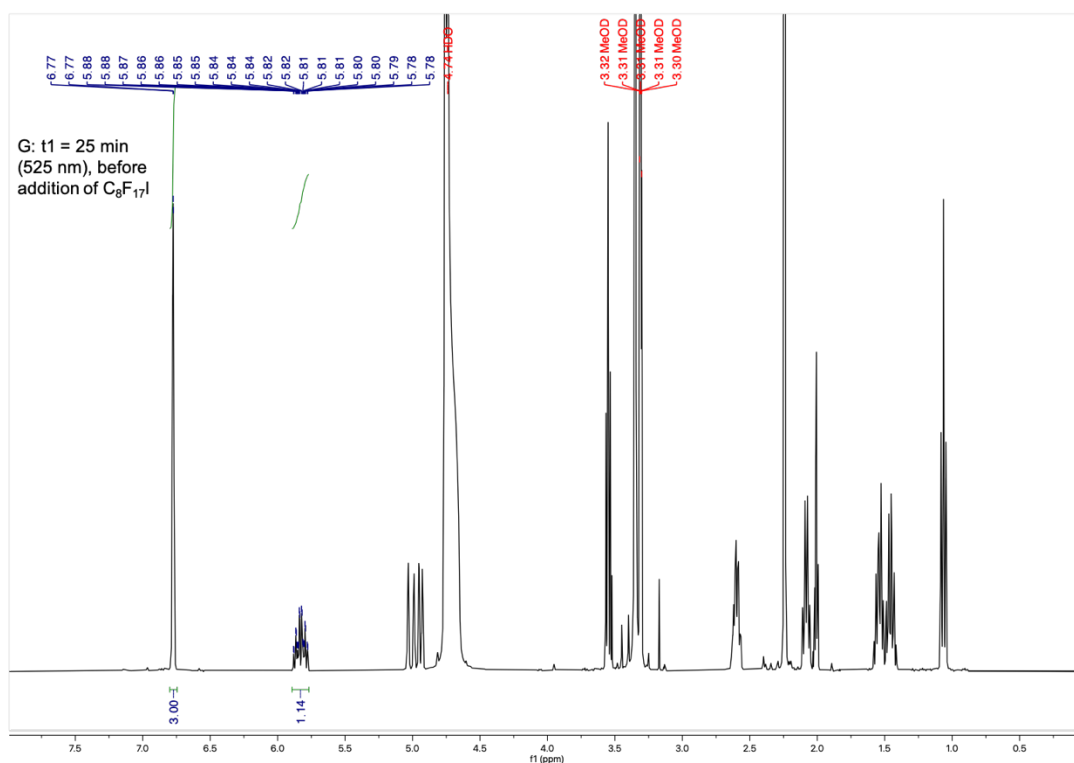


Figure S91: ^1H NMR spectrum (400 MHz) of Sample G (Wavelength-switching experiment) after 25 min irradiation at 525 nm (CD_3OD , integrated against internal standard ($3H$ (ArH)): mesitylene (15 μL)).

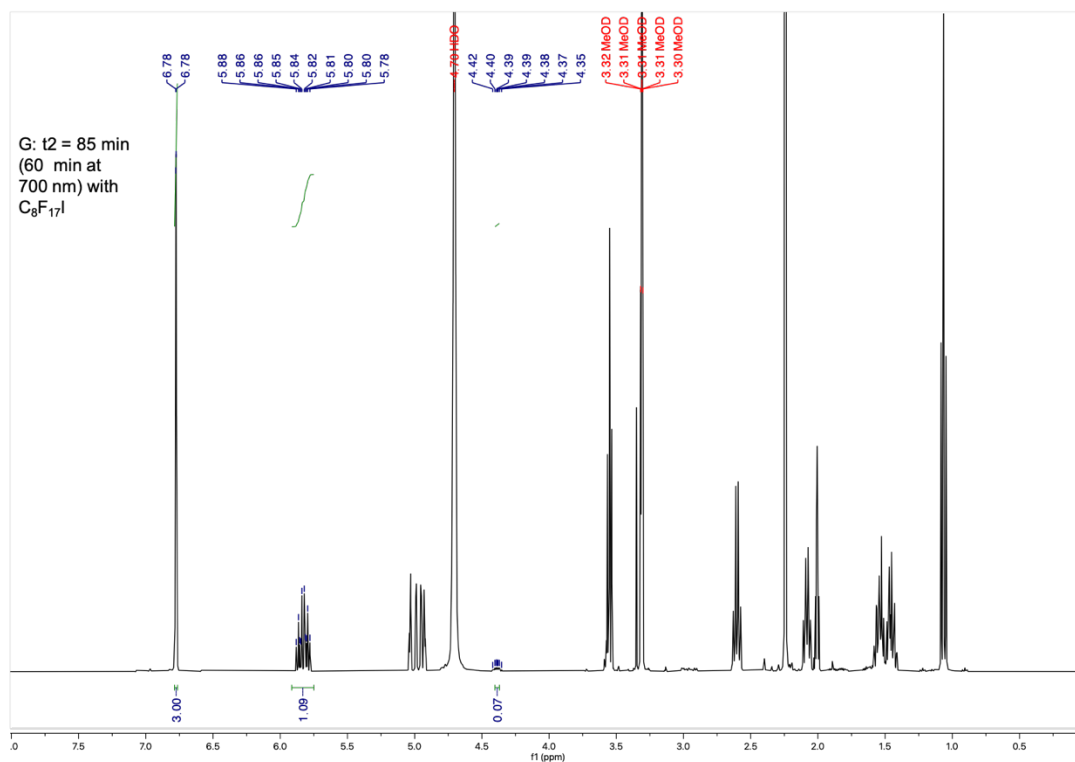


Figure S92: ¹H NMR spectrum (400 MHz) of Sample G (Wavelength-switching experiment) after addition of C₈F₁₇I and subsequent irradiation at 700 nm for 60 min (CD₃OD, integrated against internal standard (3*H* (Ar*H*)): mesitylene (15 μL)).

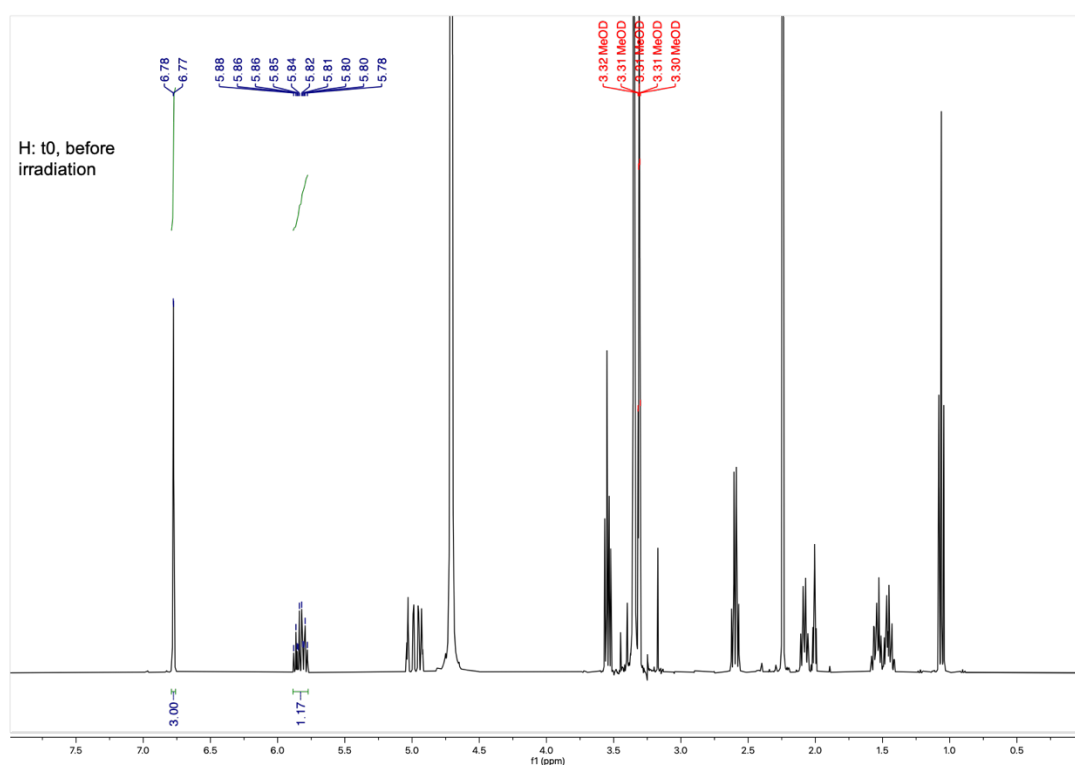


Figure S93: ¹H NMR spectrum (400 MHz) of Sample H (Wavelength-switching experiment) before irradiation (CD₃OD, integrated against internal standard (3*H* (Ar*H*)): mesitylene (15 μL)).

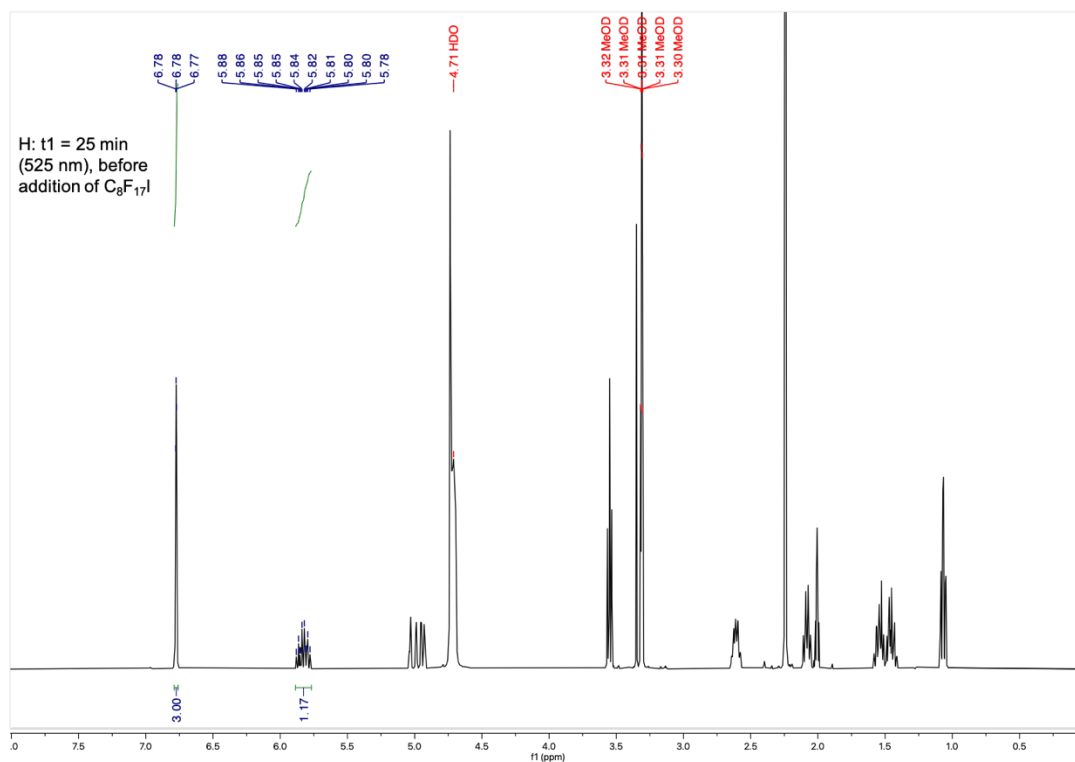


Figure S94: ¹H NMR spectrum (400 MHz) of Sample H (Wavelength-switching experiment) after 25 min irradiation at 525 nm (CD₃OD, integrated against internal standard (3*H* (Ar*H*)): mesitylene (15 μL)).

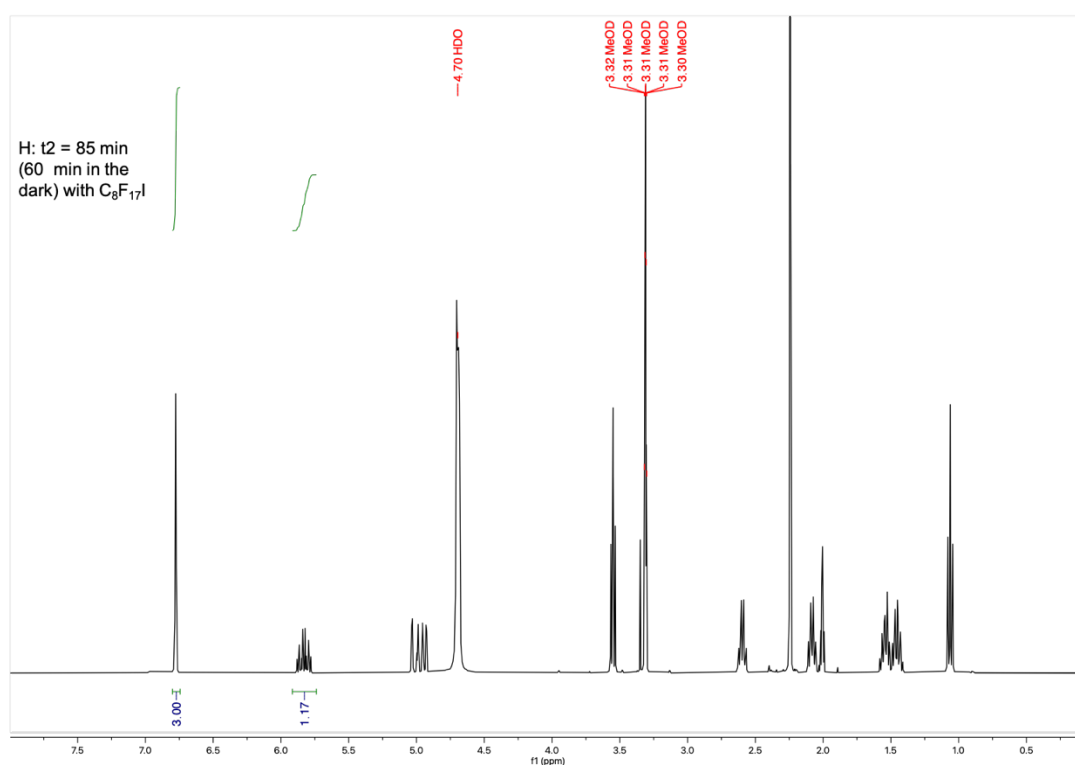


Figure S95: ¹H NMR spectrum (400 MHz) of Sample H (Wavelength-switching experiment) after addition of C₈F₁₇I and subsequent storage in the dark for 60 min (CD₃OD, integrated against internal standard (3*H* (Ar*H*)): mesitylene (15 μL)).

References

- [1] a) P. Chàbera, Y. Liu, O. Prakash, E. Thyraug, A. E. Nahhas, A. Honarfar, S. Essen, L. A. Fredin, T. C. Harlang, K. S. Kjaer, K. Handrup, F. Ericson, H. Tatsuno, K. Morgan, J. Schnadt, L. Häggström, T. Ericsson, A. Sobkowiak, S. Lidin, P. Huang, S. Styring, J. Uhlig, J. Bendix, R. Lomoth, V. Sundström, P. Persson, K. Wärnmark, *Nature* **2017**, *543*, 695-699; b) P. Chàbera, K. S. Kjaer, O. Prakash, A. Honarfar, Y. Liu, L. A. Fredin, T. C. B. Harlang, S. Lidin, J. Uhlig, V. Sundström, R. Lomoth, P. Persson, K. Wärnmark, *J. Phys. Chem. Lett.* **2018**, *9*, 459-463; c) J. Zhang, D. Campolo, F. Dumur, P. Xiao, J. P. Fouassier, D. Gigmes, J. Lalevée, *J. Polym. Sci., Part A: Polym. Chem.* **2016**, *54*, 2247-2253.
- [2] *CRC Handbook of Chemistry and Physics*, 102nd ed., CRC Press, **2021**.
- [3] a) R. G. Salomon, S. Ghosh, M. G. Zagorski, M. Reitz, *J. Org. Chem.* **1982**, *47*, 829-836; b) G. Balme, D. Bouyssi, R. Faure, J. Gore, B. Van Hemelryck, *Tetrahedron* **1992**, *48*, 3891-3902.
- [4] J. Hu, J. Wang, T. H. Nguyen, N. Zheng, *Beilstein J. Org. Chem.* **2013**, *9*, 1977-2001.
- [5] C.-J. Wallentin, J. D. Nguyen, P. Finkbeiner, C. R. J. Stephenson, *J. Am. Chem. Soc.* **2012**, *134*, 8875-8884.
- [6] M. Lumbierres, M. Moreno-Mañas, A. Vallribera, *Tetrahedron* **2002**, *58*, 4061-4065.
- [7] a) T. Rawner, E. Lutsker, C. A. Kaiser, O. Reiser, *ACS Catal.* **2018**, *8*, 3950-3956; b) X. Zou, F. Wu, Y. Shen, S. Xu, W. Huang, *Tetrahedron* **2003**, *59*, 2555-2560.
- [8] K. Matsuzaki, T. Hiromora, H. Amii, N. Shibata, *Molecules* **2017**, *22*.
- [9] T. Xu, C. W. Cheung, X. Hu, *Angew. Chem. Int. Ed. Engl.* **2014**, *53*, 4910-4914.
- [10] S. P. Pitre, C. D. McTiernan, W. Vine, R. DiPucchio, M. Grenier, J. C. Scaiano, *Sci. Rep.* **2015**, *5*, 16397.
- [11] M. A. Cismesia, T. P. Yoon, *Chem. Sci.* **2015**, *6*, 5426-5434.
- [12] P. Müller, K. Brettel, *Photochem. Photobiol. Sci.* **2012**, *11*, 632-636.